This dissertation has been
microfilmed exactly as received

69-16,575

JOHNSON, David Wilson, 1942-

THE THERMAL ISOMERIZATION OF CYCLO-PROPANE.

The University of Oklahoma, Ph.D., 1969
Engineering, chemical

University Microfilms, Inc., Ann Arbor, Michigan

Downloaded from SHAREOK. Persistent Handle URL: https://hdl.handle.net/11244/2557

THE UNIVERSITY OF OKLAHOMA

GRADUATE COLLEGE

THE THERMAL ISOMERIZATION OF CYCLOPROPANE

A DISSERTATION

SUBMITTED TO THE GRADUATE FACULTY

in partial fulfillment of the requirements for the

degree of

DOCTOR OF PHILOSOPHY

by

DAVID WILSON JOHNSON

Norman, Oklahoma

1969

THE THERMAL ISOMERIZATION OF CYCLOPROPANE

APPROVED BY

C. M. Sheppard

R. H. Murphy

F. M. Townsend

K. E. Starling

J. K. Lott

DISSERTATION COMMITTEE

ACKNOWLEDGMENTS

The author expresses his sincere appreciation to his advisory committee, Dr. C. M. Sliepcevich, Dr. G. W. Murphy, Dr. F. M. Townsend, Dr. K. E. Starling, and Dr. J. L. Lott, for their interest, direction, and assistance during this graduate program.

The efforts of Mrs. Joyce Meyer and Mr. T. Booker, who handled the graphical work, and Mrs. Ruth Kempton and Mrs. Connie Kirk, who typed the manuscript, are appreciated.

Special thanks is due to Dr. Jerry Havens, who undertook the final proofreading of this dissertation, and to Mr. Dwight Pfenning and Dr. George Bauerle, whose timely comments were well received during the experimental part of this study.

The author wishes to express his gratitude to the United States Government who, by way of an NDEA Title IV Fellowship, supported him during the first three years of this investigation, and to the Monsanto Company, who provided financial assistance during the last year of the study.

David Wilson Johnson

ABSTRACT

The homogeneous, gas-phase isomerization of cyclopropane to propylene was studied in the pressure range of 0.4 to 137 atmospheres and temperature range of 454 to 538°C. Integral rate data were obtained in a continuous flow system consisting of a tubular gold-lined reactor. The coiled reactor and preheater were maintained at constant temperature in a bath of fluidized sand heated by means of an enclosed propane burner. The burning air-propane mixture served as both a high temperature source and fluidizing medium for the sand bath. Residence times varied from 7 to 800 seconds and product conversions varied from 0.3 to 35 percent. Reactor inlet and outlet concentrations were determined by gas chromatography.

The statistical mechanical theories of Kassel, Rice and Ramsperger, and Slater predicting that the unimolecular rate constant should be a monatomically increasing function of pressure were shown to be in error. The rate constant at high pressures was shown to decrease with increasing pressure. An explanation based on the absolute reaction rate theory has been proposed to account for this observation.

The experimental Arrhenius parameters determined by Pipkin at 18 atmospheres agreed to within 0.1 percent of the 21 atmospheres parameters of this investigation. A method was proposed for computing the change in activation energy with pressure. Activation energies determined from this study and those found in the literature agreed to within an average deviation of 0.6 percent of the computed values.

TABLE OF CONTENTS

Page

LIST OF ILLUSTRATIONS. viii

LIST OF TABLES xi

CHAPTER

I. INTRODUCTION. 1

II. THEORETICAL CONSIDERATIONS. 3

General Principles of Reaction Kinetics. 3
General Theories of Chemical Reactions . 4
Unimolecular Reaction Rate Theory. . . . 7
Effect of Temperature on the Rate Constant 16
Effect of Pressure on the Rate Constant. 16
Effect of Pressure on the Activation Energy 21

III. REVIEW OF PREVIOUS WORK 23

Reaction Mechanism and Kinetics. 30
Composition at Equilibrium 33
Ranges of Pressure and Temperature . . . 34
Types of Apparatus 39

IV. DESCRIPTION OF EXPERIMENTAL APPARATUS . . . 41

Feed System. 43
Preheater and Reactor Section. 46
Product Section. 54
Auxiliaries. 56

V. EXPERIMENTAL PROCEDURE. 58

Preliminary Procedures 58
Startup Procedure. 59

Page

Run Procedure 61
Shutdown Procedure. 64
Calibrations. 65
Problems Encountered. 75

VI. ANALYTICAL PROCEDURE AND APPARATUS 76

VII. METHOD OF DATA ANALYSIS. 87

Development of an Expression for Calculation of the Specific Rate from Experimental Data 87
Calculation of Frequency Factor and Activation Energy 90
The Isothermal Behavior Assumption. 91
Estimation of the Expected Experimental Error. 93

VIII. DISCUSSION OF RESULTS. 98

IX. CONCLUSIONS. 134

NOMENCLATURE. 136

REFERENCES. 140

APPENDICES. 143

A. CALCULATION OF PHYSICAL PROPERTIES 143

B. EVALUATION OF THE EFFECTS OF LOGITUDINAL AND AXIAL DIFFUSION IN A TUBULAR REACTOR . . 149

C. COMPUTER PROGRAM FOR ANALYSIS OF EXPERIMENTAL DATA. 157

D. FLUIDIZED SAND BED DIAGRAMS. 168

E. SUMMARY OF EXPERIMENTAL DATA 174

LIST OF ILLUSTRATIONS

Figure		Page
1.	Variation of Reaction Rate with Pressure	11
2.	Characteristic Curve of Kassel, etc.	14
3.	Plot of $[\partial \ln I(T,P)/\partial P]_T$ versus P	20
4.	Effect of Pressure on Activation Energy	22
5.	Plot of $1/k_c$ versus 1/P Showing the Variation of Pipkin's Results from Theoretical Predictions	29
6.	Equilibrium Composition	35
7.	Pressure Ranges	37
8.	Temperature Ranges	38
9.	Simplified Flow Diagram	42
10.	Flow Diagram of Feed System	44
11.	Flow Diagram of Preheater and Reactor System . .	47
12.	Reactor Coupling	51
13.	Flow Diagram of Product System	55
14.	Effect of Temperature on Mueller Bridge Resistance	69
15.	Equipment Used to Measure Fluctuations in Sand Bath Temperature	72
16.	Soap Bubble Meter	74
17.	Photograph of Chromatograph	79
18.	Standard Sample Preparation Equipment	81

Figure		Page
19.	Standard Preparation Work Sheet	82
20.	Chromatograph Calibration Curve	83
21.	Typical Chromatogram	86
22.	Non-Isothermal Behavior in Reactor	94
23.	Region of Isomerization	100
24.	First Order Behavior at 496.1°C	101
25.	Arrhenius Correlation at 28 atms	103
26.	Arrhenius Correlation at 21 atms	104
27.	Arrhenius Correlation at 14.5 atms	105
28.	Arrhenius Correlation at 7.8 atms	106
29.	Arrhenius Correlation at 4.4 atms	107
30.	Arrhenius Correlation at 3.0 atms	108
31.	Arrhenius Correlation at 2.0 atms	109
32.	Arrhenius Correlation at 1.3 atms	110
33.	Arrhenius Correlation at 1.0 atms	111
34.	Plot of I(T,P) versus ℓn(P)	114
35.	Arrhenius Correlation for Infinite Pressure	116
36.	Variation of the Rate Constant with Pressure at 482.2°C	120
37.	Effect of Residence Time on the Rate Constant at 482.2 and 510°C	123
38.	Plot of 1/k versus 1/P at 482.2°C	125
39.	Comparison of Rate Constant Theories	127
40.	Comparison of k_c and RTk_a	129
41.	Variation of Activation Energy with Pressure.	130
42.	Compressibility of Cyclopropane at 482.2°C.	145

Figure		Page
43.	Error in Assuming Plug Flow	152
44.	Sample Input Data	158
45.	Sample Computer Results	167
46.	Burner Ignition System Electrical Circuit Diagrams	169
47.	Sectional Elevation of Burner for Sand Bath Heater	170
48.	Reactor Fluidized Sand Heater	171
49.	Reactor Fluidized Sand Heater--Sectional	172
50.	Reactor Fluidized Sand Heater-- Grid Plate	173

LIST OF TABLES

Table		Page
1.	Temperature and Pressure Ranges of Cyclopropane Thermal Isomerization	36
2.	Mueller Bridge Calibration Results	67
3.	Results of Chromatograph Calibration	85
4.	First Order Behavior at 496.1°C	102
5.	Summary of Runs Used In Arrhenius Correlation	113
6.	Rate Constant for Infinite Pressure	115
7.	Arrhenius Parameters for Infinite Pressure Rate Constants	118
8.	Parameters Used in Equation (VIII-2)	121
9.	Variation of Activation Energy with Pressure.	131
10.	Results of Parameter Calculations	154
11.	Summary of Experimental Runs	175

CHAPTER I

INTRODUCTION

The study of the variation of unimolecular rate constants with pressure offers a unique method for testing the statistical mechanical theories of reaction kinetics. While it is not presently possible to predict the correct value of the reaction rate from statistical mechanical developments, the ability of these methods to predict the pressure trends of rate constants is encouraging.

The variation in the rate constant with pressure for the thermal isomerization of cyclopropane has been extensively studied at pressures below one atmosphere; only recently has this reaction been studied at high pressures. The low pressure studies have substantiated the theories of Kassel, Rice and Ramsperger, and Slater which predict a decline in the rate constant with decreasing pressure. The only study of the thermal isomerization of cyclopropane conducted at pressures substantially above atmospheric pressure indicated that at sufficiently high pressures the rate constant would decrease with increasing pressure. Even though a theoretical basis was proposed for this observation, the results were not generally accepted

since the possibility of undetected polymerization clouded the validity of the experimental results.

Continuous flow systems have been successfully employed in the study of the cyclopropane isomerization reaction only by the most recent investigators. Flow systems are ideally suited for reaction studies at elevated pressures where short contact times are required.

The objectives of this investigation were (1) to obtain rate data in the previously unexplored region from 454-539°C and 1-18 atmospheres pressure, (2) to determine if the observed decrease in the rate constant with increasing pressure at high pressures was a valid observation, (3) to determine if operation of the same flow system was possible at subatmospheric and elevated pressures, and (4) to demonstrate the usefulness of a pressurized flow (non-pumped) reaction system for moderate and high pressure kinetic studies.

The reaction study was conducted in a gold-lined, tubular reactor immersed in a constant temperature bath of fluidized sand. Rate data were obtained at temperatures ranging from 454 to 539°C and at pressures from 0.4 to 137 atmospheres.

CHAPTER II

THEORETICAL CONSIDERATIONS

The material in this chapter will be divided into five sections: (1) general principles of reaction kinetics, (2) theories of chemical reactions, (3) unimolecular reaction rate theory, (4) effect of temperature on the rate constant and (5) effect of pressure on the rate constant. The main emphasis of the chapter will be to develop a foundation for later discussion.

General Principles of Reaction Kinetics

In any discussion of reaction rates, a clear and unambiguous definition of the reaction rate is required. In this work, the term reaction rate will refer to the time rate of change in the number of moles of a component per unit volume:

$$r_i = -\frac{1}{V}\frac{dn_i}{dt} \qquad \text{(II-1)}$$

Equation (II-1) is applicable to both batch and flow processes. In a batch process, V is the fixed volume of the reaction system; while in a flow process, V is the volume associated with a fixed mass. Thus, V will usually be a function of time in a flow process. Formally, the reaction

rate may be expressed as:

$$-\frac{1}{V}\frac{dn_i}{dt} = k_c\,\Phi(c_1, c_2, \ldots c_n)$$

$$= k_a\,\beta(a_1, a_2, \ldots a_n) \qquad \text{(II-2)}$$

where the specific rate constant k_c is defined in terms of concentrations and k_a is defined in terms of activities. Pipkin (P2) offers an excellent discussion concerning the continuing disagreement on the use of concentrations versus activities in rate expressions. In this work, the rate expression will be defined in terms of concentrations.

General Theories of Chemical Reactions

While the thermodynamics of matter at equilibrium is well established, the foundations of rate theory are less firm. Deducing kinetic principles from equilibrium behavior involves extrapolations which must be carried out with caution. The most useful deduction of this type was made by Arrhenius who rationalized the temperature dependence of the specific rate constant from Van't Hoff's equation for the effect of temperature on the concentration equilibrium constant. His result was:

$$k_c = A \exp\,(-E_o/RT) \qquad \text{(II-3)}$$

where k_c is the specific rate constant, E_o is termed the energy of activation and A is the frequency factor. For elementary unimolecular and bimolecular gas-phase reactions, deviations from the predicted temperature effect of Equation (II-3) are usually attributed to experimental error. The

fundamental significance of the Arrhenius development lies in the interpretation of the results in terms of "active" molecules. The proposal by Arrhenius, that equilibrium exists between normal molecules and "active" molecules which have sufficient energy for reaction, includes the two concepts fundamental to both the collision and absolute reaction rate theory: (1) equilibrium between normal and "activated" molecules and (2) the presence of an activated state.

In the collision theory of chemical reaction, reaction is assumed to occur upon collision, provided the reactants possess a certain minimum activation energy, E_o. The number of collisions occurring per unit time can be approximated by the kinetic theory equation for double collisions:

$$N = c_1 \, c_2 \, \sigma_{12}^2 \sqrt{\frac{8\pi R_1 T \, (M_1 + M_2)}{M_1 M_2}} \qquad \text{(II-4)}$$

At ordinary conditions, N is a very large number of the order 10^{28}/ml-sec. Yet, since reactions do not occur this fast, not every collision produces a reaction. To complete the development, it is assumed that only those molecules possessing a certain minimum energy, E_o, are capable of reacting upon collision. From the Maxwell-Boltzmann distribution law, the fraction of molecules possessing an energy in excess of E_o is:

$$f(E_o) = \exp\ (-E_o/RT) \qquad \text{(II-5)}$$

Therefore, the product of the number of collisions per unit time and the fraction of these collisions which produce a reaction gives the specific reaction rate:

$$\text{rate} = f(E_o)\ N = N \exp\ (-E_o/RT) \qquad \text{(II-6)}$$

Naturally this result is highly simplified, but it is useful in predicting reaction rates for simple molecules.

The activated complex or transition state theory assumes that an equilibrium exists between an activated complex (that is, a complex capable of reacting) and reactants and products:

$$A + B \leftrightarrow X \rightarrow C + D \qquad \text{(II-7)}$$

Based on this assumption, and using further statistical mechanical arguments, the specific reaction rate constant can be represented as:

$$k = \varkappa\ \frac{K_B T}{h}\ K^* = \varkappa\ \frac{K_B T}{h}\ \left[\frac{F_x'}{F_a F_b}\right] \exp\ (-E_o/RT) \qquad \text{(II-8)}$$

where: K_B = Boltzman constant

h = Planck's constant

K^* = equilibrium constant for reactants and activated complex in terms of concentrations

F_x' = partition function for activated complex with one vibrational degree of freedom removed

F_a, F_b = partition functions of A and B

$\varkappa$ = transmission coefficient accounting for the fact that not every activated molecule becomes a product

Unimolecular Reaction Rate Theory

Unimolecular reactions are those reactions which proceed through a transition state consisting of a single, activated molecule. This definition does not imply that unimolecular reactions are elementary; most are complex and involve the formation of free radicals. The thermal isomerization of cyclopropane is one of the few unimolecular reactions known to occur in a single elementary step.

When first discovered, unimolecular reactions were not understood. Their first order behavior could not be reconciled to the second order collision process. Perrin, (P1) in 1919, attempted to show that the activation was brought about by absorption of radiation. His hypothesis was discredited when further experimental work showed that many unimolecular reactions became second order at reduced pressure. In 1922, Lindemann (L4) proposed a mechanism for unimolecular reactions which was compatible with both experimental results and collision theory. His mechanism, with some refinements, remains the accepted one today.

Lindemann visualized three processes to occur simultaneously in a unimolecular reaction: (1) normal molecules collide to produce activated molecules, (2) activated molecules

collide with normal molecules and are deactivated, and (3) activated molecules decompose to form products. The mechanism is given below in equation form:

$$(1)\quad A + A \xrightarrow{k_F} A^* + A \qquad \text{(II-9)}$$

$$(2)\quad A + A^* \xrightarrow{k_B} A + A \qquad \text{(II-10)}$$

$$(3)\quad A^* \xrightarrow{k_L} B \qquad \text{(II-11)}$$

One additional assumption is needed here: that is, the assumption of an equilibrium condition between activated molecules and reactants and products. With this assumption the rates of activation and deactivation-decomposition can be equated to give:

$$k_F C_A^{\,2} = k_B C_A C_A^* + k_L C_A^* \qquad \text{(II-12)}$$

Since the net rate of reaction is:

$$r_A = -\frac{1}{V}\frac{dn_A}{dt} = k_L C_A^* \qquad \text{(II-13)}$$

the quantity, C_A^*, can be eliminated between Equations (II-12) and (II-13) to give the net reaction rate in terms of C_A alone:

$$r_A = \frac{k_L k_F C_A^{\,2}}{k_L + k_B C_A} \qquad \text{(II-14)}$$

However, the question still remains: How does the Lindemann mechanism explain the first order behavior of unimolecular reactions at high pressures and their second order behavior at low pressures?

To help explain this phenomenon, Equation (II-14) will be rearranged into the following form:

$$r_A = \frac{k_L C_A^2}{\frac{k_L}{k_F} + \frac{C_A}{k_d}} \qquad \text{(II-15)}$$

where: $k_d = k_B/k_F$

Now, at high pressures, C_A will be large and the ratio k_L/k_F will be small in comparison to C_A/k_d. Therefore, the high pressure limiting form of Equation (II-15) will be:

$$r_A = k_L\, k_d\, C_A \qquad \text{(II-16)}$$

which is a first order reaction. At low pressures, the term k_L/k_F will become much larger than C_A/k_d and the low pressure limiting form will be:

$$r_A = k_F C_A^2 \qquad \text{(II-17)}$$

a second order reaction. In testing for the Lindemann mechanism, the first order rate constant, k_c, is computed, and its reciprocal is plotted against the reciprocal of C_A. The result should be a straight line, which can be shown in the following way: Since

$$r_A = k_C\, C_A = \frac{k_L k_F C_A^2}{k_L + k_B C_A}$$

$$\text{then } k_c = \frac{k_L k_F C_A}{k_L + k_B C_A} \qquad \text{(II-18)}$$

$$\text{or} \quad \frac{1}{k_c} = \frac{1}{k_L k_d} + \frac{1}{k_F C_A} \qquad \text{(II-19)}$$

An equivalent development in statistical mechanical terms has been made by Hinshelwood (H1). Both Lindemann's and Hinshelwood's treatments either explicity or implicitly assume that all activated molecules have the same probability of reacting, regardless of their energy content. Hinshelwood's results can be summarized by the equation:

$$k_c = \frac{k_\infty}{1 + \beta/P} \qquad \text{(II-20)}$$

The term k_∞ (a supposably pressure independent rate constant referred to infinite pressure) has been universally accepted by previous investigators of unimolecular reactions as a means of reporting pressure independent rate constants.

Some departure from the linear relationship of Equation (II-19) as indicated in Figure 1, brought about basically similar refinements in the theory by Kassel (K2), Rice and Ramsperger (R2) and Slater (S1). Their contributions consisted of a statistical mechanical development which allowed for the variation in specific reaction rate with the energy level of the molecule. In the nomenclature of equation (II-18), the result of their treatment is:

$$k_c = \sum_i \frac{(k_L)_i \, (k_F)_i \, C_A}{(k_L)_i + (k_B)_i C_A} \qquad \text{(II-21)}$$

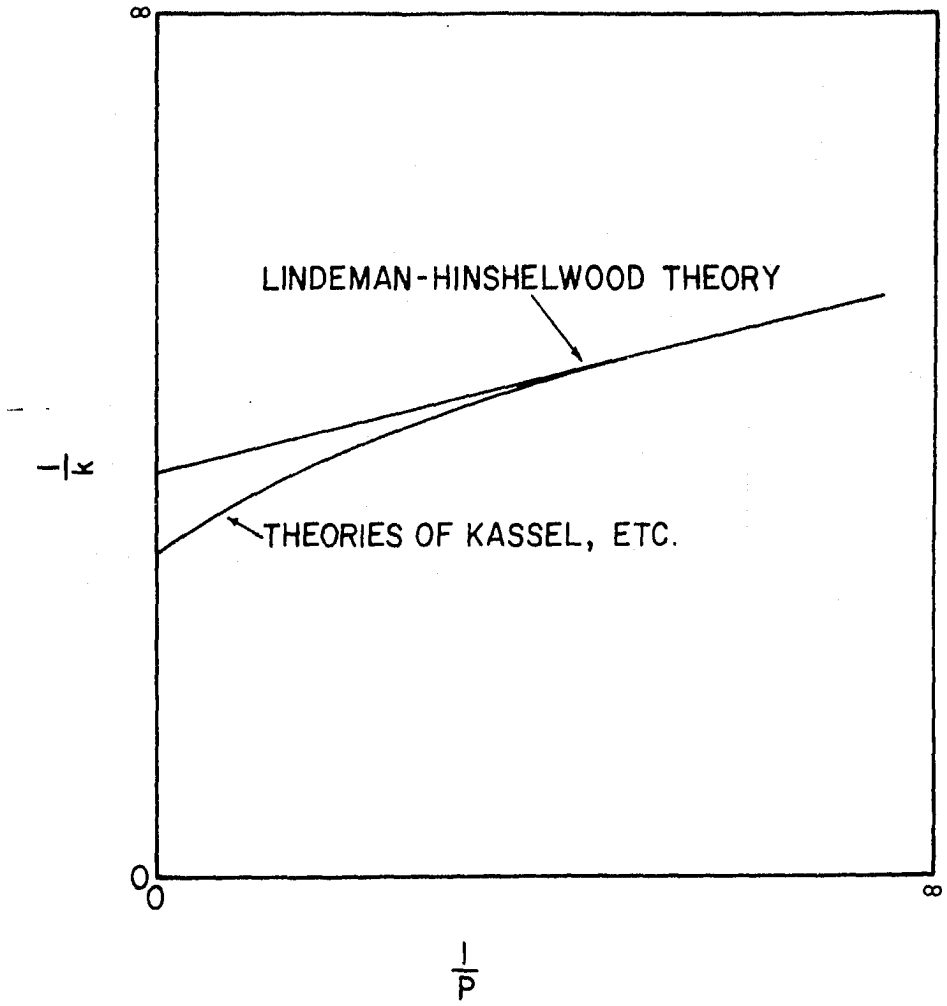


Figure 1. Variation of Reaction Rate with Pressure.

where the summation includes all energy levels of the activated molecule A*. The high pressure limiting form of (II-21) following the derivation in Equations (II-14) to (II-16) becomes:

$$k_\infty = \sum_i (k_L)_i \, (k_d)_i \qquad \text{(II-22)}$$

While the derivation of the statistical mechanical arguments of Kassel, Rice and Ramsperger or Slater are very lengthy, the results of Kassel's work will be presented since the numerical results are very similar in all treatments. Kassel found the following relation between the rate constant at pressure P and the rate constant referred to infinite pressure:

$$k(P) = k_\infty \int_0^\infty \frac{D \exp(-x/RT)\,dx}{\frac{1}{x^{s-1}} + \frac{(A/BN)}{(x+E_o)^{s-1}}} \qquad \text{(II-23)}$$

$$D = \frac{1}{\Gamma(S)\,(RT)^s}$$

$$B = 4\sqrt{\frac{\pi R_1 T}{M}}\,\sigma^2$$

where: $N \simeq 6\times10^{20} P/(R_2 T)$, molecules/ cc

A = frequency factor, molecules/sec

σ = collision diameter, cm

R = 1.987 cal/mole-°K

R_2 = 0.08205 liter-atms/mole-°K

R_1 = 8.314 x 10^7 g-cm^2/sec^2-mole-°K

Γ = gamma function, $\Gamma(n) = \int_0^\infty e^{-x} x^{n-1} dx$

S = effective number of oscillators

T = temperature, °K

M = molecular weight

Thus, it is possible to calculate the ratio, k/k_∞, with a knowledge of pressure, temperature, collision diameter and the number of oscillators. The term, I(T,P), will be used to denote the integral in Equation (II-23), i.e.:

$$I(T,P) = \int_0^\infty \frac{D \exp(-x/RT)\,dx}{\frac{1}{x^{\frac{s-1}{2}}} + \frac{(A/BN)}{(x+E_o)^{s-1}}} \qquad \text{(II-24)}$$

Testing of the theory is accomplished by plotting $\ell n\ (k/k_\infty)$ against $\ell n(P)$ to obtain the curve shown in Figure 2.

For the cyclopropane isomerization, Slater has attempted to calculate directly the specific rate of reaction from a vibrational analysis of the molecule. Using both a classical harmonic oscillator model (52) and a quantum harmonic oscillator model (53), Slater was able to predict the characteristic shape of the curve in Figure 2.

As previously mentioned, investigators of the cyclopropane isomerization reaction have expressed their results in terms of the pressure independent rate constant, k_∞. In determining the dependence of k_∞ on temperature, all investigators have chosen the Arrhenius form:

$$k_\infty = A_\infty \exp(-E_\infty/RT) \qquad \text{(II-25)}$$

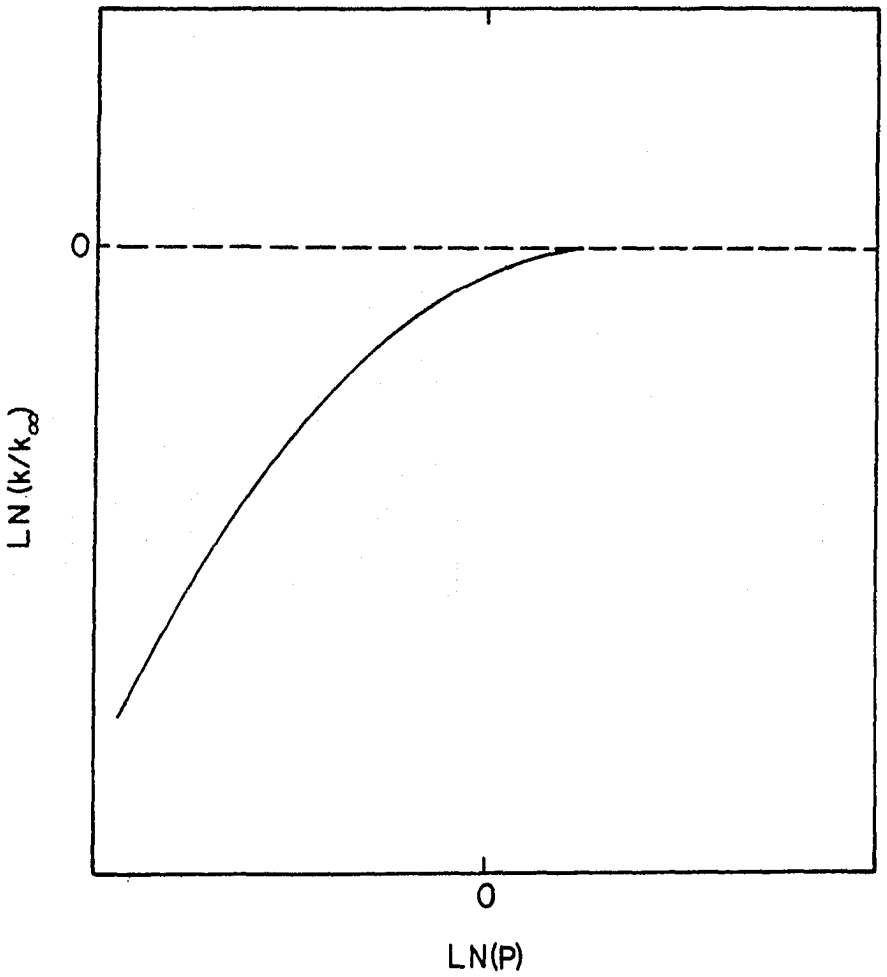


Figure 2. Characteristic Curve of Kassel, etc.

It is interesting to investigate the restrictions placed upon unimolecular reaction rate theories by this assumption. Slater (S1) has found the following restrictions (implications) imposed by the Arrhenius form on the classical harmonic oscillator models:

(1) The minimum energy for dissociation is the Arrhenius parameter E_o.

(2) The specific rate for molecules of very high energy is A, the Arrhenius frequency factor.

(3) The (average) specific rate must be a particular function of the classical weight factors.

For the quantum oscillator model, an additional restriction is observed:

(4) The only model giving the Arrhenius rate is that of a set of degenerate oscillators.

The unimolecular models of Kassel, Rice and Ramsperger, and Slater reduce to the Arrhenius form for k_∞. However, Hinshelwood's development gives a somewhat different temperature dependence:

$$k_\infty = k_1 \exp(-b_1) \{b_1^{n-1}/(n-1)! + b_1^{n-2}/(n-2)! + \ldots + 1\} \qquad \text{(II-26)}$$

where $b_1 = E_1/RT$

E_1 and E_o can be related by the following equation:

$$E_o = E_1/\{1 + (n-1)/b_1 + \ldots (n-1)!/b_1^{n-1}\} \qquad \text{(II-27)}$$

Effect of Temperature on the Rate Constant

The variation of the specific rate constant with temperature is accurately represented by the Arrhenius equation:

$$k = A \exp(-E_o/RT)$$

or in differential form:

$$\frac{\partial k}{\partial T} = kE_o/RT^2 \qquad \text{(II-32)}$$

$$\frac{\partial \ell n\ (k)}{\partial\ (1/T)} = -\frac{E_o}{R} \qquad \text{(II-38)}$$

Variation in the rate constant referred to "infinite" pressure, k_∞, has also been adequately representated by the Arrhenius equation.

Effect of Pressure on the Rate Constant

The effect of pressure on the specific rate constant can be predicted from the unimolecular reaction models of Kassel (K1), Rice and Ramsperger (R2), or Slater (S1). The primary effect is a decrease in rate constant with decrease in pressure as shown in Figure 2.

While the "fall off" curves of Kassel, etc. have been verified at pressures below one atmosphere, there is some reason to believe that at sufficiently high pressures, these characteristic curves are inadequate in expressing the dependency of the rate constant on pressure. The reasons

for this view will be briefly discussed below.

In the development presented by Kassel, the pressure dependency of the rate constant is theorized to come from an inability of the reaction system to maintain equilibrium between activated molecules and reactant molecules. That this effect is paramount at low pressures is shown by the agreement between theoretical predictions of rate constant variation with pressure and experimental observations. However, at higher pressures, the reaction system changes from a system of essentially ideal gases to a system of real, non-ideal gases. The effect of these non-idealities have not been considered by the treatments of Kassel, etc.

Quantitatively, these "non-ideal" effects can be determined by use of the absolute reaction rate theory, but with a new interpretation given to the transmission coefficient. The transmission coefficient is generally thought of as a probability factor relating the number of activated species which become products to the number of activated species which are proceeding toward the product state. With this interpretation, the transmission coefficient is not a function of pressure and the absolute reaction rate theory is incapable of predicting the observed decline in rate constant with decreasing pressure at low pressures for unimolecular reactions. If, however, the transmission coefficient is considered to be the ratio between the number of activated molecules at some pressure, P, and the

equilibrium number of activated molecules available at some pressure approaching infinity, then the transmission coefficient becomes pressure dependent. The theoretical treatments of Kassel, etc. make this assumption and Equation (II-23), in effect, becomes the transmission coefficient. The "new" (at least in interpretation) absolute reaction rate theory becomes:

$$k_c = I(T,P)\ \frac{K_B T}{h}\ K^* \qquad \text{(II-32)}$$

where $I(T,P)$ is defined by Equation (II-24) all other terms remaining as in Equation (II-8).

The effect of pressure on the rate constant at either high or low pressures can be predicted from Equation (II-32) by direct differentiation:

$$\ln k_c = \ln I(T,P) + \ln K^* + \ln \frac{K_B T}{h}$$

$$\left[\frac{\partial \ln k_c}{\partial P}\right]_T = \left[\frac{\partial \ln I(T,P)}{\partial P}\right]_T + \left[\frac{\partial \ln K^*}{\partial P}\right]_T \qquad \text{(II-33)}$$

Now, K^* can be expressed in the following manner utilizing the Lewis fugacity rule:

$$K_f^* = \frac{x^* f^*}{x_A f_A} = \frac{x^*}{x_A}\ \frac{f^*}{f_A} = K^* \frac{f^*}{f_A}$$

$$\text{or} \qquad K^* = K_f^*\ \frac{f_A}{f^*} \qquad \text{(II-34)}$$

where K_f^* is the pressure independent fugacity equilibrium constant,

f* is the fugacity of the activated species and f_A is the fugacity of the reactant. In terms of Equation (II-34), Equation (II-33) becomes:

$$\left[\frac{\partial \ell n\, k_c}{\partial P}\right]_T = \left[\frac{\partial \ell n\, I(T,P)}{\partial P}\right]_T + \left[\frac{\partial \ell n\, (f_A/f^*)}{\partial P}\right]_T + \cancel{\left[\frac{\partial \ell n\, K_f^*}{\partial P}\right]_T}^{\,0} \qquad \text{(II-35)}$$

Since fugacity is defined in the following manner:

$$RT\, d(\ell n\, f) = \bar{V} dP$$

where $\bar{V}$ is the molar volume, then Equation (II-35) can be written as:

$$\left[\frac{\partial\, \ell n\, k_c}{\partial P}\right]_T = \left[\frac{\partial\, \ell n\, I(T,P)}{\partial P}\right]_T - \frac{\bar{V}^* - \bar{V}_A}{RT} \qquad \text{(II-36)}$$

where $\bar{V}^*$ is the molar volume of the activated species and $\bar{V}_A$ is the molar volume of the reactant. Equation (II-36) is the final equation relating the change in the rate constant with pressure.

The statistical mechanical theories of Kassel, Rice and Ramsperger, and Slater assume that the effect of pressure on the rate constant is due to a displacement from equilibrium of the activated molecules. Thus, the last term in Equation (II-36) is zero and their equation which relates the rate constant to pressure is:

$$\left[\frac{\partial \ell n\, k_c}{\partial P}\right]_T = \left[\frac{\partial \ell n\, I(T,P)}{\partial P}\right]_T \qquad \text{(II-37)}$$

The absolute reaction rate theory, on the other hand, assumes that the pressure effect resides in the equilibrium constant, K*, i.e., that the pressure dependence of the rate constant is:

$$\left[\frac{\partial \ell n\, k_c}{\partial P}\right]_T = -\frac{\bar{V}^* - \bar{V}_A}{RT} \qquad \text{(II-38)}$$

The term $\left[\frac{\partial \ell n\, I(T,P)}{\partial P}\right]_T$ can be found by numerical differentiation of values obtained from Equation (II-24). The result is a curve similar to the one shown in Figure 3 below. The numerical value of this term decreases rapidly with

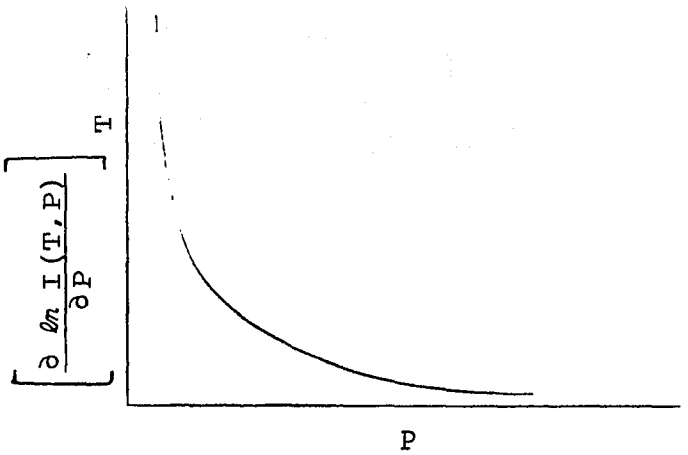


Figure 3. Plot of $[\partial\, \ell n\, I(T,P)/\partial P]_T$ versus P.

increasing pressure, becoming very small at pressures above 30 atmospheres. The second term to the right of the equality, $\frac{\bar{V}^* - \bar{V}_A}{RT}$, can only be roughly estimated since values of $\bar{V}^*$, the molar volume of the activated complex, are not known. However, it seems reasonable to assume that because the activated complex is similar to the reactant, except for

some stretching of a critical bond (see Gonikberg (G1) p. 77), that its molar volume is greater than the reactant. Therefore, this term is probably a small positive number which increases slowly with increasing pressure.

At low pressures, the first term will be much larger than the second term to the right of the equality in Equation (II-36) and the rate constant will increase with increasing pressure. At sufficiently high pressures, the second term should predominate the equation (the first term approaches zero at high pressures) and the rate constant will decrease with increasing pressure. At some pressure, P_m, the rate constant will show a maximum value as the two terms in Equation (II-36) cancel and the derivative with respect to pressure vanishes.

The implications of this development on the rate constant at infinite pressure, k_∞, and some numerical results are discussed in Chapter VIII.

Effect of Pressure on the Activation Energy

The effect of pressure on the activation energy, E_o, can be found using the Arrhenius form for the rate constant:

$$k_c = A \exp(-E_o/RT)$$

$$\ln k_c = \ln A - E_o/RT$$

at any pressure, P, E_o can be found from:

$$E_o\ (P) = \frac{R[\ell n\ k_c(P,T_2) - \ell n\ k_c(P,T_1)]}{[(1/T_1) - (1/T_2)]} \qquad \text{(II-39)}$$

at low pressures (below 2 atmospheres) where Equation (II-32) varies insignificantly (see Chapter VIII) from Equation (II-34) the pressure dependence of the activation energy can be more easily computed by using the following:

$$E_o = - \frac{R\ \partial \ell n\ (k_c)}{\partial (1/T)}$$

$$k_c = k_\infty \times I(T,P)$$

$$E_o = \frac{-R\ \partial \ell n\ (k_\infty)}{\partial (1/T)} - \frac{R\ \partial \ell n\ [I(T,P)]}{\partial (1/T)}$$

$$E_o = E_\infty - \frac{R\ \partial \ell n\ [I(T,P)]}{\partial (1/T)} \qquad \text{(II-40)}$$

Here, E_∞ is the hypothetical "infinite" pressure activation energy defined by the relationship:

$$k_\infty = A_\infty \exp\ (-E_\infty/RT) \qquad \text{(II-41)}$$

The general effect of pressure on the activation energy is shown in Figure 4.

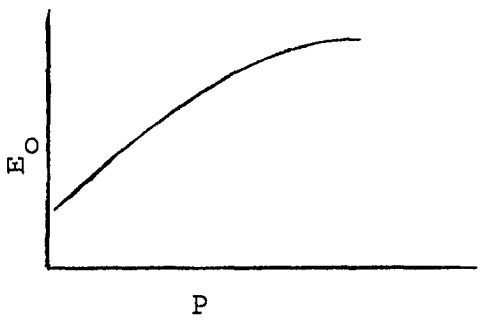


Figure 4. Effect of Pressure on Activation Energy.

CHAPTER III

REVIEW OF PREVIOUS WORK

Despite its appearance of simplicity, the thermal isomerization of cyclopropane is an extensively studied reaction. Past interest in the reaction has been primarily the result of two considerations: (1) the homogeneous gas phase reaction is one of the few elementary unimolecular reactions occurring in the absence of free radical chain mechanisms and (2) the reaction is useful in testing the unimolecular reaction rate theories which predict a decline in the first order rate constant with reduced pressure.

Trautz and Winkler (T1) in 1922 made the first significant study of cyclopropane thermal isomerization. At the time of the Trautz and Winkler investigation, the statistical theories of unimolecular reactions had not been developed, and the need for a study of rate constant dependence on pressure was not apparent. Their experiments were conducted at approximately 75.5 cm of mercury and in the temperature range of 350 to 650°C. The reaction was accomplished in flow-type reactors constructed of either quartz or porcelain tubes. They found the reaction to be homogeneous and of first order, but some surface catalysis was indicated

in the porcelain tubes. At the higher temperatures, decomposition occurred; products of the decomposition were reported to be: hydrogen, carbon, methane, ethylene and propylene. The work of Trautz and Winkler has been criticized by Kassel (K1) and Chambers and Kistiakowsky (C1) because a reaction preheater was not used. The activation energies of 63.9 to 65.0 kilocalories per mole, for the temperature range of 550 to 650°C, are reasonably close to values reported by later investigators, but their frequency factor of 1×10^{14} was much too low.

Chambers and Kistiakowsky (C1) were the first to demonstrate the pseudo-unimolecular behavior in the thermal isomerization of cyclopropane. At 499.5°C their first-order rate constant was observed to decrease 43.5 percent upon decreasing the pressure from 70.26 to 1.27 cm of mercury. Values of k_∞ were obtained by finding the 1/k intercept in a plot of 1/k versus 1/P. The k_∞ values were fitted to the Arrhenius equation, with the following parameters:

$$\log (k_\infty) = 15.17 - \frac{65{,}000}{2.3\ RT}$$

where T is degrees Kelvin, k is in sec^{-1} and $R = 1.987 \frac{cal}{mole\text{-}°K}$

Chambers and Kistiakowsky also found that by choosing 3.9×10^{-8} cm as the collision diameter and thirteen as the number of degrees of freedom, the experimental values of k/k_∞ were in close agreement with the values of k/k_∞ computed from the equations derived by Kassel (K2).

Despite the overwhelming evidence of unimolecular behavior for the thermal isomerization of cyclopropane found in the Chambers and Kistiakowsky investigation, Corner and Pease (C3) attempted to demonstrate, through the effect of added gases, the existence of a chain mechanism for the isomerization. Their mechanism was based on the formation of a trimethylene di-radical. With a quasi-unimolecular reaction, added gases are expected to increase the reaction rate, while the rate may either increase or decrease in the case of a chain mechanism. However, in the Corner and Pease mechanism no change was expected. The added gases were hydrogen, ethylene, propylene and n-butane. With exception of decomposing n-butane, which accelerated the reaction, the added gases had little effect and the results were inconclusive.

Almost a decade passed before decisive results were reported on the effects of added gases. A clear cut restoration of the first-order rate constant was demonstrated by Pritchard, Sowden and Trotman-Dickenson (P3) when a number of gases were added to cyclopropane at an initial pressure of 0.01 to 0.1 cm of mercury. Their results were of sufficient precision to demonstrate, beyond reasonable doubt, the unimolecular character of the cyclopropane isomerization reaction.

With the pressure range of cyclopropane isomerization extended to a much lower region in the work of Pritchard et al., ample data were available to Slater (S2) to permit a thorough check of his theoretically predicted unimolecular

reaction rate for cyclopropane isomerization. Slater considered the cyclopropane molecule to be a classical vibrating system. Two models were proposed: in the first, the reaction was assumed to occur when vibration carried a hydrogen near a carbon in another methylene group; while in the second model, isomerization was assumed to result from the over stretching of a carbon-carbon bond. Slater's theory fell short of predicting the experimentally observed frequency factor (4×10^{14} theoretical versus 15×10^{14} experimental). However, two important points were established: (1) the shape of the log (k/k_∞) versus log (P) curve was confirmed without the use of any arbitrary parameters and (2) the hydrogen migration model gave results which were in closer agreement with experimental observations. Although not entirely due to this study, the hydrogen migration mechanism has become the generally accepted mechanism.

Langrish and Pritchard (L1) in studying the effect of temperature on the plot of log (k/k_∞) versus log (P) found the high pressure rate constant to be represented by:

$$\log (k_\infty) = 15.85 - \frac{67,500}{2.303\ RT}$$

They observed no change in the curve with temperature, as their data at 483 and 505°C could not be distinguished from previous data at 491°C (P3).

In 1959, Slater (S1) presented a quantum harmonic oscillator model to explain the temperature dependence of

unimolecular rate constants. However, Falconer, Hunter and Trotman-Dickenson's (F1) results agreed more closely with the Arrhenius form than with Slater's model. The experiments of Falconer, et al. were designed to yield data of sufficient precision to test the Slater theory. Their runs were conducted at 30 cm of mercury in the temperature range from 420 to 535°C. Their results are summarized in the equation:

$$\log (k_{30}) = 15.296 - \frac{65,084}{2.303\ RT}$$

Upon extending their results to infinite pressure, they found:

$$\log (k_{\infty}) = 15.45 - \frac{65,600}{2.303\ RT}$$

Kennedy and Pritchard (K3) extended the low pressure region of the thermal isomerization of cyclopropane to 6×10^{-5} cm of mercury. It was their purpose to observe the change in reaction kinetics as the mean free path of the molecules approached the dimensions of the reaction vessel. At 490°C and 10^{-4} cm of mercury, the reaction became first-order again, where the mean free path was approximately 7 cm, compared with the vessel diameter of 13 cm. The return to first order kinetics was the expected result as collision with the walls of the reaction vessel, rather than in the gas phase, became the primary source of activation. Kennedy and Pritchard reported an activation energy of 57.2 ± 2 kilocalories at a pressure of 8×10^{-4} cm of mercury (0.0000105 atm).

Davis and Scott (D2) extended the temperature range of reliable data to 620°C. Their measurements were at atmospheric pressure and were conducted in a Pyrex glass, flow-type reactor. They reported an atmospheric pressure rate constant of:

$$\ell n(k_1) = 36.1923 - \frac{66,950}{RT}$$

Upon combining their data with that of previous investigators (C1, C3, L5), they obtained the following relation of k_∞ to temperature:

$$\ell n(k_\infty) = 35.431 - \frac{65,570}{RT}$$

The most recent study of the thermal isomerization of cyclopropane was conducted by Pipkin (P2). Pipkin was the first investigator to study the reaction at pressures substantially above atmospheric (18-137 atms); his high pressure activation energies agree favorably with those found by Davis and Scott. Pipkin's runs were conducted in a flow-type system consisting of a gold-lined, tubular reactor. His results show, beyond reasonable doubt, the non-catalytic nature of gold toward the cyclopropane isomerization reaction. Pipkin observed a reversal of the trend for the rate constant to increase with increasing pressure. This effect is shown in Figure 5. Possible explanations for this effect were hypothesized to be: (1) undetected polymerization or, (2) non-ideal behavior at the high reaction pressures.

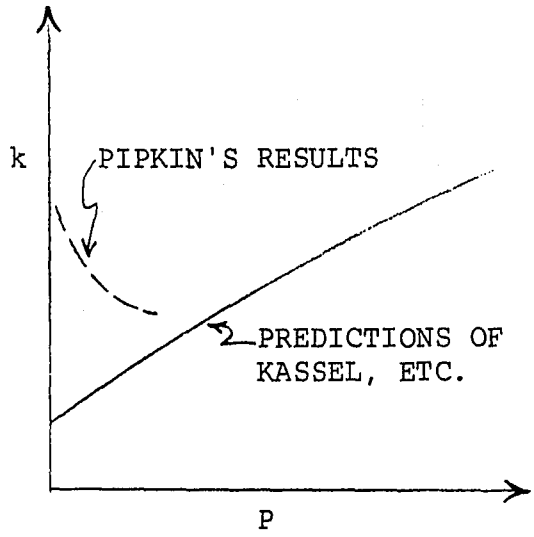


Figure 5. Plot of $1/k_c$ versus $1/P$ Showing the Variation of Pipkin's Results from Theoretical Predictions.

Reaction Mechanism and Kinetics

It is generally accepted that the thermal isomerization of cyclopropane is one of the few elementary unimolecular reactions. In Pyrex apparatus the reaction has been found to be homogeneous and at atmospheric pressure the reaction is of first order. In agreement with unimolecular reaction rate theory, the first order reaction rate constant shows a pressure dependence as pressure is reduced, and a region of second order behavior exists.

The reaction mechanism studies can be divided into two phases: (1) unimolecular versus free radical chain theory and (2) after acceptance of the unimolecular course, determination of whether the reaction occurs through hydrogen migration or overstretching of a c-c bond. Since the reaction mechanism is not the primary interest in this investigation, the past work on structural mechanism will be briefly reviewed.

As previously mentioned, Corner and Pease (C3) proposed a free radical chain mechanism to explain their data as well as that of Chambers and Kistiakowsky. Corner and Pease postulated that the trimethylene di-radical was formed, followed by the reactions:

$$C \xrightarrow{k_1} R$$

$$R \xrightarrow{k_2} C$$

$$R \xrightarrow{k_3} P$$

$$R + C \xrightarrow{k_4} 2P$$

Here, C signifies cyclopropane, R the trimethylene di-radical and P propylene. With the usual assumption of steady state free radical concentration, the rate equation for change in cyclopropane concentration becomes:

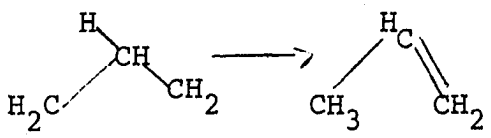
$$\frac{dc}{dt} = k_1 C\left[\frac{k_3 + 2k_4 C}{k_2 + k_3 + k_4 C}\right]$$

By proper selection of the ratio, $k_3/(k_2 + k_3)$ and k_3/k_4, Corner and Pease were able to show a constant value of k_1 over their pressure range. They were also able to demonstrate this constancy for the data of Chambers and Kistiakowsky by using a different ratio for $k_3/(k_2 + k_3)$.

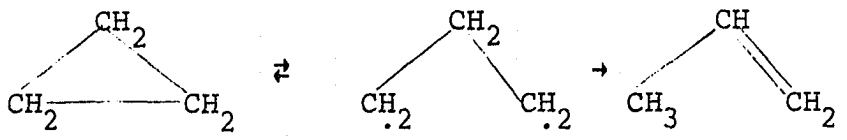
Since the addition of an inert gas should have no effect on the rate constant with the free radical chain mechanism and should increase the rate constant for a unimolecular reaction, this procedure was the logical means for determining the proper mechanism. However, the initial pressures of the Corner and Pease study were not low enough to produce a significant effect and their results were inconclusive. The unimolecular character of the reaction was strongly indicated in the later, added-gas experiments of Pritchard et al. The intramolecular, or purely physical, nature of the cyclopropane isomerization reaction is the accepted view today.

In their early study of the thermal isomerization of cyclopropane, Chambers and Kistiakowsky (C1) proposed the two structural mechanisms favored by later investigators.

In the first, a hydrogen "migrates" or "disproportionates" along a c-c bond causing a rupture of a second c-c bond and doubling of a third:



The classical vibrational analysis of Slater (S2) has favored this mechanism. In the second mechanism, the initial, and rate determining-step is the rupture of a c-c bond, followed by rearrangement of the di-radical produced:



Several isotope studies have been made in an attempt to choose between the two mechanisms. Lindquist and Rollefson (L5) and Weston (W1,W2) have investigated the relative rates of isomerization for cyclopropene and cyclopropane -t_1 (t_1 = tritium), while Rabinovinc, Schlag and Wiberg (R1) have similarly studied the relative rates using cyclopropane -d_2. The most recent study was conducted by Blades (B3) using cyclopropane -d_6. As pointed out by Blades, the results of these studies have not been conclusive. Since the arguments by Blades favoring the first structural mechanism are very convincing, the hydrogen "migration" mechanism is generally favored today.

Composition at Equilibrium

Pipkin (P2) has presented a complete discussion relating composition at equilibrium to absolute temperature. The results of his work will be briefly outlined.

The composition of a reacting cyclopropane-propylene mixture at equilibrium can be found by use of the relation:

$$\ell n\ (K_c) = -\Delta G°/RT \qquad \text{(III-1)}$$

where K_c is the concentration equilibrium constant and $\Delta G°$ is the ideal gas free energy change for the reaction. Equation (III-1) is valid only if non-ideal effects of pressure are negligible, such as can be expected at the elevated temperatures needed to perform the isomerization reaction. $\Delta G°$ can be computed from a knowledge of: (1) heat capacities, (2) heat of reaction at one temperature, and (3) values of entropy at one temperature. The derivation is outlined below:

$$\frac{\partial\ (\Delta G°/T)}{\partial T} = \frac{-\Delta H°}{T^2} \qquad \text{(III-2)}$$

$$\frac{\Delta G°}{T} = \int_{T_1}^{T} \frac{-\Delta H°}{T^2}\, dT + I_1 \qquad \text{(III-2)}$$

$$\Delta G° = \Delta H° - T\Delta S° \qquad \text{(III-4)}$$

$$\Delta H° = \int_{T_1}^{T} \Delta C_p°\, dT + I_2 \qquad \text{(III-5)}$$

Pipkin found the following relation for $\Delta G°$:

$$\Delta G° = -5.532\ T\ \ell n\ T + 0.007632\ T^2 - 1.5565 \times 10^{-6} T^3 + 25.89\ T - 8913.5\ \text{cal/g-mole} \qquad \text{(III-6)}$$

In view of the most recent data available for the functions needed in the computation, this result appears valid. Figure 6 is a plot of $\ell n\ (K_c)$ versus $T(°K)$ calculated from Equations (III-1) and (III-6).

Ranges of Pressure and Temperature

Prior to the work of Pipkin, the term "high pressure," when referred to the cyclopropane isomerization, meant a region only slightly above atmospheric pressure. Obviously, this terminology is not now applicable since Pipkin's investigations were performed up to 138 atmospheres (2000 PSIG). The highest pressure employed previous to the work of Pipkin was 91 cm of mercury in the investigation of Corner and Pease. Most investigations have been in the "interesting" region far below atmospheric pressure.

Excluding the early, and somewhat uncertain, work of Trautz and Winkler and the isotope studies, reliable data for the cyclopropane isomerization reaction has been obtained from 420 to 620°C. The greatest range of temperature, 454 to 593°C, was covered in Pipkins' investigation.

Table 1 summarizes the cyclopropane isomerization studies to date. Figures 7 and 8 graphically display the ranges of pressure and temperature covered by the various investigations.

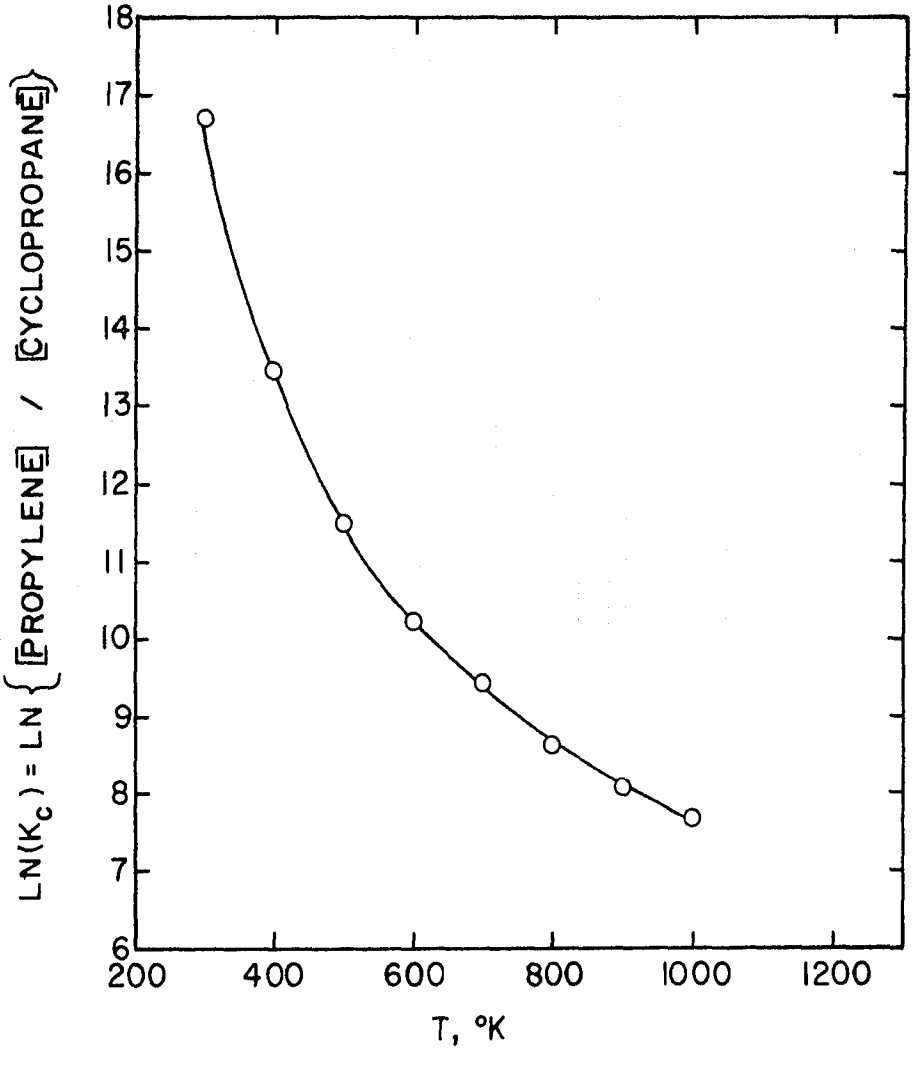


Figure 6. Equilibrium Composition.

TABLE 1

TEMPERATURE AND PRESSURE RANGES OF CYCLOPROPANE THERMAL ISOMERIZATION STUDIES

Number	Reference	Year	Pressure (atms)	Temperature (°C)
1	Trautz and Winkler (T1)	1922	1	350-650
2	Chambers and Kistiakowsky (C1)	1934	0.017-1	470-519
3	Corner and Pease (C3)	1945	0.013-1.2	440-520
4	Pritchard, Sowden and Trotman-Dickenson (Pe)	1952	9.2×10^{-5} - 0.11	470-490
5*	Weston (W2)	1955	5.3×10^{-4} - 0.92	406-492
6*	Lindquist and Rollefson (L5)	1956	0.21-0.27	447-555
7*	Rabinovich, Schlag and Wibert (R1)	1958	0.02	414-474
8	Langrish and Pritchard (L1)	1958	--	483-505
9	Falconer, Hunter and Trotman-Dickenson (F1)	1961	0.395	420-535
10*	Blades (B3)	1961	2.3×10^{-4} - 1.0	407-514
11	Kennedy and Pritchard (K3)	1963	0.79×10^{-6} - 0.92×10^{-3}	477-517
12	Davis and Scott (D2)	1964	~1.0	546-620
13	Pipkin (P2)	1964	18-137	454-593
14	This Investigation	1968	0.395-137	454-538

*Isotope studies.

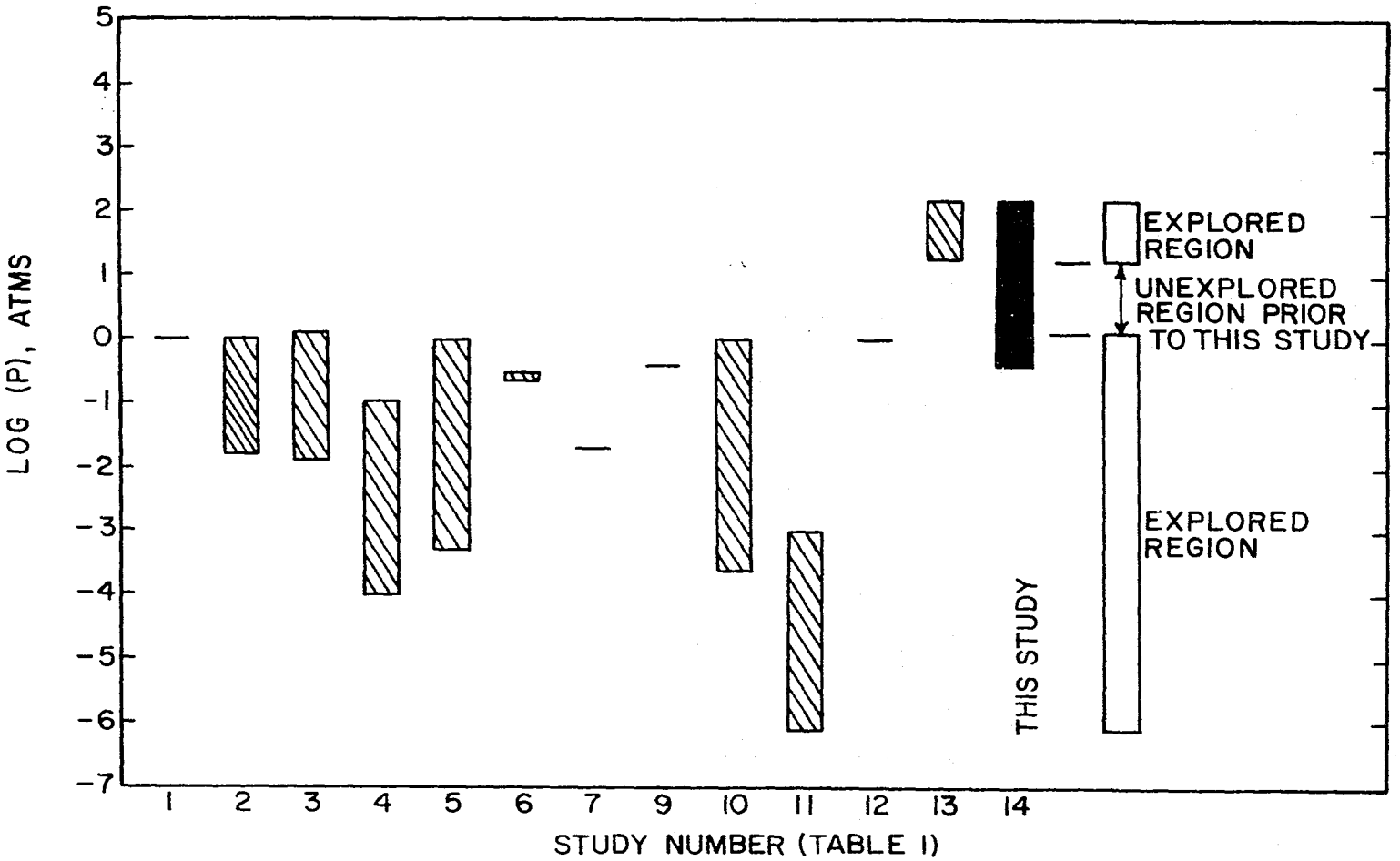


Figure 7. Pressure Ranges.

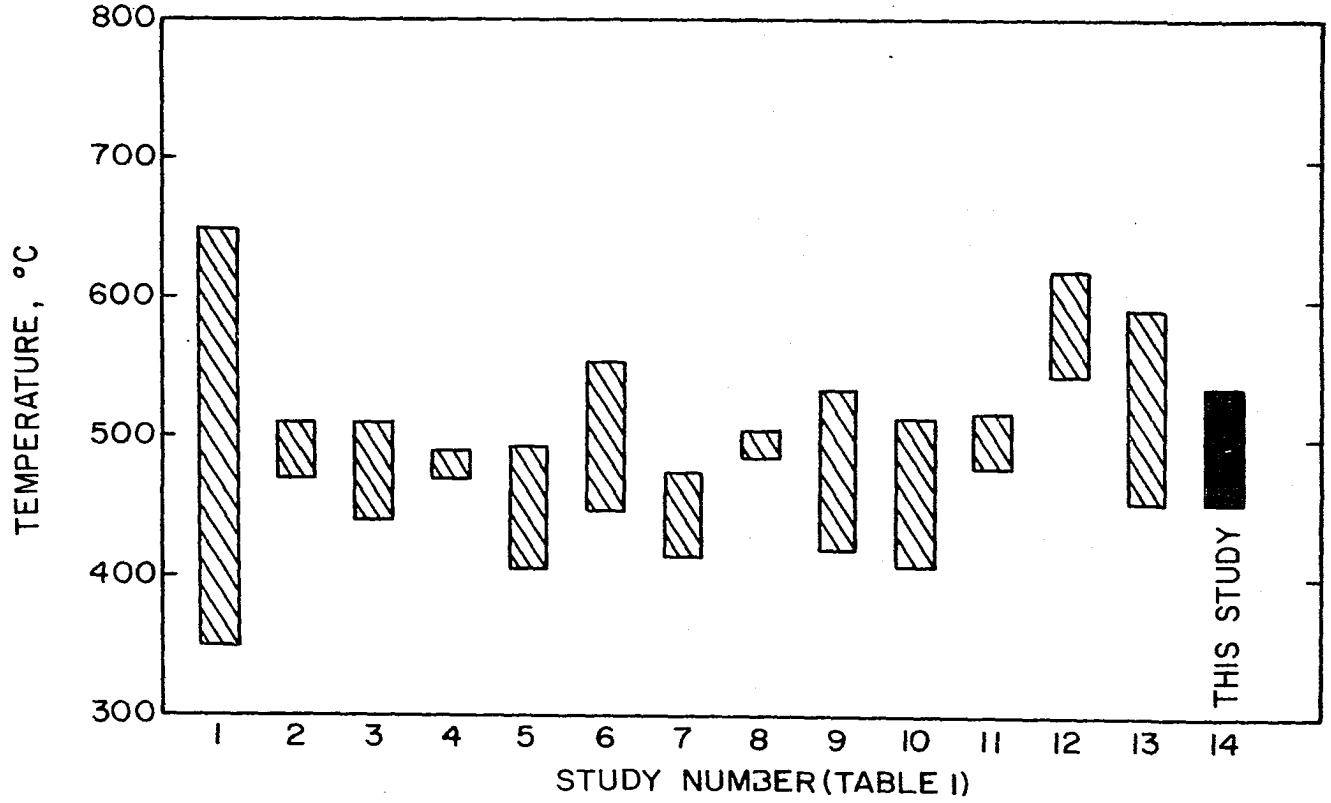


Figure 8. Temperature Ranges.

Types of Apparatus

The majority of cyclopropane thermal isomerization studies have been conducted in batch type apparatus constructed of Pyrex glass. Flow reactors have been used in only three instances; in the early work of Trautz and Winkler, in the recent work of Davis and Scott, and in the most recent work of Pipkin. As previously mentioned, the work of Trautz and Winkler was criticized because of their failure to use a reaction preheater.

Flow reactors were not used extensively by early investigators because their flow dynamics were not well understood. Many investigators employed reactors of low length to diameter ratios with small diameter inlet and outlet connections. This arrangement is favorable to channeling, thus producing erroneous residence times. In many instances, plug flow has been erroneously assumed. The plug flow assumption is valid for the studies of Davis and Scott and Pipkin. In Appendix B the effect of radial and axial diffusion is investigated and their anticipated effect on the residence time noted.

All batch thermal isomerization studies have been conducted in glass vessels of some type. Pyrex glass has been used in most cases; however, silica glass and quartz have been used in some studies. Chambers and Kistiakowsky and Davis and Scott have demonstrated that the reaction is homogeneous in Pyrex glass. Surface effects were shown

to be absent upon addition of Pyrex packing to the reactor in each case.

Gold was introduced as a suitable reactor material by Pipkin. His reactor consisted of a gold tube (or lining) mechanically bonded to an outer stainless steel tube. This arrangement produced a non-catalytic inner surface and a strong outer binding. Since at the temperatures needed to produce significant cyclopropane isomerization (500°C), glass reactors are not usable above atmospheric pressure, Pipkin's reactor design opened a new area for the isomerization study.

CHAPTER IV

DESCRIPTION OF EXPERIMENTAL APPARATUS

All of the previous studies of the thermal isomerization of cyclopropane, with the exceptions of the early work of Trautz and Winkler (T1) and the most recent investigations of Davis and Scott (D2) and Pipkin (P2), have been conducted in batch reaction systems. Only in the study made by Pipkin (P2) have materials other than glass or quartz been used successfully for the reactor. Flow systems fell into early disfavor due to erroneous assumptions concerning plug flow and certain "streaming" phenomena which occur at reduced pressures. However, the work of Davis and Scott demonstrated the usefulness of a continuous flow system. Pipkin's study demonstrated the facility of a flow system for studying kinetics at elevated pressures; it also showed that gold is noncatalytic to the thermal reaction of cyclopropane.

In this investigation, the thermal isomerization of cyclopropane to propylene was accomplished with the equipment indicated in the process flow diagram of Figure 9.

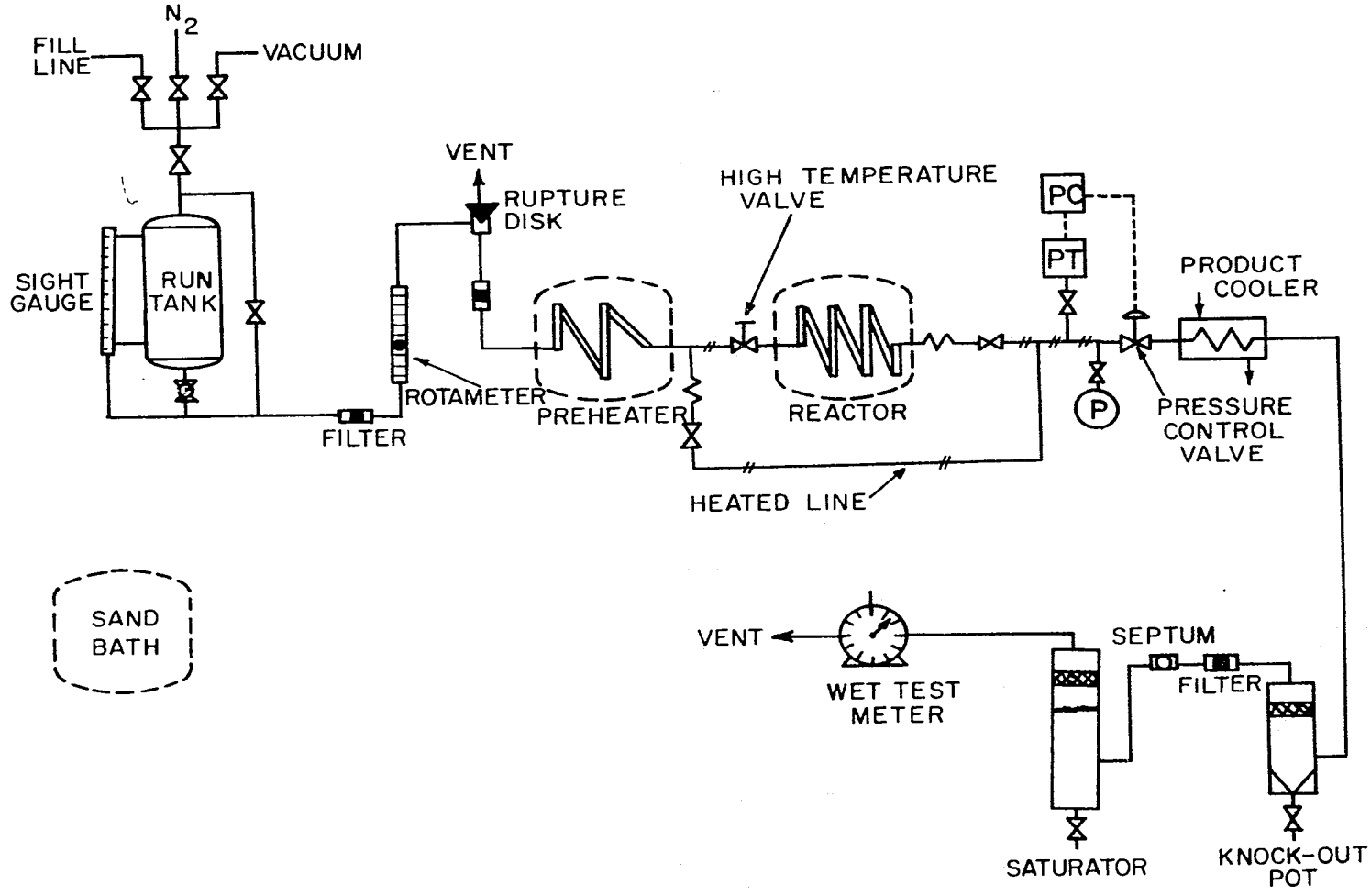


Figure 9. Simplified Flow Diagram.

The process involved flowing pure cyclopropane from storage to a gold lined preheater, and then to a gold lined tubular reactor. Both preheater and reactor were immersed in a constant temperature bath of fluidized sand. Product gases were throttled through a pressure control valve into a product cooler, followed by a knock-out pot, and gas measuring system. For further discussion, the equipment may be conveniently divided into four sections: (1) feed system, (2) preheater and reactor system, (3) product system and (4) auxillaries. The analytical equipment used to analyze the reactants and products is discussed in Chapter VI.

Feed System

The main components of the feed system were the cyclopropane storage drum, nitrogen pressurizing system, run tank and calibrated sight glass, flow rotameters, and flow control valve. Figure 10 shows a more detailed view of the feed system.

The storage drum was constructed from a 142.2 cm (56-inch) length of 20.3 cm (8-inch), Schedule 80, carbon steel pipe and two 20.3 cm (8-inch), Schedule 40, carbon steel pipe caps. Capacity of the storage tank was approximately 82.3 liters. Due to the potential hazards of storing liquefied hydrocarbon gases indoors and the high cost of cyclopropane ($10.50 per liquid liter), several precautions were taken to insure leak-free service from the storage tank

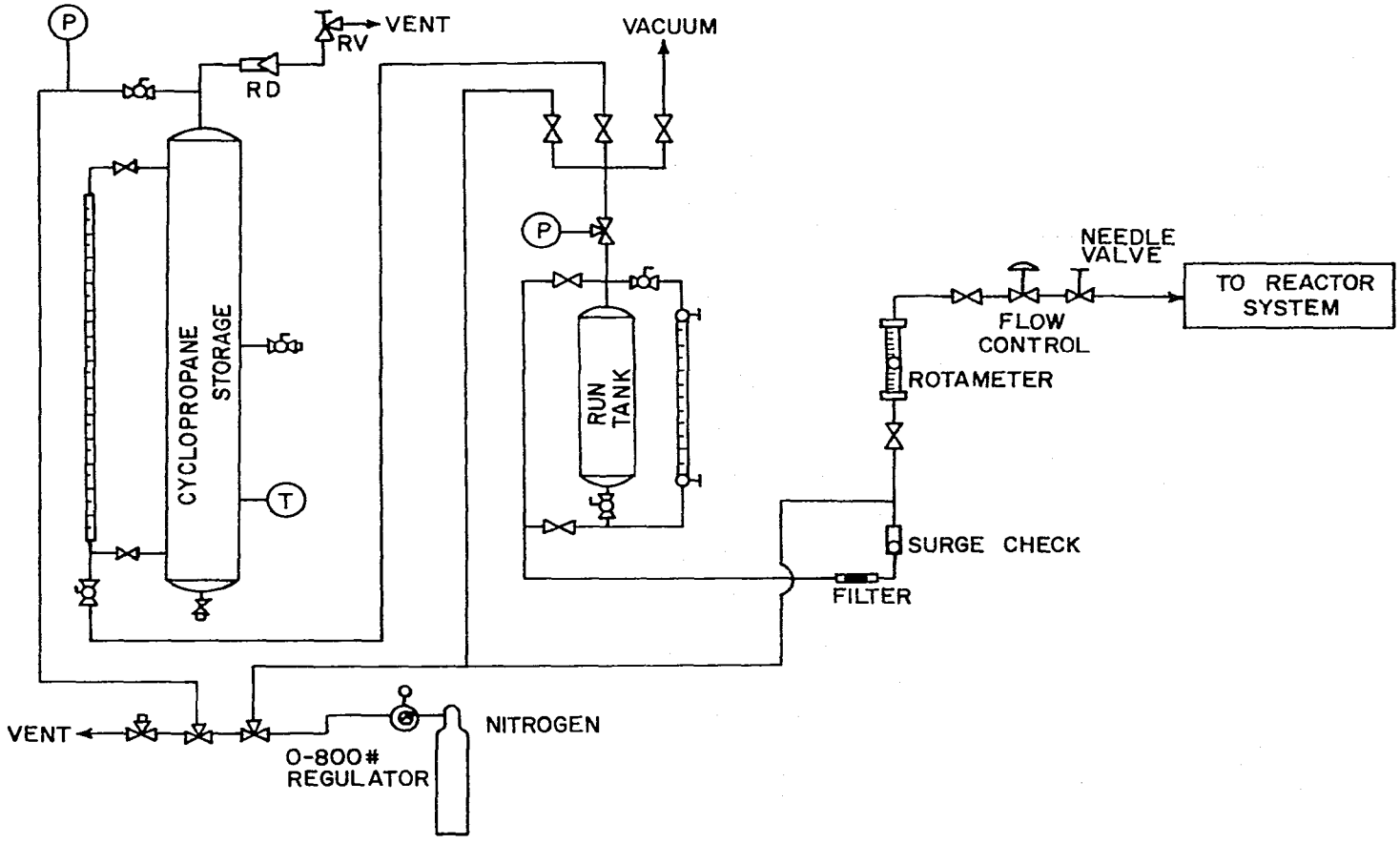


Figure 10. Flow Diagram of Feed System.

and connecting piping. First, all threaded connections were made with teflon as the thread sealant. Second, all ball valves connected to the storage drum had the Underwriter's Laboratory approval for liquefied hydrocarbon gas service. Third, relief protection was provided by a rupture disk and relief valve in series, with the former on the drum side. The rupture disk-relief valve system was used because relief valves are seldom leak-free, and one would not want to risk loosing a complete charge of cyclopropane when using a rupture disk alone. Both the rupture disk and relief valve were set to relieve at 21.4 atmospheres (300 PSIG). Normal storage pressure was 13.6 atms, 6.8 atms due to the vapor pressure of cyclopropane and 6.8 atms from nitrogen pressurization. The storage tank was also equipped with a pressure gauge, sight glass and thermometer.

The run tank was constructed from a 66 cm (26-inch) length of 10.2 cm (nominal 4-inch ID), Schedule 40, 304 stainless steel pipe and two 10.2 cm (nominal 4-inch ID), Schedule 40, 304 stainless steel end caps. Capacity of the run tank was slightly over 7.48 liters liquid. The run tank was equipped with a Jerguson sight glass, type R-20. To provide protection in the event of guage glass failure, the sight glass was equipped with gauge valves which contained ball check valves functioning on the excess surge valve principle. Calibration of the sight gauge revealed an average internal

volume of 2.839 ml per cm of length. The run tank was hydrostatically tested to 171 atms (2500 PSIG) before use.

Cyclopropane flowed, either under nitrogen pressure or its own vapor pressure, from the run tank, through a sintered metal filter, surge check valve, flow rotameter and flow control valves to the preheater and reactor section. The flow rotameter, a Fischer and Porter Model 10A1700 with Tube size 02, was used to indicate flow continuity during a run. As installed, the rotameter had a safe working pressure of 28.9 atms (410 PSIG). A Brooks Model 8800, constant differential flow controller was used in series with a Nupro Model "M" needle valve to control cyclopropane flow rates. For runs above 29 atms the rotameter and flow controller were bypassed. All connecting lines used in the feed system were either 6.35 mm OD by 3.18 mm ID or 3.18 mm OD by 1.59 mm ID, type 304 stainless steel tubing. Connections were made with Ermeto fittings.

Preheater and Reactor Section

Cyclopropane from the feed system passed thru a ball check valve, rupture disk and sintered metal filter before entering the preheater. Figure 11 show a more detailed view of the preheater and reactor section.

Originally, the preheater was constructed from a 6.35 mm OD by 3.18 mm ID, type 316L stainless steel tube of 457 cm length. This tube was lined with a 0.76 mm thickness

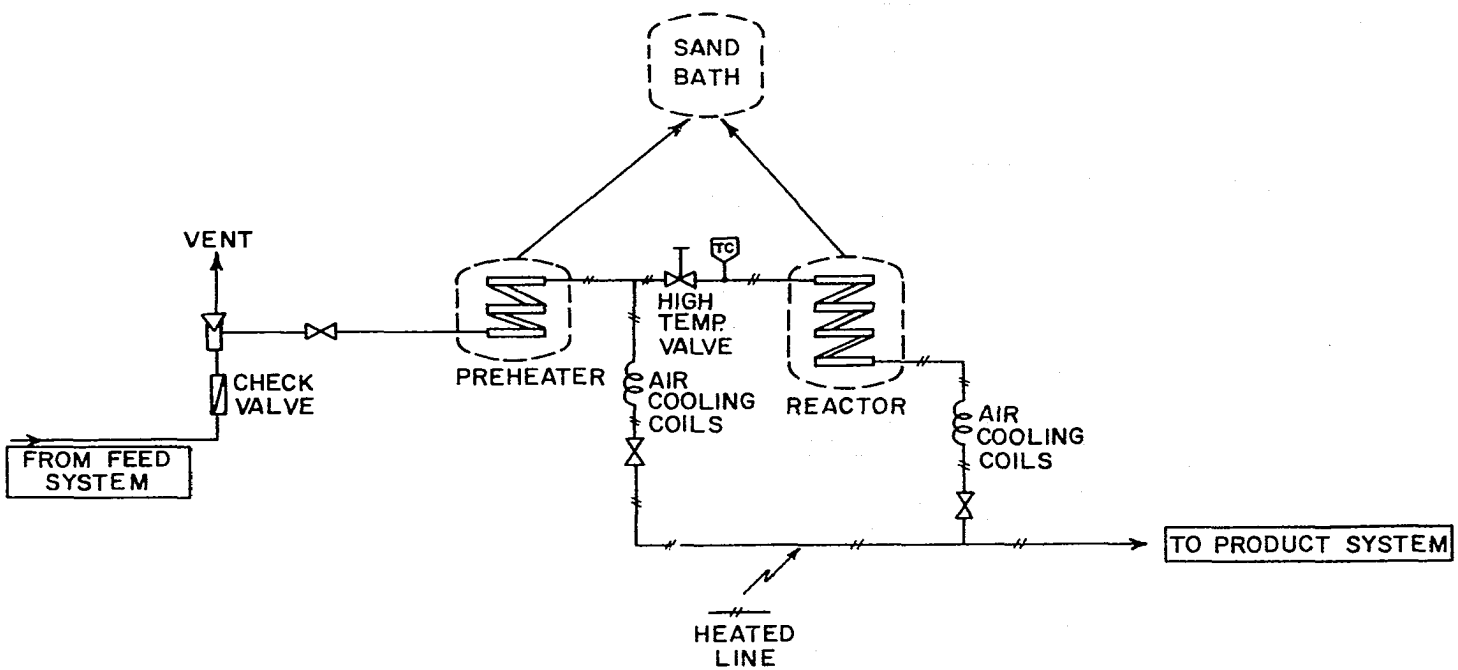


Figure 11. Flow Diagram of Preheater and Reactor System.

of gold, leaving an internal diameter of 1.75 mm. All connecting tubing which carried heated gases was constructed similarly. After approximately half of the runs had been completed, the gold in the preheater tubing "necked" at several positions in the tube; subsequently a new preheater, constructed from a 3.18 mm OD by 1.59 mm ID by 457 cm length of type 316 stainless tubing, was installed for the remainder of the runs. The preheater was immersed in a constant temperature bath of fluidized sand, which will be discussed shortly.

After passing through the preheater, the reactant gases could pass into the reactor or could bypass the reactor in order to obtain preheater conversion levels. All tubing, connecting preheater to reactor and lying outside the constant temperature bath, was kept at reaction temperature by the use of Nichrome heating wires embedded in the tubing insulation. The outside tubing temperature was continuously monitored from a chromel-alumel thermocouple imbedded between tubing and insulation.

The reactor was constructed from a 1.43 cm (9/16 inch) OD by 0.95 cm (3/8 inch) ID by 487.7 cm (16 feet) length of type 316L stainless steel tubing. This tubing and the original preheater tubing were lined with a 0.76 mm thickness of gold by Engelhard Industries, Inc. The lining was accomplished by first inserting a cold gold sleeve into straight lengths

of the tubing and then by pulling a "torpedo" thru the gold to press it firmly onto the stainless steel. As lined, the preheater, reactor and connecting tubing contained 3.33 kilograms of gold.

Coiling of the reactor tubing was accomplished on a lathe, using a 15.2 cm (6 inch) pipe as a spool and an improvised wiper die. A uniform coil spacing was obtained by welding an unlined 1.91 cm OD tube to the spool with a uniform spacing between coils. The lined tubing was then wound on the spool using the welded tubing as a guide. After expanding, the final coil diameter was 19.1 cm (7.5 inches).

The constant temperature bath for both preheater and reactor was a fluidized sand bath designed and previously used by Pipkin (P2). Since Pipkin's discussion of the sand bath's operation is valid for this investigation, only a brief summary will be presented.

The fluidized sand bath consisted of three sections: (1) a burner section, (2) a fluidized sand section and (3) a sand disengaging section. As Pipkin explained:

"In brief, operation of the fluidized sand heating system involves heating a controlled volume of air which, upon passing through a grid-plate distributer, fluidizes a charge of sand in which the gold-lined reactor coil is immersed. The air-flue gas mixture leaving the fluidized bed then passes through a disengaging section in which all

but the smallest entrained particles of sand are removed. Control of the base heat supply for maintenance of bath temperature was accomplished by hand regulation of propane flow to the burner. Trim heat for the final control of bath temperature was supplied by a heating element immersed in the sand. Electric power to this trim heater was regulated by a temperature controller with a resistance thermometer sensing element." Details of the fluidized sand heating system are shown in Appendix D.

Air for fluidization was regulated at 2 atms by a Fisher No. 95L pressure regulator. The flow of air was controlled by hand adjustment of a standard brass globe valve.

Coupling of the reactor to the connecting tubing was accomplished using a modified 6M44C8 coupling designed by Autoclave Engineers, Inc. as shown in Figure 12. All other couplings in the reactor and preheater section were made using Ermeto fittings of the proper size. The Ermeto fittings performed extremely well during the runs. Repeated temperature cyclings from room temperature to reaction temperature (454-538°C) had no effect on the leak-free performance of the fittings. Several times during the course of the experimental work, these fittings were dismantled and remade; after each dismantling, the reaction system was hydrostatically tested for leaks at 137 atms and found leak-free.

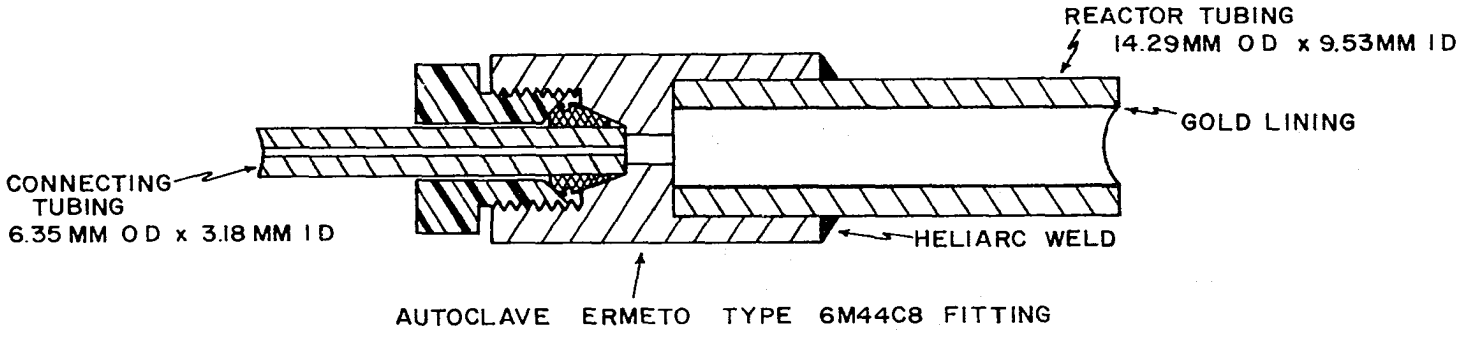


Figure 12. Reactor Coupling.

Reactor volume was determined, both before and after coiling, by filling with distilled water. The volume in both instances was found to be 239.9 ± 0.1 ml.

All lines leading from the reactor or preheater to the pressure control valve were insulated and heated to 166°C by Nichrome wire imbedded in the insulation. Product gas temperature was monitored on a Honeywell Brown recorder using an Autoclave Engineers type STC 2200 thermocouple block assembly, fitted with an iron-constantan thermocouple. Air flow was visually indicated on a Barton Model 200 pressure differenital indicator with a range of 50.8 cm of water. A 12.9 mm sharp edged orifice served as a pressure differential generator for the Barton indicator.

The basic heat load for the bed was supplied by a propane burner designed by John Zink Company. A sectional elevation of the burner is shown in Appendix D. The burner was designed for a heat output of 7,560 Kcal/hr. Commercial propane, regulated to 1.6 atms by a Matheson No. 70A pressure regulator, was used as fuel for the burner. Propane flow was regulated by adjustment of a stainless steel needle valve and indicated by a Matheson No. 622 PBV rotameter with a No. 604 tube. As a safety feature, a BASO device, activated by a shielded thermocouple in the burner flame, was used to stop propane flow to the burner in the event of a flame-out. As shown in Appendix D, the burner was ignited using a spark ignitor located inside the burner.

Final control of the temperature of the fluidized sand bed was accomplished using a Bayley, Model 96, Precision Temperature Controller modified for use to 650°C. Under actual operating conditions, the instrument was capable of sensing temperature deviations of 0.2°C. Trim heat from the controller was supplied to a 675-watt Chromalox catridge heater located in a horizontal copper well directly above the distribution plate. A Rosemount Engineering Company, Model 104 MA, platinum resistance thermometer served as the primary temperature sensor for the sand bath. Sensor resistance was measured using a Leeds and Northrup, Model 8067 Mueller Bridge and Hewlett Packard, Model 419 A, electronic null detector. Two chromel-alumel thermocouples in conjunction with a Leeds and Northrup Micromax Recorder were used to monitor the sand bath's temperature continuously. One of these thermocouples, a Conax WTG-24-B2 Safetywell Assembly, was located near the top of the fluidized sand and extended approximately 20.3 cm into the bath. The other thermocouple was placed in a retractable well above the fluidizing section, and from this position, it could be used to traverse the entire sand-filled portion of the bath. Switching was provided so that either thermocouple could more precisely read on a Honeywell, Model 2745 potentiometer.

Product Section

Reactor pressure was regulated by throttling the product gases with a Research Controls, ¼-inch, 304 stainless steel, diaphram-operated, control valve with P2, P4 or L trim as required. Control air for the valve was supplied by a Bristol, Series 650, Metagraphic pressure transmitter and Foxboro M-58 Consotrol pressure controller.

Reactor pressure was indicated on either a 7.8, 35, 70, or 140 atmospheres Heise pressure gauge. Scale divisions were respectively: 0.007, 0.07, 0.14, 0.14 atms. All gauges were dead weight tested before use.

Product gases from the pressure control valve passed to a product cooler where cooling was accomplished by counter-current flow of chilled water. The cooling coil was constructed from 3.35 meters of 6.35 mm stainless steel tubing. Following the cooler was a copper knock-out pot designed to trap any liquid products of the reaction. The knock-out pot was constructed from a 36 cm length of 2.54 cm diameter copper pipe with a 2.54 cm thick brass wool demister located at the top of the receiver.

Gases from the knock-out pot passed thru a sintered metal filter before entering the product sampling system. As shown in Figure 13, products could be sampled by syringe and needle thru a septum or collected in sample bottles for later analysis. Following the sampling system was a gas

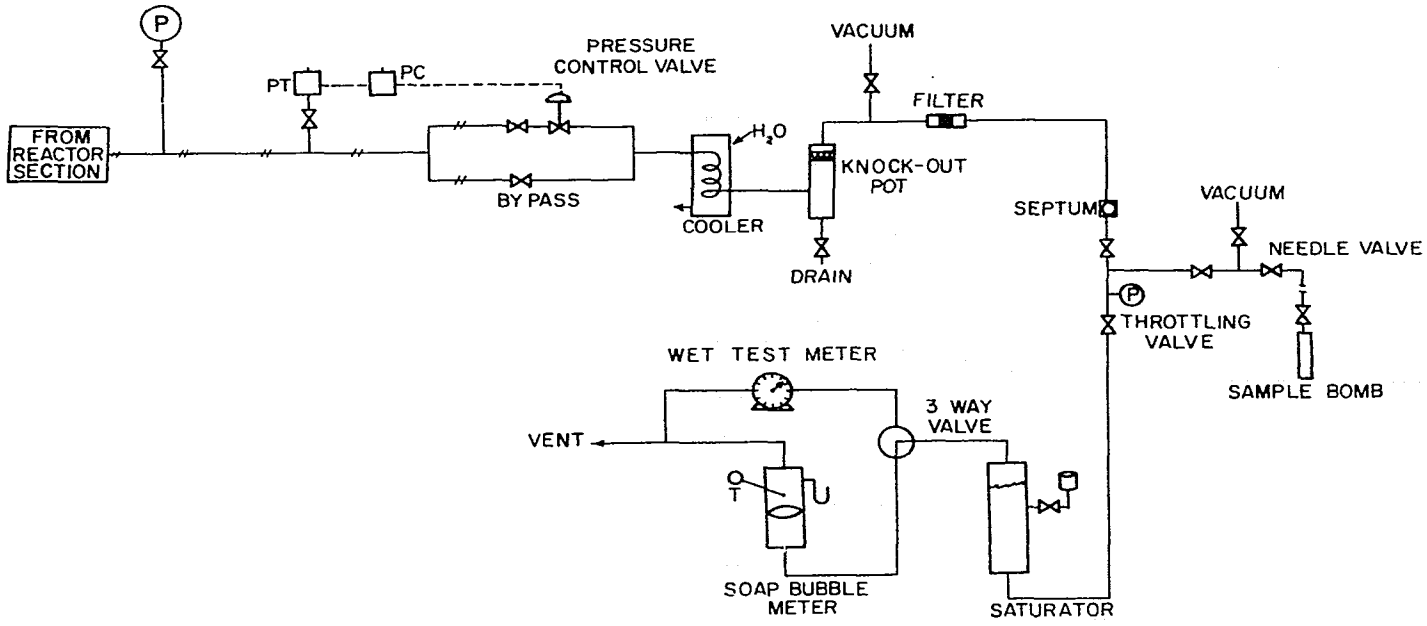


Figure 13. Flow Diagram of Product System.

saturator constructed of clear plastic. Final measurement of product flow rates could be obtained using either a Precision Scientific, Model 3110-12, wet test meter or a soap bubble meter of the author's design.

Auxiliaries

The chilled water system used to provide cooling water for the product cooler consisted of a Copeland Model E75C refrigeration unit, a small Eastern circulating pump and a 114-liter chilled water reservoir. The chilled water reservoir was insulated with fiberglass. Water was circulated by the Eastern pump thru Tygon tubing to the product cooler and back to the resevoir.

The run tank, sand bath and most of the connecting tubing were housed in a high pressure cell constructed of 6.35 mm thick, cold-rolled steel. Further safety precautions included a spray nozzle located over the equipment and an explosion proof exhaust fan. The spray nozzle was connected thru a solenoid valve to a water line. Activation of the solenoid valve was accomplished by a switch located on the front of the cell. The exhaust fan prevented the accumulation of explosive vapors in the cell.

A Welch, Duo Seal, Model 1400 Vacuum pump served as an evacuation medium for the reaction system and sampling system. High pressure nitrogen for purging and pressurization

was provided by "K" bottles of nitrogen connected to the system by way of a Victor Model LR17BSS pressure regulator (range: 1.7-55 atms) or a Victor Model GD-710 pressure regulator (range: 28-408 atms).

CHAPTER V

EXPERIMENTAL PROCEDURE

The experimental procedure chapter is divided into six sections: (1) preliminary procedures, (2) startup procedure, (3) run procedure, (4) shutdown procedure, (5) calibrations and (6) problems encountered.

Preliminary Procedures

Due to the valuable "hindsight" obtained from the work done by Pipkin (P2) on a similar apparatus, the preliminary procedure consisted mainly of determining workable startup, run and shutdown routines. Approximate control settings for the various pressure and temperature control instruments were also obtained during these "dry" runs.

The "dry" runs were conducted with technical grade propane in the system. It was felt that the similarity in properties between propane and cyclopropane would allow operating knowledge gained in the dry runs to be transferred directly to data runs with cyclopropane. Only five "dry" runs were required before sufficient information for the operation of a data run was obtained. In general, these "dry" runs proceeded very smoothly and predictably.

Startup Procedure

By far the most time consuming procedure during a startup was the heating of the fluidized sand bed. Approximately 7 hours were required to bring the sand bath to a stable condition at the highest temperature level (538°C). Thus, the first item of the startup procedure was ignition and heat-up of the fluidized sand bath.

The first step in the sand bath ignition involved initiation of air flow through the sand bed. Air flow rate was regulated at 283 std liters/min [15.6°C (60°F), 1 atms] and the propane flow rate adjusted to a reading of 5 on the rotameter glass float (4.9 g/min). The burner was then ignited using the enclosed ignition system as shown in Appendix D. A BASO device prevented propane flow in the event of a flame failure. The circuit diagram of the BASO device is shown in Appendix D. After successful ignition, the propane and air flow rates were maintained at their ignition levels for 15 to 30 minutes. The air rate was then increased to 419 std liters/min, and the propane rate was increased to its maximum value of 11 on the rotameter (10.9 g/min). Propane feed was continued at this rate until the sand bath temperature came within 10°C of the required run temperature; then the propane rate was decreased to an intermediate point between the maximum rate and the estimated base load rate. When the bath temperature reached the required run

temperature, the propane rate was reduced to the base load which would allow the Bayley temperature controller to hold the run temperature. This two-step, propane-feed reduction minimized a sharp drop in bath temperature and subsequent slow temperature recovery characteristic of a one-step, propane-rate decrease. After attaining initial temperature control at the required temperature, bath temperature was closely monitored for 1 hour to insure that no transient effects were present.

During the sand bath warmup period, a slow flow of nitrogen at 4.4 atms was maintained in the reactor and pre-heater sections. This procedure served to supply a flow rate so that the pressure control valve could be placed in operation and the operation of flow meters could be observed. After the sand bath temperature reached 330°C, all product line and transfer-line heaters were placed in operation. Powerstats were adjusted to give a transfer-line temperature within ± 8°C of the bath temperature and a product-line temperature of about 165°C. At this same time, the refrigeration unit for the chilled water system was started, as was the water circulating pump. If product samples were to be taken using the septum located in the product tubing downstream of the product cooler (see Figure 13), the chromatograph was warmed up approximately two hours before the start of a run. When samples were taken in sample bombs, the chromatograph was not warmed up, as the samples could be analyzed easily the

following day. Details of chromatograph operation can be found in Chapter VI.

Prior to initiation of a run, the cyclopropane level in the run tank was checked, and cyclopropane was transferred from the storage tank to the run tank if necessary.

Run Procedure

When temperature control was established in the sand bath and all auxiliary systems were functioning correctly, run procedures were initiated. First, nitrogen flow through the reaction system was discontinued, followed quickly by the start of a flow of cyclopropane. Depending on the pressure levels to be used during a run, cyclopropane was available from the run tank in either liquid or gaseous form. If runs were to be made at the high pressure level, 4.4 to 137 atms (50-2000 PSIG), nitrogen pressure, 1.7 or more atms in excess of the run pressure, was placed on the run tank. Cyclopropane was then moved in a liquid form through the feed system to the preheater and reactor. For the low pressure runs, 0.395 to 4.4 atms, pure gaseous cyclopropane at its vapor pressure (6.8 atms at 25°C) was reduced to 5.7 atms, by a regulator and sent to the feed system. In either case, cyclopropane flow was maintained at a high rate for 30 minutes to insure a complete purging of the system. Cyclopropane flow was then reduced to the required run rate.

After establishing the required flow rate at each pressure level, from 15 to 30 minutes, depending on the system flow rate, were allowed for steady state to be established. The lower flow rates were allowed the longest times to approach steady state. At each pressure level data was recorded for at least three observation periods. For each observation reactor pressure, temperature and flow rate were recorded. A sample run data sheet has been included in Appendix C. If product samples were taken at the septum port, a chromatographic analysis was also obtained for each observation period. When samples were taken by use of a sample bomb, the sample was taken prior to the last observation period. At least three chromatograms were prepared from each sample bomb and averaged to obtain the bomb composition. Flow rates and reactor pressure permitting, a material balance was made for each pressure level. To obtain a material balance, the run tank sight glass was isolated from the run tank, and the level change was observed for a specified number of revolutions of the wet test meter. Total inlet and outlet flows could then be calculated and compared. Material balance results are included in Appendix E.

Since both reactor inlet and outlet concentrations are needed to obtain the specific rate constant (see "Method of Data Analysis," Chapter VII), preheater outlet (reactor inlet) concentrations were obtained in the following manner.

At the end of a series of runs at various pressures, the run tank was valved off from the feed system, and the entire reaction train pressure was decreased to 4.4 atms. This procedure was accomplished by opening the pressure control bypass valve or the emergency vent valve. Nitrogen was then admitted to the reaction train at 4.4 atms, and a strong flow was maintained for 15 minutes. This procedure served to purge effectively all cyclopropane from the reactor. Nitrogen pressure was increased to the maximum run pressure, and the reactor was isolated (valved off) from the reaction train by closing the reactor inlet and outlet block valves. The preheater outlet valve was opened, and a run procedure was started exactly as previously described. Various reaction pressures and flow rates were reproduced with the reactor bypassed. The preheater outlet concentrations were obtained by use of the septum or sample bomb facilities.

Due to the large heat capacity of the sand bed, several hours were required to change from one temperature to another. Therefore, the unit was brought on stream each day for only one temperature of operation. Pressure levels were more easily changed, so each day's operation consisted of a run at one temperature level and several pressure levels. If no difficulties were encountered, four or five data points, i.e. pressure levels, could be obtained during each run.

At the end of a run at a given pressure, the knock-out pot drain was opened to check for liquid product.

During periods of operation, the barricaded cell was entered only to perform the necessary valving operations.

Shutdown Procedure

The first step in the shutdown was to discontinue the flow of cyclopropane from the run tank to the feed system. Then the pressure control bypass valve was opened and the system relieved of pressure until the pressure was below 4.4 atms. Nitrogen, at approximately 4.4 atms, was then admitted to the feed system at a high flow rate. Nitrogen flow was continued at this rate for at least 15 minutes in order to purge the preheater and connecting tubing of cyclopropane. Directly following the establishment of nitrogen flow to the feed system, the flow of propane to the sand bath burner was stopped. Air flow to the bath was continued at the normal run rate in order to aid the cooling process. The reactor block valves were then opened and nitrogen flow directed through the entire reaction system. Also during this period, the transfer line and product line heaters were shut off and these lines were allowed to cool.

When the reaction system was sufficiently purged of cyclopropane, the nitrogen pressure in the system was increased to 28.2 atms simultaneously with a decrease in the nitrogen flow. A low flow of nitrogen was continued until

the sand bath temperature decreased to 200°C. The preheater and reactor were then blocked in at 28.2 atms, and the air flow to the sand bed was stopped. The valve on the sand collection pan was opened to a container provided to catch the small amount of sand that flowed through the grid plate. The final two steps in the shutdown procedure were to shut off the refrigeration unit and circulating pump and to bleed the excess nitrogen pressure from the run tank.

Calibrations

Temperature of the fluidized sand bed which housed both reactor and preheater was measured, excepting runs R4 through R9, with a calibrated platinum resistance thermometer. In actuality, runs R1 to R4 were made using a platinum resistance thermometer. However, this thermometer was inadvertantly ruined after run R3. A calibrated chromel-alumel thermocouple was used in the interim period while the resistance thermometer was being replaced. Runs R10-R24 were conducted using the new thermometer.

Both resistance thermometers used in this study were obtained from Rosemount Engineering Company and carried the nominal model number of 104MA. The thermometers were calibrated by Rosemont per their schedule GF (0 to 1220°F) and were guaranteed to represent the international temperature scale to $\pm$ 0.3°C ($\pm$ 0.5°F) within this range. The thermometers

were also guaranteed to retain their calibration for a period of at least one year. The resistance-temperature relations of both sensors were fitted to a cubic polynomial to within 0.001°C from 450 to 660°C. Denoting the first thermometer by 1 and the second by 2 the following relation was found:

$$T_1(°C) = -217.978 + 12.4348(R) + 0.004228(R^2) + 0.0002011(R^3).$$

$$T_2(°C) = -218.788 + 12.4370(R) + 0.002331(R^2) + 0.0002237(R^3)$$

where: R = resistance, ohms

Thermometer resistances were measured using a modified model 8067, Leeds and Northrup Mueller Bridge. The modification consisted of adding a nominal resistance of 40 ohms to the bridge so that thermometer resistances could be measured in the high temperature range (65 ohms at 620°C). The auxillary resistance was a Leeds and Northrup, Model 191445, Wheatstone Bridge adjusted to approximately 40 ohms. The Mueller Bridge was calibrated per Leeds and Northrup instructions using a calibrated and temperature compensated, 10-ohm, standard resistance (L & N Model 4025B). Correction factors obtained from five separate calibrations are shown in Table 2. The effect of temperature on the bridge was found to be represented by the relation:

TABLE 2

CORRECTIONS FOR MUELLER BRIDGE @ 25°C

Indicated Resistance (ohms)	Actual Resistance (ohms)	Remarks
10.0	10.0053	10 Ω tap
20.0	20.0107	20 Ω tap
30.0	30.0165	30 Ω tap
40.0	40.0219	40 Ω tap
1.0	1.0004	
2.0	2.0008	
3.0	3.0013	
4.0	4.0017	
5.0	5.0021	
6.0	6.0024	
7.0	7.0028	
8.0	8.0032	
9.0	9.0036	
10.0	10.0041	$\underline{\overline{X}}$ setting
0.1	0.1001	
0.2	0.2002	
0.3	0.3002	
0.4	0.4003	
0.5	0.5004	
0.6	0.6004	
0.7	0.7004	
0.8	0.8004	
0.9	0.9004	
1.0	1.0004	0.$\underline{\overline{X}}$ setting

$$\frac{R_{ACTUAL}}{R_{OBS}} = 0.99933 + 3.607 \times 10^{-5} T_B - 4.30 \times 10^{-7} T_B^2$$

where: R_{ACTUAL} = actual resistance, ohms

R_{OBS} = observed resistance, ohms

T_B = bridge temperature, °C

The actual calibration curve is shown in Figure 14. After the Mueller Bridge was calibrated, the auxiliary resistance was also calibrated using the Mueller Bridge. The temperature-resistance relationship of the auxiliary resistance was found to be:

$$R_{ACTUAL} = 40.0421 + 1.834 \times 10^{-4} T_B$$

Null points for the resistance temperature measurements were indicated on a Hewlett-Packard, Model 419A, null detector. With a 4-milliampere current flowing to the resistance thermometer, a 0.001 ohm change in sensor resistance could be observed using the 100 microvolt range of the null detector (maximum sensitivity of null detector was 3 microvolts). At the highest temperature level of this study, 538°C (1000°F), a 0.001 ohm change corresponded to a 0.01°C change in temperature. Thus, the sensitivity of temperature measurement, when using the resistance thermometer, was much greater

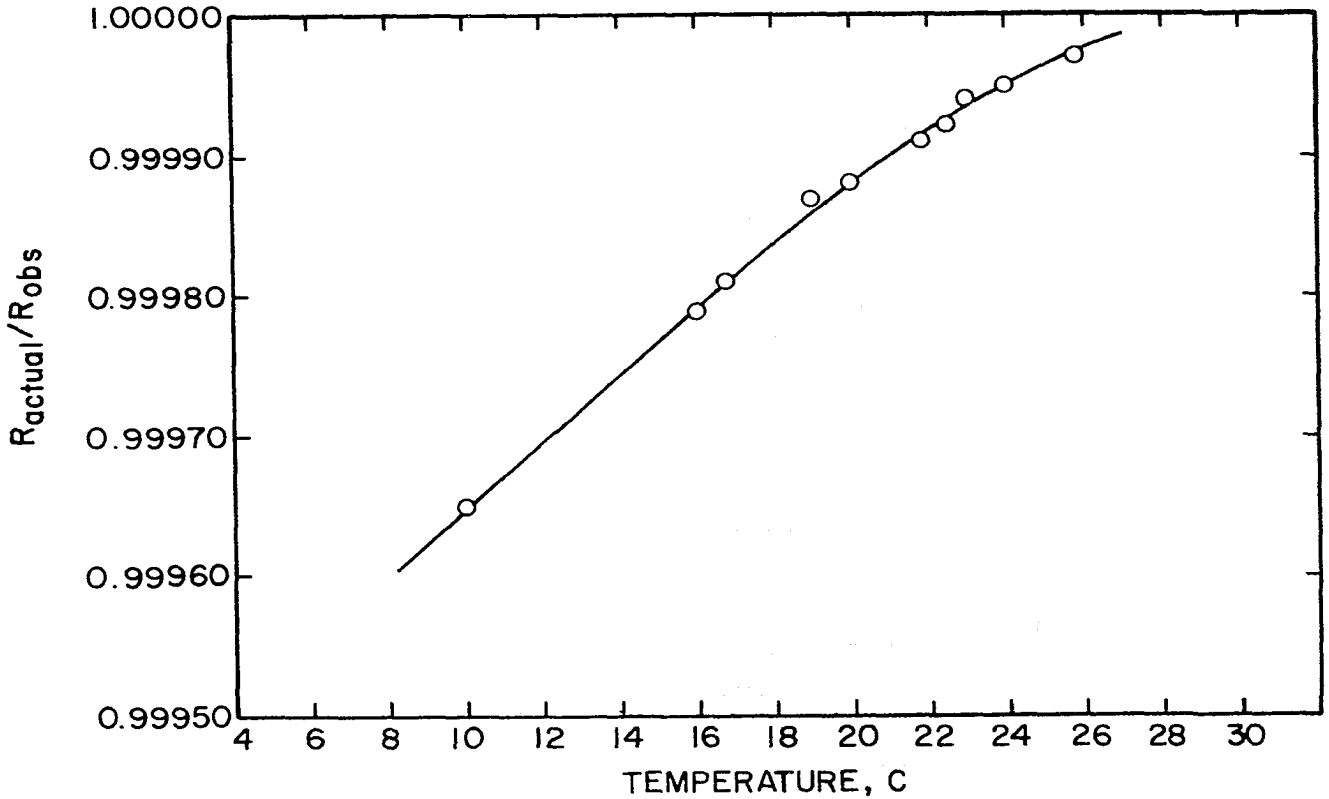


Figure 14. Effect of Temperature on Mueller Bridge Resistance.

than the calibration of the thermometer. The maximum error expected in the bath temperature, when using the resistance thermometer, was no greater than 0.3°C.

As previously mentioned, the temperature sensor used for runs R4 through R9 was a chromel-alumel thermocouple. The temperature-emf relationship of this thermocouple had previously been investigated using a calibrated platinum-platinum rhodium thermocouple as a standard and a Leeds and Northrup, Model A2 calibration furnace as the constant temperature source. These data were combined with data obtained from the "in place" calibration of the thermocouple to yield the relation:

$$T(°C) = 17.44 + 23.277 \times MV$$

where: MV = emf of the thermocouple, millivolts

Random checks of this correlation with temperatures measured by the second resistance thermometer showed deviations between the two of less than 0.3°C.

The emf generated by the chromel-alumel thermocouple was measured on a Honeywell, Model 2745, Rubicon potentiometer. Comparison of this instrument with a Leeds and Northrup K-3 potentiometer indicated that readings were accurate to $\pm$ 0.003 millivolts. A Hewlett-Packard 419A null detector served as a galvonometer for the potentiometer. Reference junction temperature was measured using a calibrated mercury

thermometer, graduated to 0.1°C. As described, thermocouple temperature measurements were felt to be accurate to within ± 0.4°C.

Stability of the sand bath temperature during a run was generally excellent. Figure 15 shows some test equipment used to record bath temperature fluctuations during several runs. Results of these tests indicated that bath temperature variations of less than ± 0.3°C occurred during a run. These results agreed well with the observed low and high temperatures measured during a run.

As previously mentioned, reactor pressure was measured using either a 7.8, 35, 70 or 140 atmospheres Heise pressure gauge.

Pressure fluctuations about the controller set point were less than 0.03 atms. Reactor pressure was measured from a tap 1.2 meters downstream of the reactor, but, at the low flow rates used, the pressure drop corrections were felt to be negligible. Generally, pressure drops through the entire system were less than 0.14 atms.

The wide range of flow rates used in this investigation, 0.5 to 155 cc/sec (gas at STP), made the use of two separate flow metering systems necessary. Flows in the range of 0.5 cc/sec to 11 cc/sec were metered with a calibrated soap bubble meter. Basically, the soap bubble meter consisted of a glass tube of uniform diameter, with suitable connections for gas inlet and outlet, temperature measurement, pressure measurement

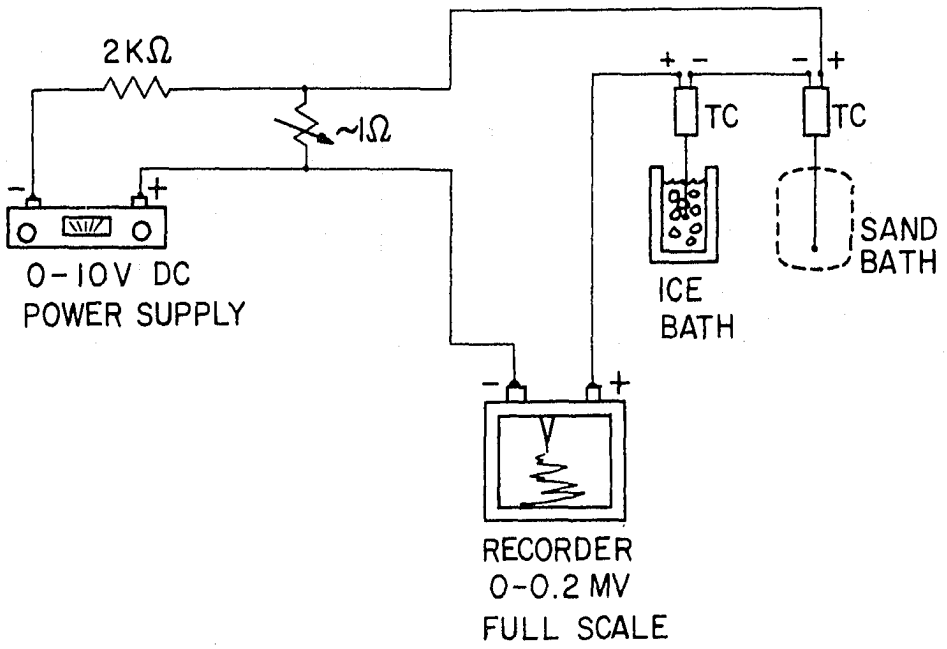


Figure 15. Equipment Used to Measure Fluctuations in Sand Bath Temperature.

and soap bubble formation. In operation, the time for a soap bubble to sweep between two graduations was measured and, with the knowledge of the volume between the graduations, the volumetric flow rate was found. Figure 16 is a schematic of the soap bubble meter. Flow rates in the range, 10 cc/sec to 155 cc/sec were measured using a Sargent Model 3110 Wet Test meter. Reported accuracy of this type meter is 0.5 percent. Several measurements were made in the region of flow rates for which both meters overlapped to determine the consistancy of the meters. The absolute average difference between the two meters was 0.63 percent.

Reactor volume was determined before and after coiling by filling the reactor with a known volume of water. Within experimental precision, the reactor volume was the same both before and after coiling, 239.9 ± 0.1 cc. Reactor length was measured before coiling and found to be 486.2 ± 0.3 cm.

Weight balance calculations were made by observing the change in level in the run tank sight gauge during a specified number of revolutions of the wet test meter. The sight gauge was calibrated and found to have an average internal volume of 2.839 ± 0.005 ml per cm of length. Pipkin's values of liquid cyclopropane density, 0.600 ± 0.006 grams/cc at 23.9°C and 0.594 ± 0.006 grams/cc at 29.8°C, were used in the material balance calculations. Considering the precision of the liquid density values, material balance calculations were felt to be accurate within ± 2 percent.

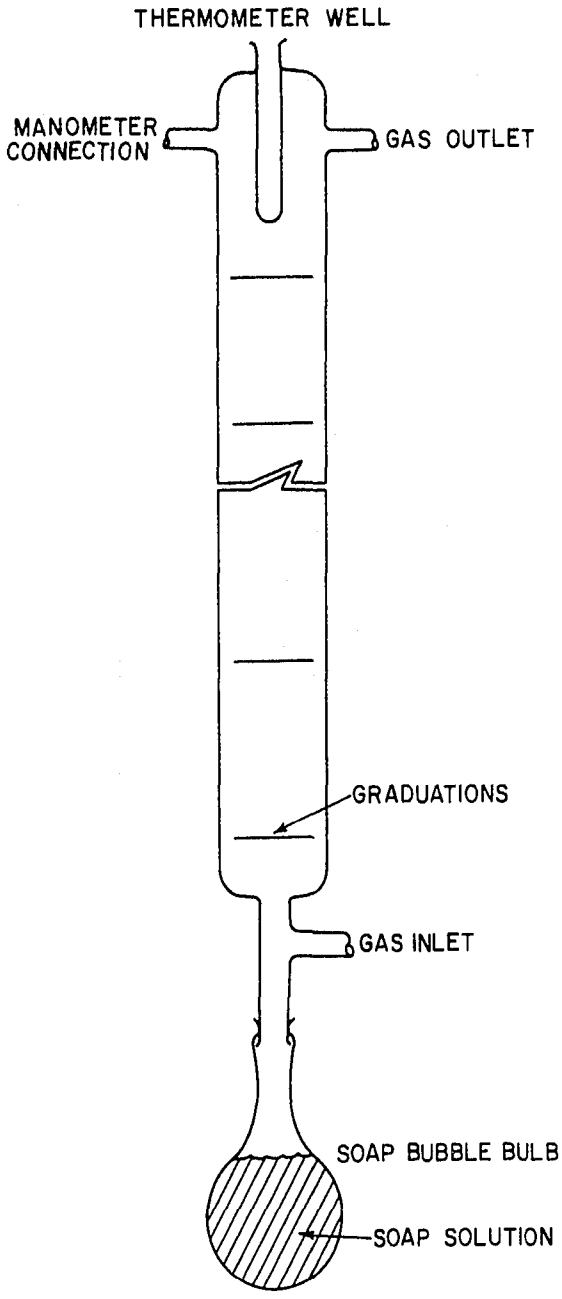


Figure 16. Soap Bubble Meter.

Problems Encountered

Aside from the lengthy period required to heat up the fluidized sand bath, data runs proceeded smoothly and with little difficulty. The most aggravating problem was the repeated plugging of the reaction preheater at the 538°C (1000°F) temperature level. This plugging was caused by a "necking" of the gold lining in the preheater at points where constriction type fittings (i.e., Ermeto fittings) were used. Since this type of plug could not be burned or blown out, the entire sand bath had to be disassembled and the preheater removed for repairs. After the third failure of this type, the gold lined preheater was replaced by an equivalent length of 3.18 mm stainless steel tubing; no further plugging occurred.

Another problem was caused by the small amount of control heat available to the sand bath. In several instances, changes in room temperature were sufficiently large to cause a shift of perhaps 1°C in the bath temperature. The control heat load, 675 watts, was not able to change the bath temperature by this amount, and adjustment of the propane fuel rate was required to restore the run temperature. This problem was not considered serious since its only consequence was to lengthen the time required for a run.

CHAPTER VI

ANALYTICAL PROCEDURE AND APPARATUS

Previous investigators of the thermal isomerization of cyclopropane have used many different methods to analyze product and reactant gases. Trautz and Winkler (T1) observed that the density at -80°C of cyclopropane-propylene mixtures was essentially additive and used this property as the basis for their analysis. Since they performed the experimental work in a flow system, the necessary quantity of gases were available for the density determination. Most subsequent investigators have conducted experimental work in batch systems and, consequently, used analytical techniques suitable for small quantities of gas. Chambers and Kistiakowsky (C1) absorbed propylene in a 3 percent aqueous neutral solution of potassium permanganate for their analysis. Other absorption techniques involved the use of mixtures of mercuric acetate and mercuric nitrate by Pritchard, Sowden and Trotman-Dickenson (P3) and a solution of mercuric sulfate in 22 percent sulfuric acid by Weston (W2).

Corner and Pease (C3) used selective catalytic hydrogenation for analysis of their samples. In their method, the

sample to be analyzed, along with hydrogen, is passed first over a mercury-poisoned nickel catalyst, which converts the propylene to propane, and then over an unpoisoned nickel catalyst which hydrogenates the cyclopropane.

Recent investigators have favored infrared spectrophotometry and gas chromatography in their analysis. Lindquist and Rollefson (L5) and Roberts (R3) reported techniques involving infrared spectrophotometry. However, most investigators have favored gas chromatography. Temperatures and columns have varied greatly among investigators. Blades (B3) chose a column of dodecyl phthalate at room temperature; Falconer, Hunter and Trotman-Dickenson (F1) used a 30.5 cm column of activated alumina followed by a 91.4 cm column of firebrick containing 20 percent of ethylene glycol saturated with silver nitrate. Kennedy and Pritchard (K3) reported a chromatographic method using a 20 percent molar $AgNO_3$/glycol on firebrick at -30°C. In the most recent investigation, Pipkin (P2) employed a 10 percent by weight loading of tricresyl phosphate on firebrick at 61.7°C.

This investigation employed chromatographic analysis using helium as the carrier gas and a 3.2 mm (1/8-inch) diameter by 244 cm long column packed with Porapack type "T." Porapack "T" was chosen because it is in an extremely effective packing for separating C_1, C_2, C_3, and higher hydrocarbons. By suitably choosing conditions, ethane-ethylene, propane-propylene or propylene-cyclopropane mixtures can be separated on a single column.

A Hewlett Packard, F and M, Model 700 gas chromatograph equipped with dual thermal conductivity detectors, automatic attenuator and linear temperature programmer was used as the analytical unit in the investigation. The chromatographic results were recorded on a Hewlett Packard Model 17503A 1-millivolt recorder. The recorder was equipped with a Disc integrator of 0.1 percent accuracy. Figure 17 is a photograph of the chromatographic equipment.

Chromatograph operating conditions were determined by trial as no separations of propylene-cyclopropane mixtures have been reported in the literature for the Porapack "T" columns. Best operating conditions were found to be:

Temperature of column = 110°C
Temperature of detector = 240°C
Flow rate of carrier gas = 10 ml/min
Attenuation = as required
Detector current = 150 MA

Using these operating conditions, a sample could be analyzed in approximately 4 minutes.

Nine cyclopropane-propylene standard samples were prepared in the following manner: (1) an evacuated cylinder of approximately 350 grams was weighed on an analytical balance to 0.01 gram, (2) The cylinder was placed in an ice bath and cyclopropane gas condensed into it, (3) the cylinder

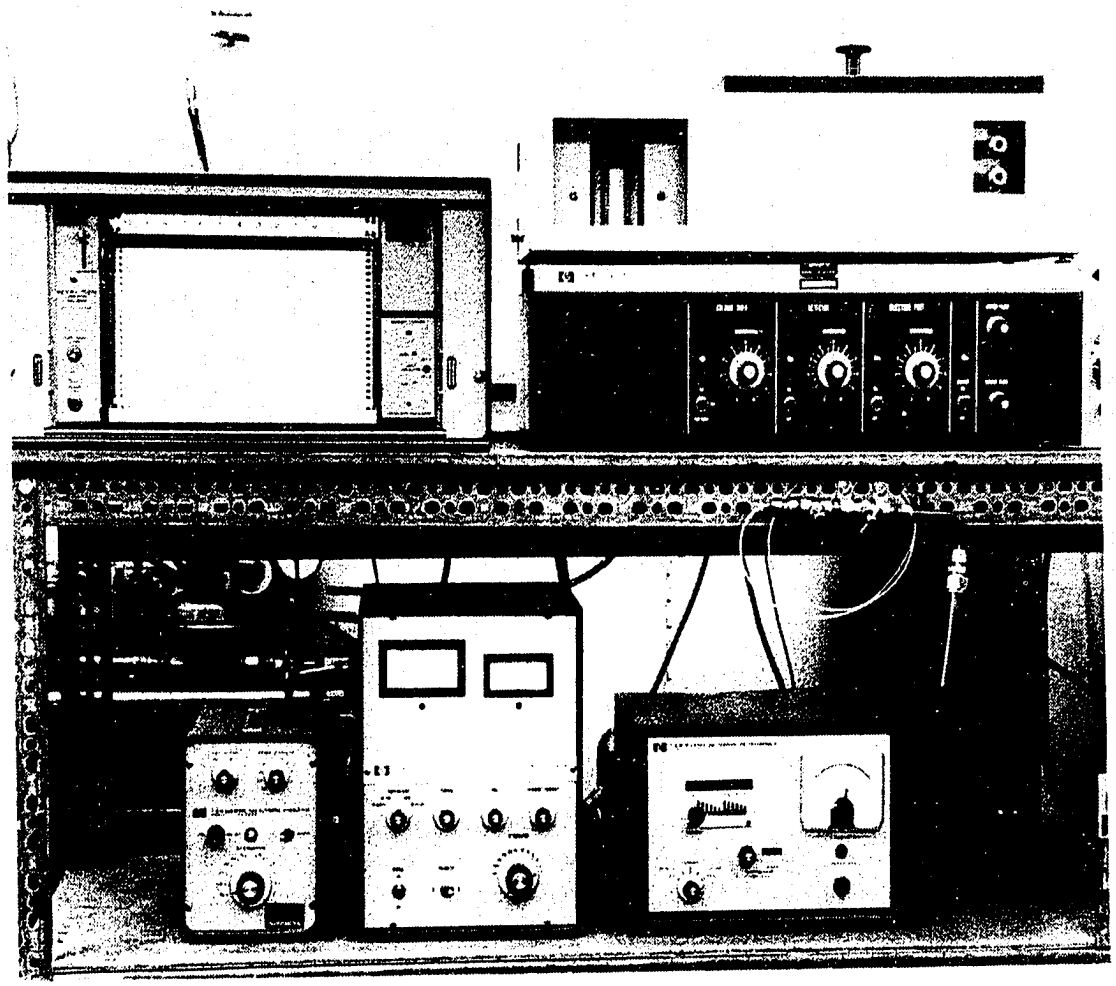
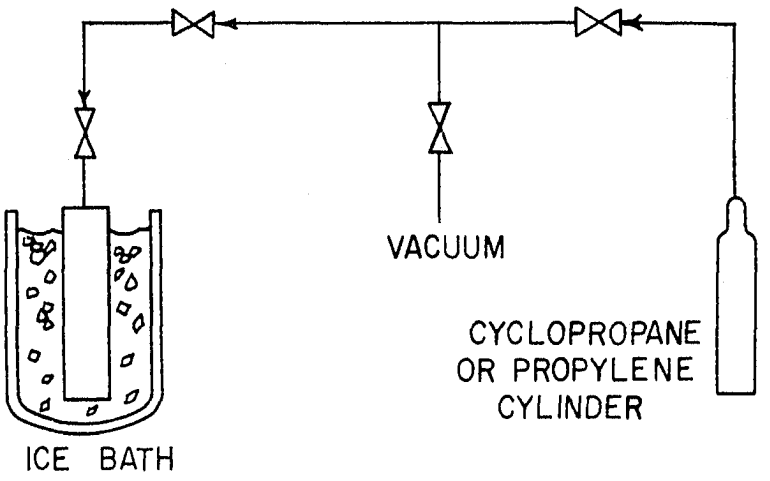


Figure 17. Photograph of Chromatograph.

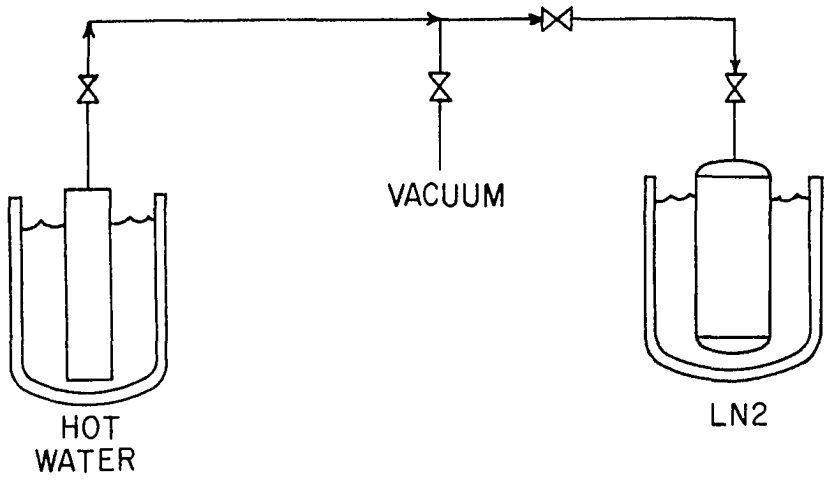
and cyclopropane were again weighed (4) the cylinder was again placed in the ice bath and propylene gas was allowed to condense into the cylinder (5) the cylinder plus cyclopropane and propylene were weighed (6) the contents of the cylinder were transferred to a bomb of 3.3 liters capacity by placing the larger bomb in a liquid nitrogen bath and distilling the contents of the cylinder into it. The complete transfer of the gases was confirmed by weighing the cylinder after the transfer. This weight always agreed to within 0.01 gram of the evacuated weight. In this manner standard samples of high accuracy could be prepared for later calibration work. Figure 18 shows the standard preparation equipment, and Figure 19 is a sample work sheet used in preparing the standards. Anesthetic grade cyclopropane from Ohio Chemical and Surgical Equipment Company and research grade propylene from Phillips Petroleum Company were used to prepare the standards. Chromatographic analysis of these materials indicated the following purities:

Cyclopropane	- 99.74	mole percent cyclopropane
	0.26	mole percent propylene
Propylene	- 99.99	mole percent propylene
	<0.01	mole percent impurities

The calibration curve determined using the nine standard samples is shown in Figure 20. Each data point on the curve is the average of at least nine chromatographic analyses taken



SAMPLE PREPARATION



SAMPLE TRANSFER

Figure 18. Standard Sample Preparation Equipment.

CHROMATOGRAPH STANDARD DATA SHEET

Date: 11-18-67

Sample No. 4

Chromatograph Bomb No. 4

1. Weight Empty Cylinder 342.58g
2. Weight Cylinder + Cyclopropane . . . . . 377.94 g
3. Weight Cylinder + Total Gases 378.22g
4. Weight Cyclopropane (2-1) 35.36g
5. Weight Total Gases (3-1) 35.64g
6. Percent Cyclopropane (4/5 x 100) 99.21
7. Percent Propylene (100.00-6) 0.79
8. Correction to Gas Percentages for Purity . . . 0.9974

Gas	Percent	Normalized
Cyclopropane	99.21	98.95
Propylene	0.79	1.05
Other	0.00	0.00

Comments:

Weight after transfer = 342.59 g

Figure 19. Standard Preparation Work Sheet.

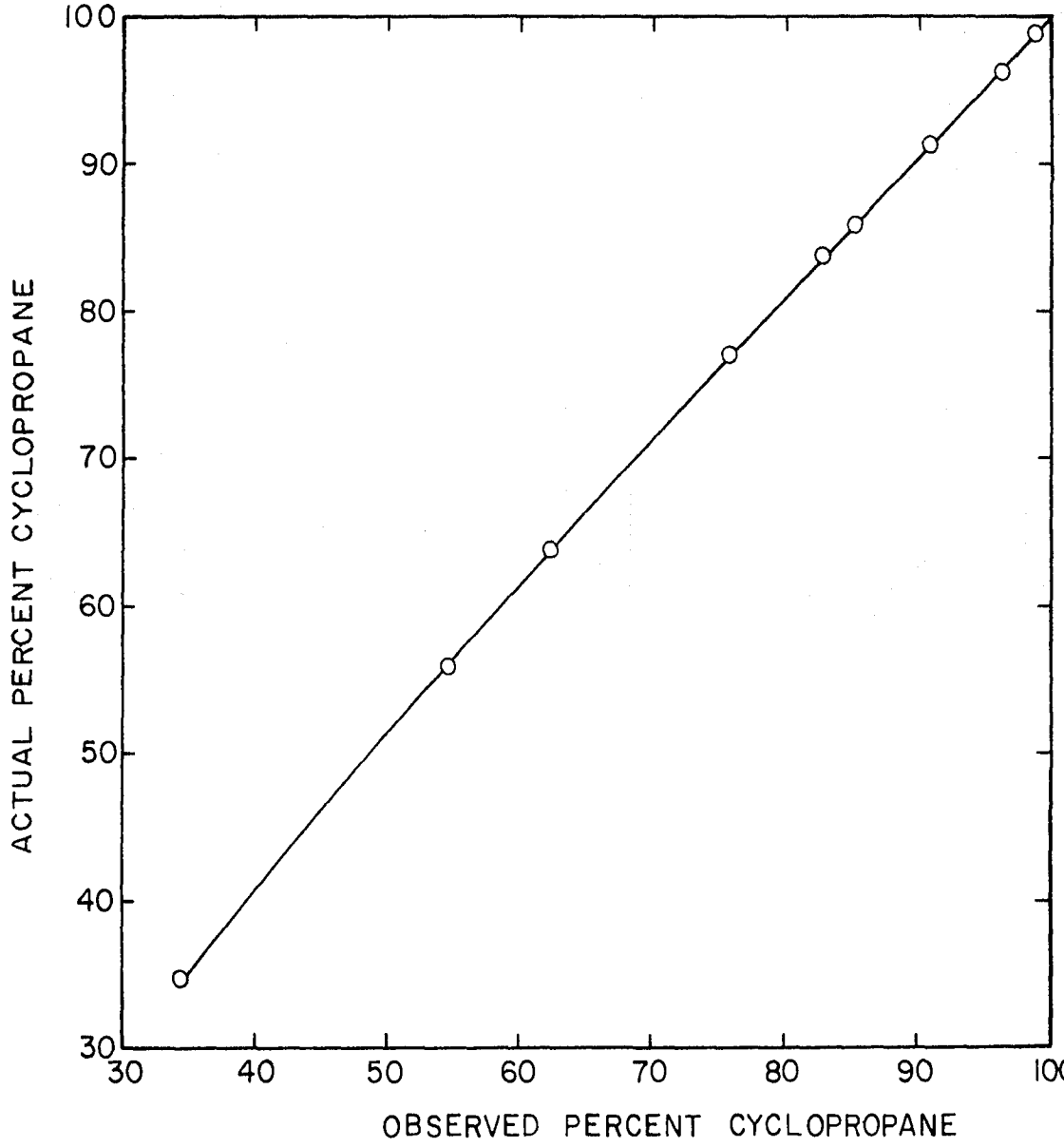


Figure 20. Chromatograph Calibration Curve.

over a 5 month period. Randomly picked standard samples were analyzed during the investigation to insure that the calibration remained valid. The calibration can be represented analytically by the following equations:

$$X_A = 0.9490(X_o) + 0.0511 \qquad \text{(VI-1)}$$

for $0.76 < X_o \leq 1.00$

$$X_A = 0.9700(X_o) + 0.0256 \qquad \text{(VI-2)}$$

for $.50 \leq X_o \leq .76$

where: X_A = actual cyclopropane mole fraction

X_o = observed cyclopropane mole fraction

Table 3 gives the results of the calibrations and the absolute average percent deviation of each sample.

Area ratios were used in the calibration in preference to peak heights for two reasons: (1) preliminary experiments showed the area method to be insensitive to minor variations in flow rate and temperature, thus providing for a long lasting calibration and (2) peak areas were readily available since the recorder contained a Disc integrator. Three or more product samples were analyzed for each run of this study. A typical chromatogram is shown in Figure 21. Using this method of analysis, errors in product gas analysis were felt to be less than 0.5 percent.

TABLE 3

RESULTS OF CHROMATOGRAPH CALIBRATION

Sample Number	Actual percent	Observed percent	Percent Deviation from Mean
1	77.19	75.99	0.28
2	91.42	90.91	0.10
4	98.95	98.97	0.01
5	96.34	96.16	0.03
6	83.72	82.89	0.04
7	55.95	54.57	0.09
8	63.74	62.39	0.05
9	34.71	34.79	1.75
10	85.96	85.19	0.09

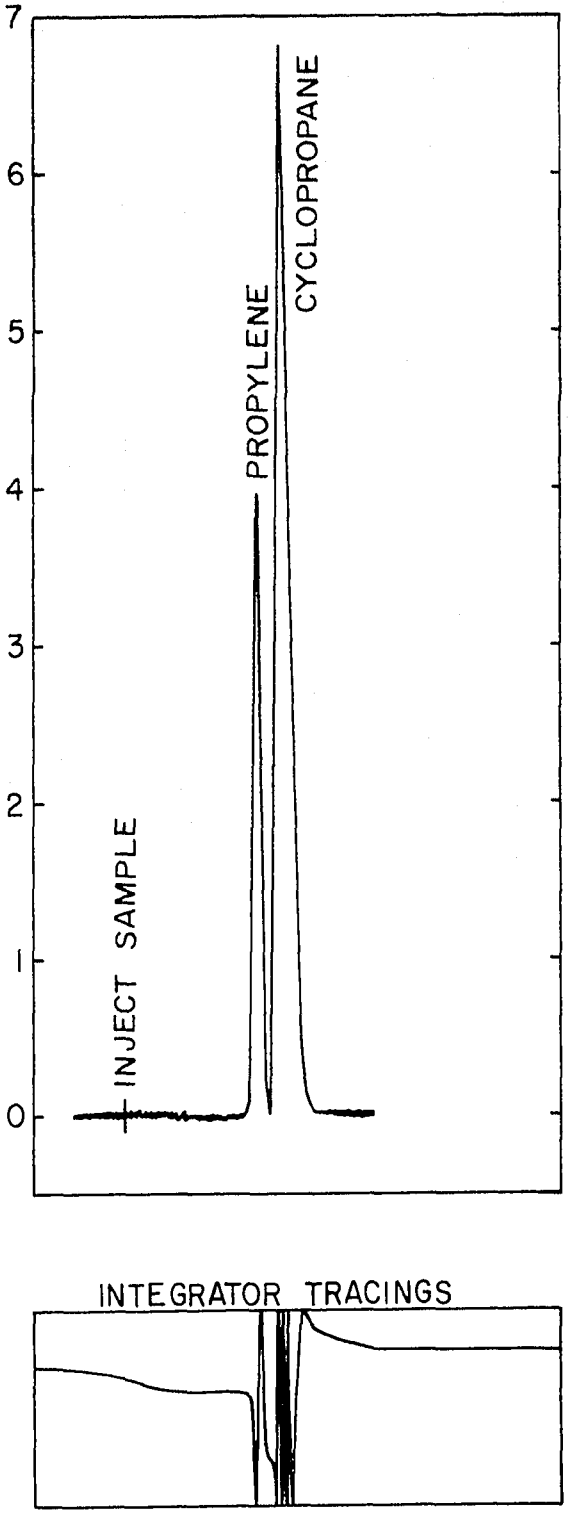


Figure 21. Typical Chromatogram.

CHAPTER VII

METHOD OF DATA ANALYSIS

In this study, specific rate constants were obtained from integral rate data utilizing the assumptions of steady state, negligible axial diffusion, plug flow and isothermal behavior. The assumption of plug flow and negligible axial diffusion is fully investigated in Appendix B. The result of this study confirms the validity of the axial diffusion and plug flow assumptions. The isothermal behavior assumption will be considered later in this chapter.

Development of an Expression for Calculation of the Specific Rate Constant from Experimental Data

The general equation of continuity for component A in a reacting binary mixture is (B2):

$$\frac{\partial C_A}{\partial t} + \nabla \cdot C_A V^* = \nabla \cdot C_A D_{AB} \nabla y_A - r_A \qquad \text{(VII-1)}$$

where C_A is the concentration of A in moles/liter, V^* is the molar average velocity in cm/sec, D_{AB} is the binary diffusion coefficient in cm^2/sec, y_A is the mole fraction of A and r_A is the reaction rate in moles/liter-sec.

Since the isomerization of cyclopropane involves no change in the number of moles present, the divergence of the molar average velocity is zero; because cyclopropane and propylene have the same molecular weight, the molar average velocity, V^*, is equivalent to the mass average velocity, v. Equation (VII-2) becomes:

$$\frac{\partial C_A}{\partial t} + v.\nabla C_A = D_{AB} \nabla^2 C_A - r_A \qquad \text{(VII-3)}$$

In terms of cylindrical coordinates, Equation (VII-3) is:

$$\frac{\partial C_A}{\partial t} + v_r \frac{\partial C_A}{\partial r} + v_z \frac{\partial C_A}{\partial z} = D_{AB} \left[\frac{1}{r} \frac{\partial}{\partial r} \left(r \frac{\partial C_A}{\partial r} \right) + \frac{\partial^2 C_A}{\partial z^2} \right] - r_A \qquad \text{(VII-4)}$$

Making the final assumptions of steady state, negligible axial diffusion, plug flow and isothermal behavior serves to eliminate the following terms:

$$\frac{\partial C_A}{\partial t} = 0 \text{ steady state}$$

$$v_r \frac{\partial C_A}{\partial r} = 0 \text{ plug flow}$$

$$\frac{1}{r} \frac{\partial}{\partial r} \left(r \frac{\partial C_A}{\partial r} \right) = 0 \text{ plug flow}$$

$$\frac{\partial^2 C_A}{\partial z^2} \simeq 0 \text{ negligible axial diffusion}$$

Thus, Equation (VII-4) reduces to:

$$\langle v \rangle \frac{dC_A}{dz} = - r_A \qquad \text{(VII-5)}$$

which will be the basic equation for developing an expression for the specific rate constant, k_c, from experimental data. The rate term, r_a, for a first order reaction is:

$$r_a = k_c C_A$$

Utilizing this relation in Equation (VII-5) and integrating over the reactor length gives:

$$\int_{C_{A_i}}^{C_{A_o}} \frac{dC_A}{C_A} = - \int_0^L \frac{k_c}{\langle v \rangle} dz = - \frac{k_c}{\langle v \rangle} \int_0^L dz$$

$$\ln \left[C_{A_o} / C_{A_i} \right] = - \frac{k_c L}{\langle v \rangle}$$

but: $\tau = L/\langle v \rangle$ = residence time

$$\ln \left[C_{A_o} / C_{A_i} \right] = - k_c \tau$$

and: $C_A = X_A \rho$

therefore:

$$\ln \left[X_{A_i} / X_{A_o} \right] = k_c \tau \qquad \text{(VII-6)}$$

continuing: $$\tau = \frac{V\rho_r}{F_o\rho_o}$$

where F_o is the volumetric flow rate at STP (15.56°C, 60°F and 1.0 atms), ρ_r is the density at reactor conditions, V is the reactor volume, and ρ_o is the density at standard conditions. The final equation used to evaluate k_c was:

$$k_c = \frac{F_o\rho_o}{V\rho_R} \ln\left[\frac{X_{Ai}}{X_{Ao}}\right] \qquad \text{(VII-7)}$$

or

$$k_c = \frac{1}{\tau} \ln\left[\frac{X_{Ai}}{X_{Ao}}\right] \qquad \text{(VII-8)}$$

First order behavior is confirmed by plotting $\ln (X_{Ai}/X_{Ao})$ versus τ to obtain a straight line passing through the origin with a slope of k_c.

Specific rate constants were calculated with Equation (VII-7) by use of an IBM 360-40 computer. The computer program used for these calculations is shown in Appendix C. Figure 44 shows a sample output obtained when analyzing the run data. A sample input data form is shown in Appendix C.

Calculation of Frequency Factor and Activation Energy

As discussed in Chapter II, the Arrhenius equation is almost exclusively used to express the variation of k_c with temperature. In logarithmic form the Arrhenius equation is:

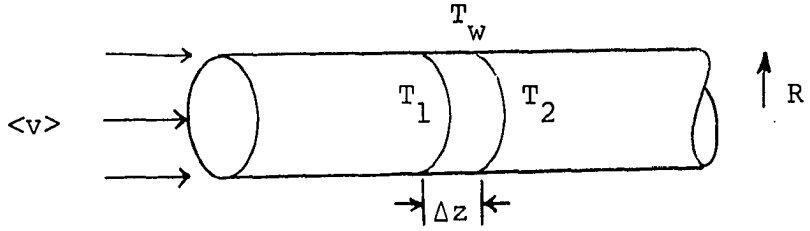
$$\ell n\ (k_c) = \ell n\ (A) - E_o/RT \qquad \text{(VII-9)}$$

Upon plotting $\ell n\ (k_c)$ versus $1/T$, a straight line is obtained whose slope is $-E_o/R$ and whose intercept is $\ell n\ (A)$. For each pressure level investigated, a least squares line of Equation (VII-9) was obtained from the experimental data.

The Isothermal Behavior Assumption

Since the requirement of isothermal behavior is implicitly implied in many of the assumptions used to derive Equation (VII-7), some discussion of isothermal behavior is obviously in order.

Consider a reacting gaseous binary mixture flowing in a tubular reactor of length L. With the following assumptions: (1) plug flow, (2) constant physical properties, and (3) negligible viscous heating, an energy balance on a segment of length ΔZ (see below) gives:



$$(\rho\ C_p\ \langle v\rangle\ T_1 - \rho\ C_p\ \langle v\rangle\ T_2)(\pi R^2) = -(\pi R^2 \Delta Z)\Delta H_{rxn} + H(2\pi R \Delta Z)\ (T - T_w)$$

$$\rho\ C_p\ \langle v\rangle\ \pi R^2\ (T_1 - T_2) = -\pi R^2 \Delta Z \Delta H_{rxn} + 2\pi R \Delta Z H\ (T - T_w) \qquad \text{(VII-10)}$$

dividing by $\pi R^2 \Delta Z$ gives:

$$\frac{\rho\, C_p \langle v\rangle\, (T_1-T_2)}{\Delta Z} = -\Delta H_{rxn} + \frac{2H(T-T_w)}{R} \qquad \text{(VII-11)}$$

Taking the limit as $\Delta Z \to 0$:

$$\rho\, C_p \langle v\rangle \frac{dT}{dZ} = \Delta H_{rxn} - \frac{2H(T-T_w)}{R} \qquad \text{(VII-12)}$$

where: ΔH_{rxn} = heat generation due to reaction

H = overall heat transfer coefficient

T_w = wall temperature

now: $\Delta H_{rxn} = \rho\, X_i\, k_c\, H_{rxn} \exp(-k_c Z/\langle v\rangle)$

H_{rxn} = heat of reaction

Letting: $\theta = T/T_w$

$\chi = Z/L$

we have:
$$\frac{d\theta}{d\chi} = \frac{X_i\, LH_{rxn}\, k_c \exp(-k_c L\chi/\langle v\rangle)}{C_p \langle v\rangle\, T_w} - \frac{2HL(\theta-1)}{\rho\, C_p \langle v\rangle R} \qquad \text{(VII-13)}$$

with the initial condition: $\theta = 1$ at $\chi = 0$

Equation (VII-13) and its initial condition were solved using a 3rd order Runge-Kutta approximation to $d\theta/d\chi$. The maximum non-isothermal effect was estimated to have occurred in run R3-400 as this run was conducted at the highest temperature level (537.8°C). The following

variables were used in solving Equation VII-13:

H_{rxn} = 185 cal/g

ρ = 18.0 g/l

L = 487 cm

C_p = 0.753 cal/g-°K

T_w = 811 °K

R = 0.40 cm

X_i = 0.9925

<v> = 10.0 cm/sec

H = 19.5, 24.5, 40.7, 68 x 10^{-4} cal/cm^2-sec

The results of the solution are presented in Figure 22. As shown, the temperature rise is a strong function of the heat transfer coefficient, H. However, the non-isothermal effects are small and can be neglected for purposes of rate analysis.

Estimation of the Expected Experimental Error

The purpose of this section is to provide an estimate of the error involved when calculating the rate constant using Equation (VII-7). Since the results are only an estimate, it will be assumed that all errors in the independent variables (i.e., measured variables) contribute independently to the total error. Thus to estimate the error of a function, $y = \Phi(a, b, c, \ldots Z)$ the following relationship may be used:

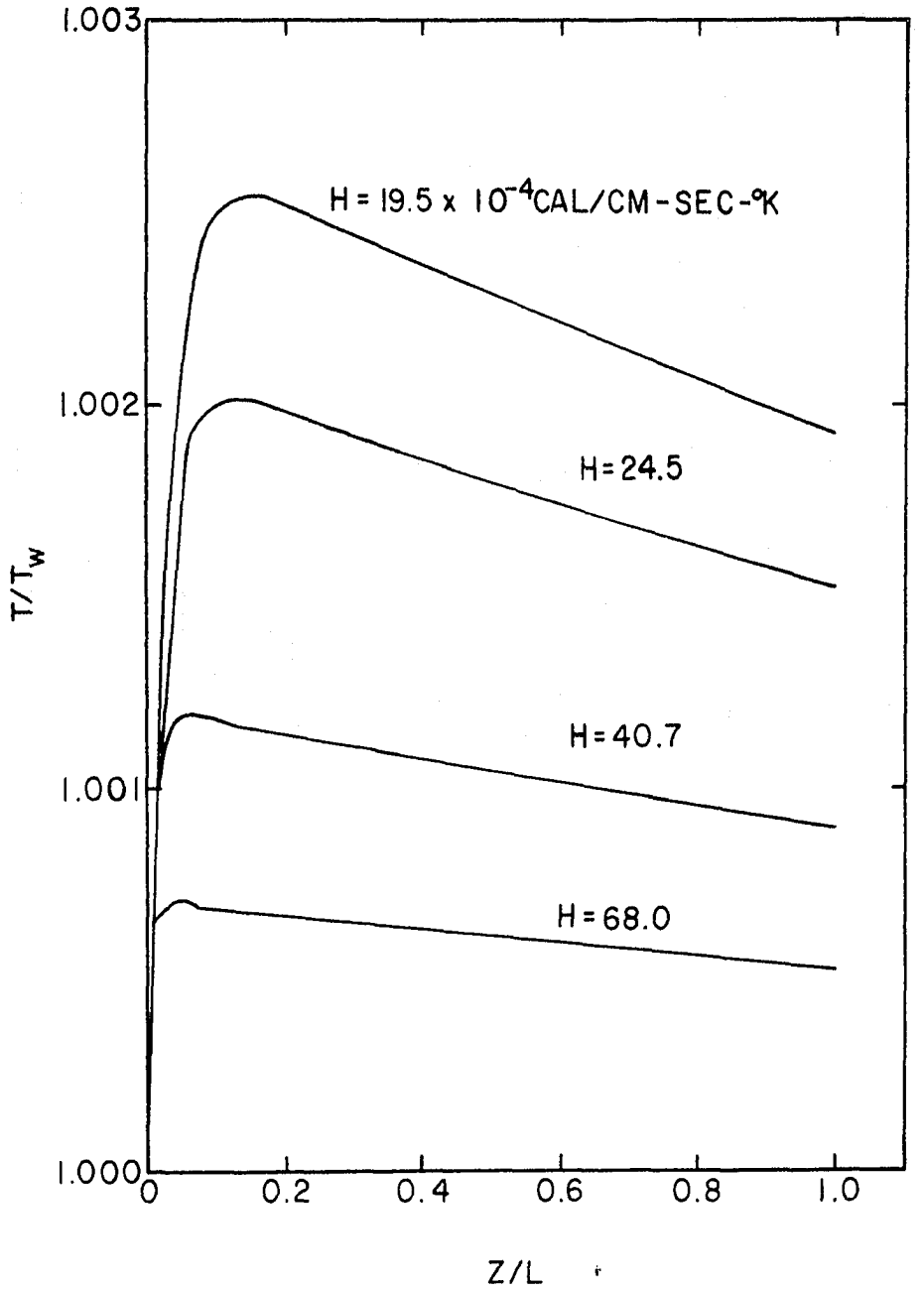


Figure 22. Non-Isothermal Behavior in Reactor.

$$dy = \frac{d\Phi}{da}\,\Delta a + \frac{d\Phi}{db}\,\Delta b + \ldots \frac{d\Phi}{dZ}\,\Delta Z$$

where a is known to within Δa, etc. for b to Z. Thus for the specific rate as computed by Equation (VII-7):

$$k_c = \frac{F_o \rho_o}{V\ \rho r}\ \ell n \left[X_{A_i} / X_{A_o} \right]$$

Letting $(X_{A_i} / X_{A_o}) = \beta$ and $\rho_o / \rho_R = \alpha$,

$$K_c = \frac{F_o \alpha}{V}\ \ell n\ [\beta] \qquad \text{(VII-17)}$$

The estimated deviations of all measured variables are:

Temperature	± 0.3°C
Flow Rate	± 0.5%
Pressure	± 0.03 atms
Concentration	± 0.5%
Reactor Volume	± 0.1 ml

These deviations produced the following "expected" variations in the parameters of Equation (VII-17).

F_o	± 1%
α	± 0.5%
V	± 0.1 ml
ρ	± 0.5%

The "expected" error in the specific rate constant is then:

$$dk_c = \frac{\alpha}{V} \ell n\ (\beta)\ dF_o + \frac{F_o}{V} \ell n\ (\beta)\ d\alpha$$
$$- \frac{F_o \alpha}{V^2} \ell n\ (\beta)\ dV + \frac{F_o \alpha}{V\beta}\ d\beta$$

Using the run variables of run R7-300:

$$F_o = 56.90 \pm 0.57 \text{ ml/sec}$$
$$\alpha = 0.1329 \pm 0.00066$$
$$\beta = 1.194 \pm 0.006$$
$$V = 239.9 \pm 0.1 \text{ ml}$$

then

$$dk_c = \frac{0.1329}{239.9} (.57) \ell n\ (1.194) + \frac{56.9}{239.9} (.0066) \ell n\ (1.194)$$
$$- \frac{56.9\ (.1329)}{239.9)^2} (-0.1) \ell n\ (1.194) + \frac{56.9\ (.1329)\,(.006)}{(239.9)\,(1.194)}$$

$$dk_c = 5.6 \times 10^{-5} + 2.8 \times 10^{-5} + 2.3 \times 10^{-6} + 1.58 \times 10^{-4}$$

$$dk_c = 24.4 \times 10^{-5}$$

The computed rate constant at these conditions was $k_c = 56.47 \times 10^{-4}$ which gives an estimated error of 4.3 percent or ± 2.15 percent.

While the value of ± 2.2 percent is the "expected" error involved when computing the rate constant, an error analysis must also be separately considered for the absolute

temperature. Using the Arrhenius equation, the temperature error can be found for run R7-300 as:

$$k_c = A \exp\ (-\ E_o/RT)$$

$$dk_c = \frac{k_c\ E_o}{RT^2}\ dT$$

$$dk_c = \frac{56.57 \times 10^{-4}\ (66{,}494)\ (.3)}{1.987\ (811.2)^2} = 8.6 \times 10^{-5}$$

or a ± 1.5 percent error. Thus, the total "expected" error in the rate constant is ± 4 percent. This figure, ± 4 percent, should be interpreted as a realistic error estimate for the conditions of this investigation. This author does not feel that the maximum error of this investigation can exceed ± 10 percent.

CHAPTER VIII

DISCUSSION OF RESULTS

This chapter is devoted to a discussion of the experimental results of this investigation in terms of the theoretical development of Chapter II after being analyzed by the methods presented in Chapter VII. In summary, rate data were obtained in a gold-lined tubular reactor for the following range of variables:

	Range	Units
Pressure	0.4-137 5.8-2014.	atms psia
Temperature	454-539 850-1000	°C °F
Residence Time	7-810	sec
Feed Rate	0.54-155	ml/sec
Conversion	0.3-34.4	percent

Table 11 of Appendix E summarizes the results of all experimental runs.

With the exception of runs R20 and R23, all runs in this investigation were conducted at residence times which were sufficiently low so that reactions other than the cyclopropane isomerization were negligible. Chromatographic

analysis of the run samples showed no traces of pyrolysis products (methane, ethylene, ethane, polymers) except for small amounts, < 0.5%, at the highest temperature level. Further, all runs were designed to fit well within the so-called "region of isomerization" defined by Pipkin (P2) and shown in Figure 23. Only one "small" drop of liquid product was recovered from the knock-out pot during the course of the study. The above evidence points strongly to the fact that the reaction investigated was, in fact, the thermal isomerization of cyclopropane.

Of the 94 data points taken during the course of the investigation, 80 were available for correlation. All of these points fall within the shaded region of Figure 23.

First order behavior was shown by plotting $\ell n(X_i/X_o)$ versus residence time, τ, and by obtaining a straight line passing through the origin with slope equal to k_c. Figure 24 shows this plot at the 496°C (925°F) temperature level. Infinite pressure rate constant lines are shown for the results of Davis and Scott (D2), $\ell n\ k_\infty = 35.431 - 65{,}570/RT$, and for the results of this investigation, $\ell n\ k_\infty = 35.984 - 66{,}316/RT$.

Sufficient data were obtained at nine pressure levels to construct Arrhenius plots. As Figures 25 to 33 show, the plots of $\ell n\ k_c$ versus 1/T followed the expected straight line

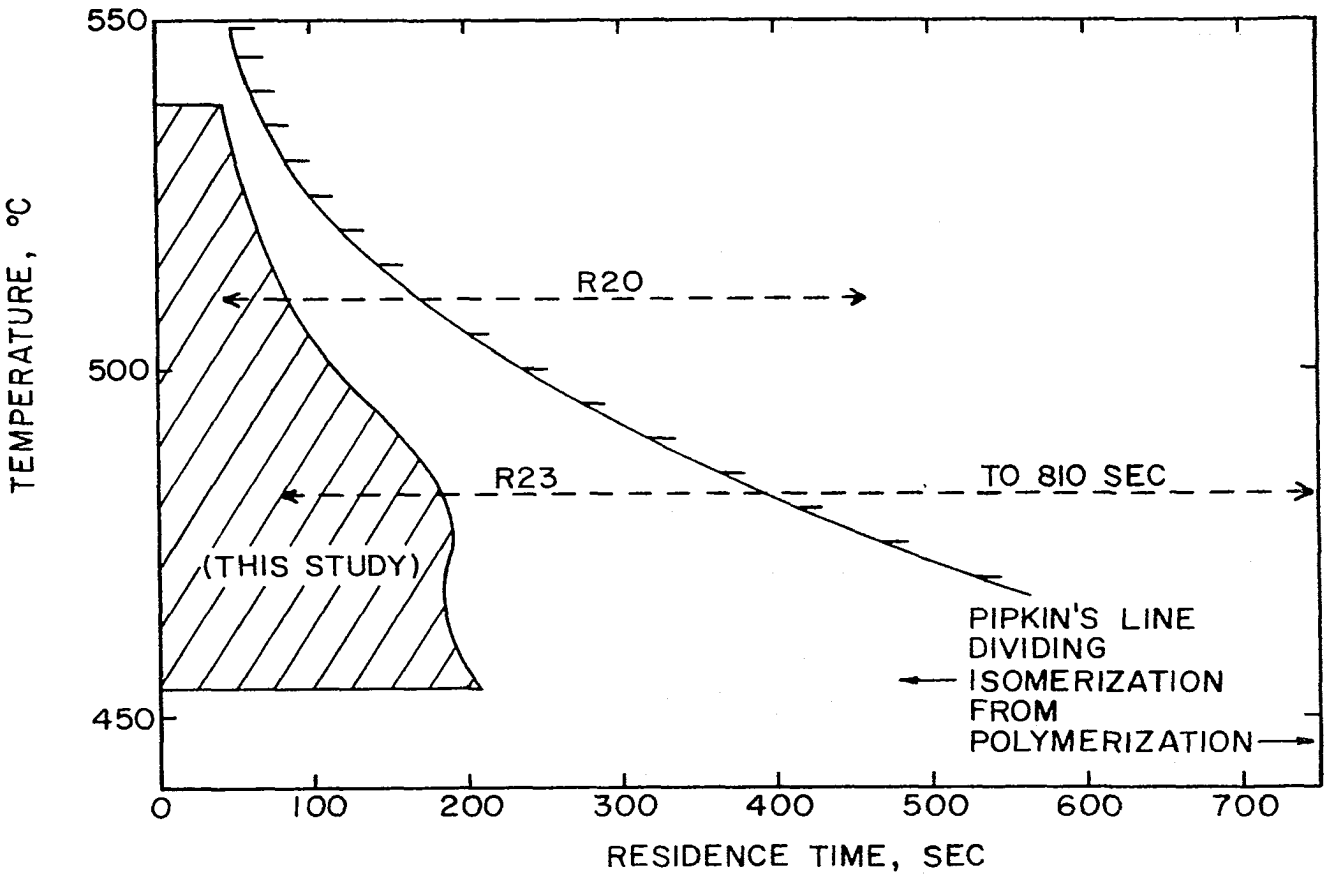


Figure 23. Region of Isomerization.

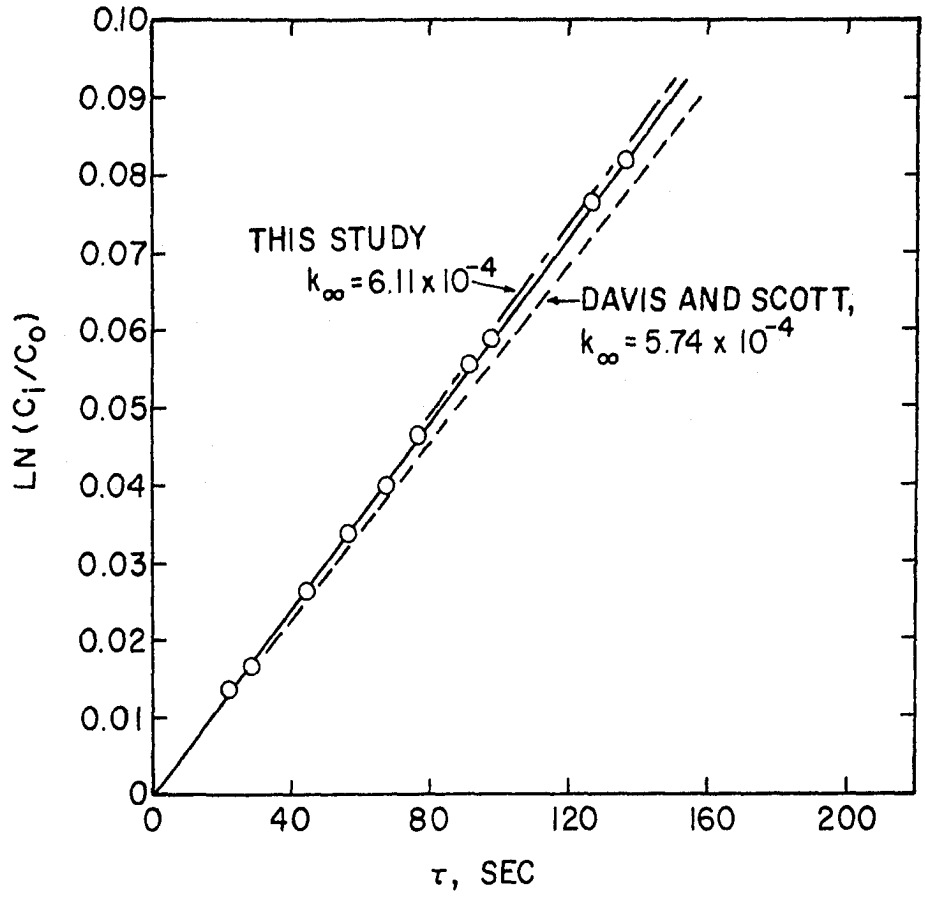


Figure 24. First Order Behavior at 496.1°C.

TABLE 4

FIRST ORDER BEHAVIOR AT 496.1°C (925°F)

τ (sec)	$\ln(C_i/C_o)$
23.1	0.0134
29.0	0.0167
43.7	0.0258
45.2	0.0262
56.5	0.0335
67.0	0.0397
69.3	0.0400
76.5	0.0462
91.3	0.0550
97.6	0.0588
127.1	0.0764
135.8	0.0820
136.4	0.0820

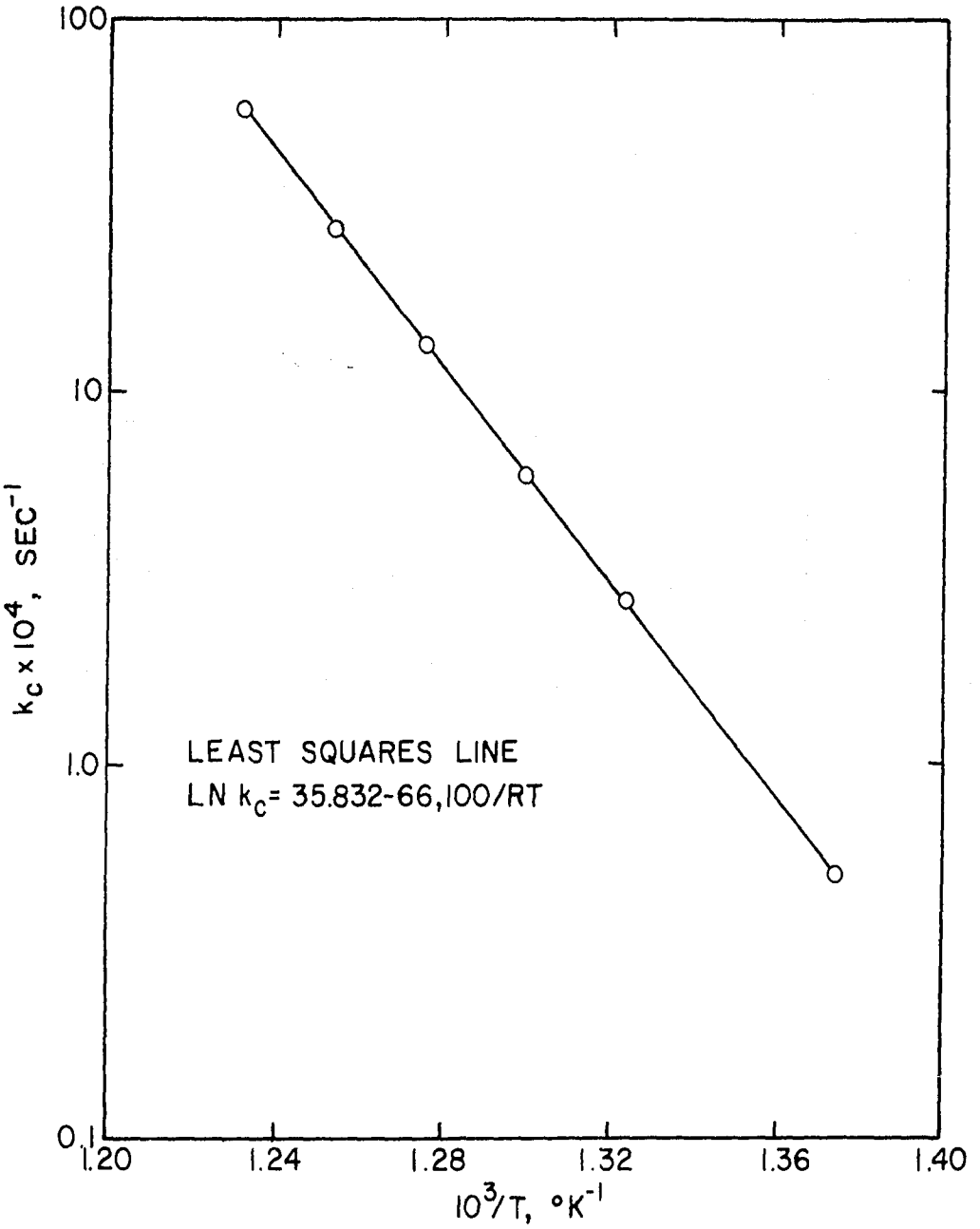


Figure 25. Arrhenius Correlation at 28 atms.

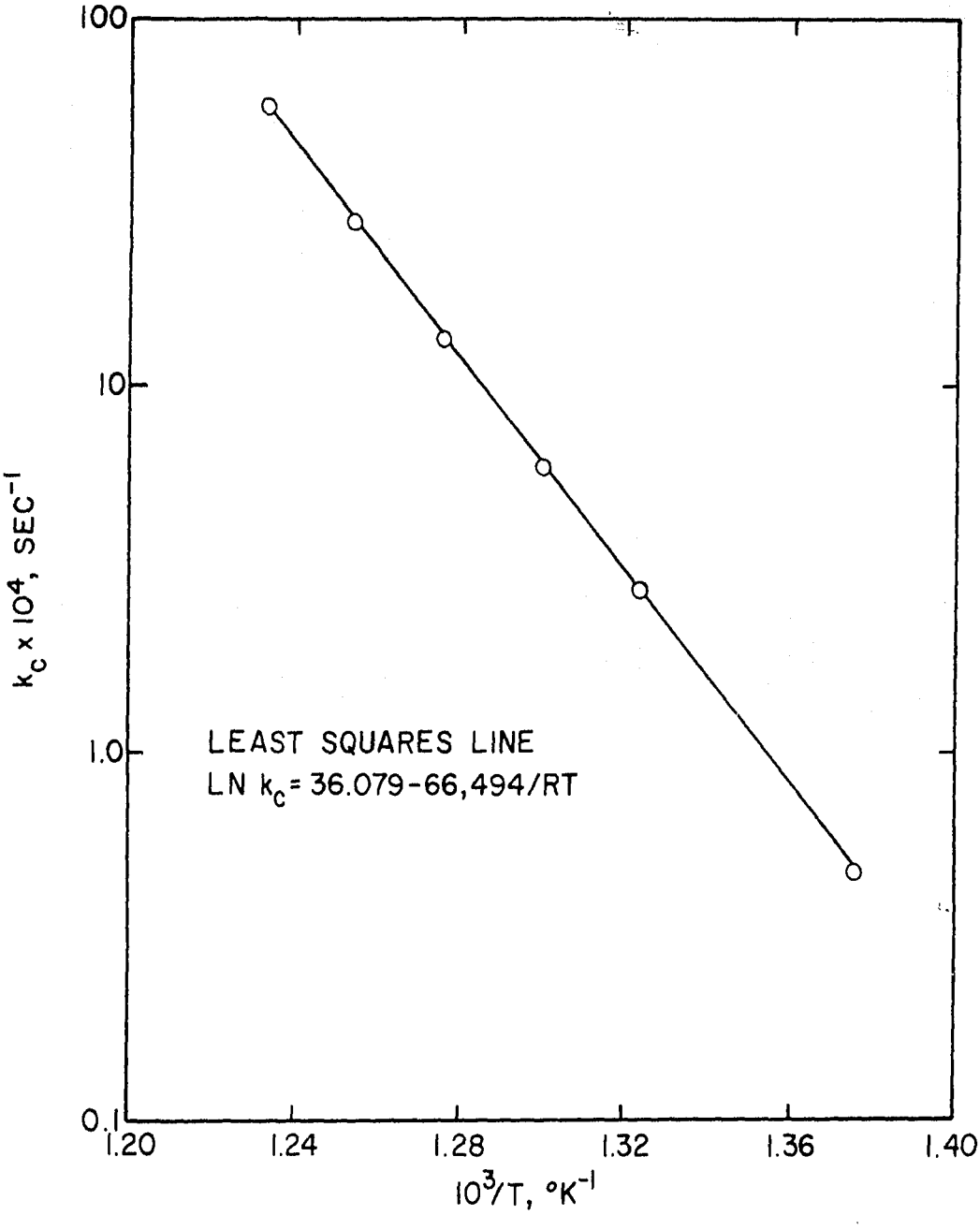


Figure 26. Arrhenius Correlation at 21 atms.

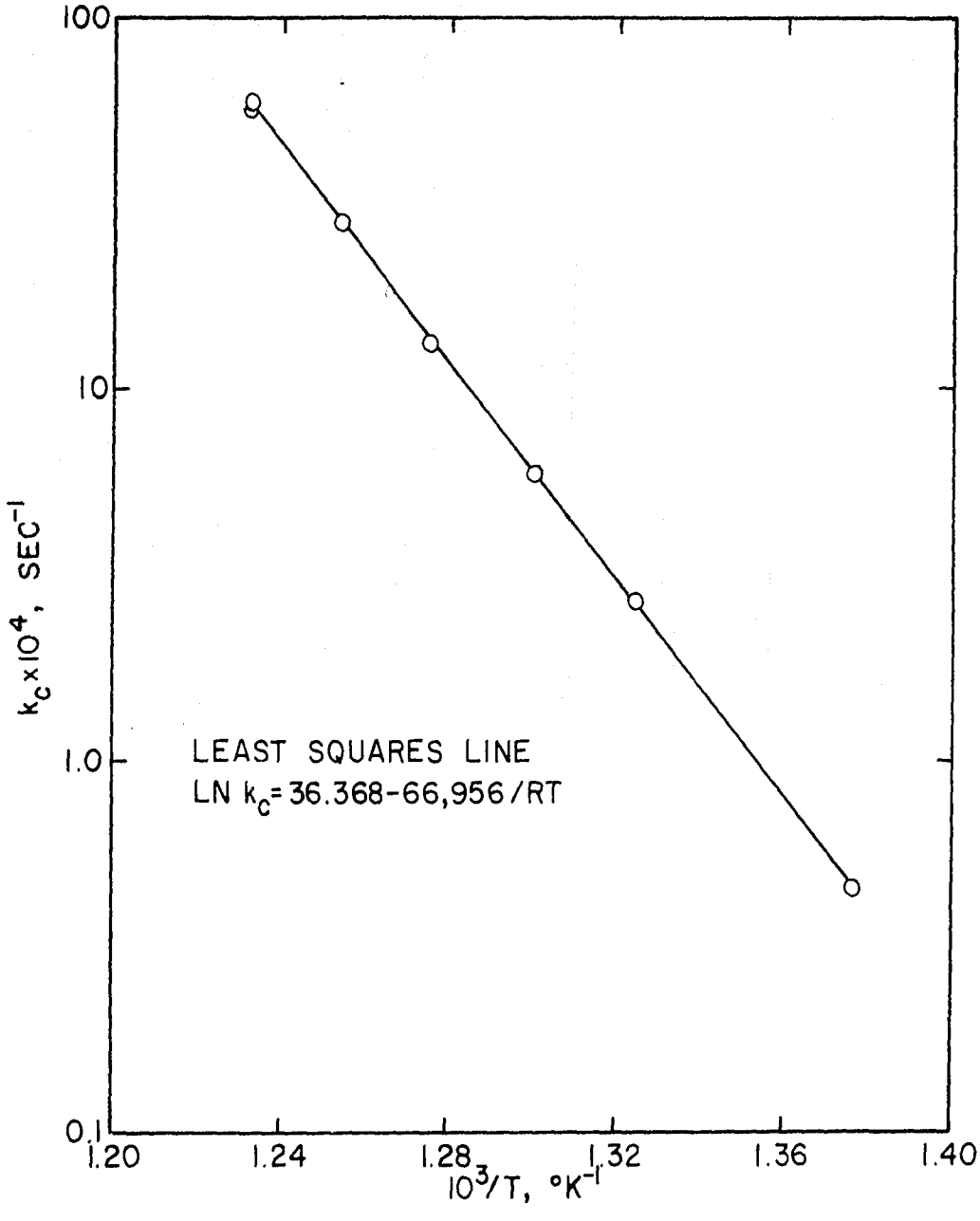


Figure 27. Arrhenius Correlation at 14.5 atms.

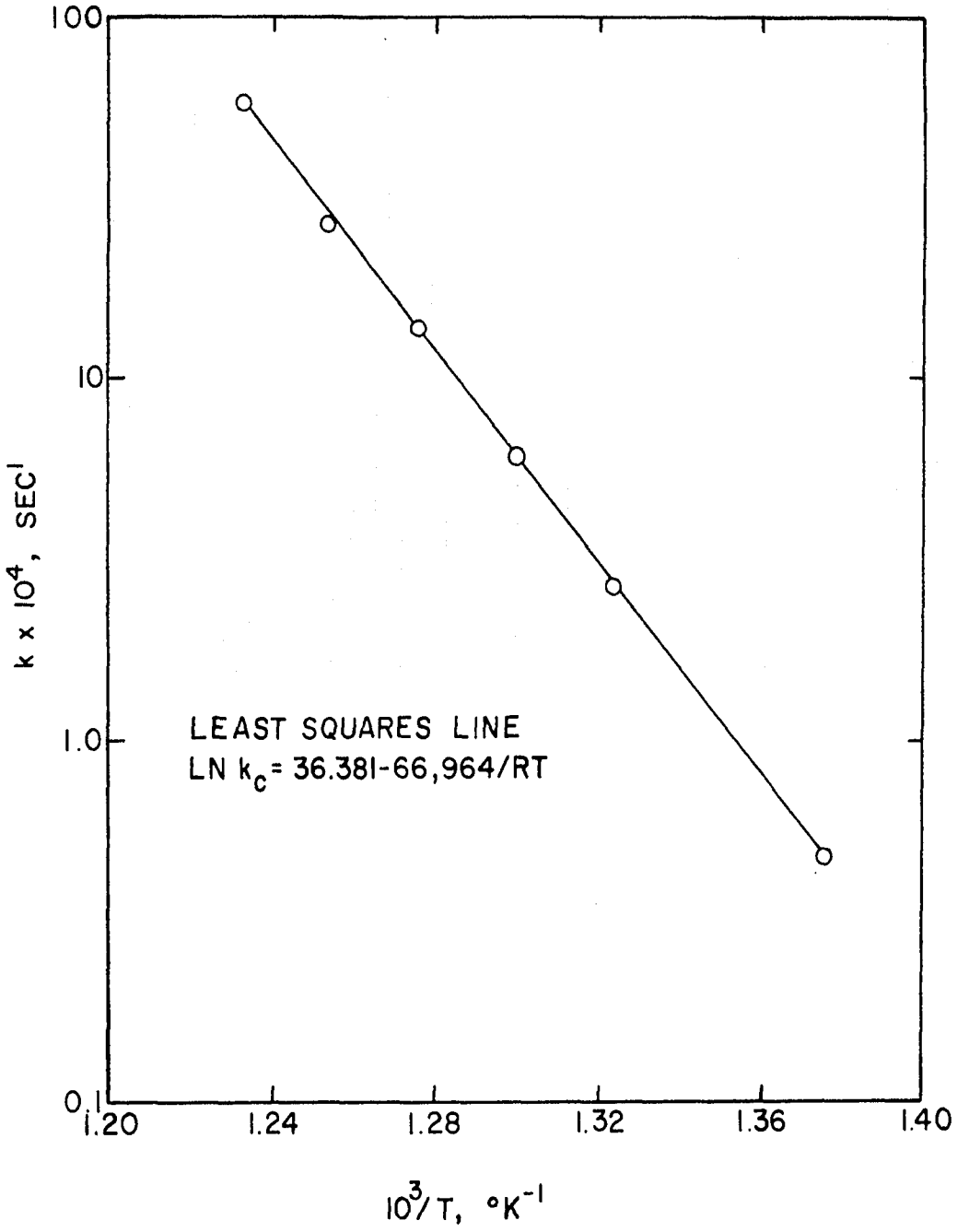


Figure 28. Arrhenius Correlation at 7.8 atms.

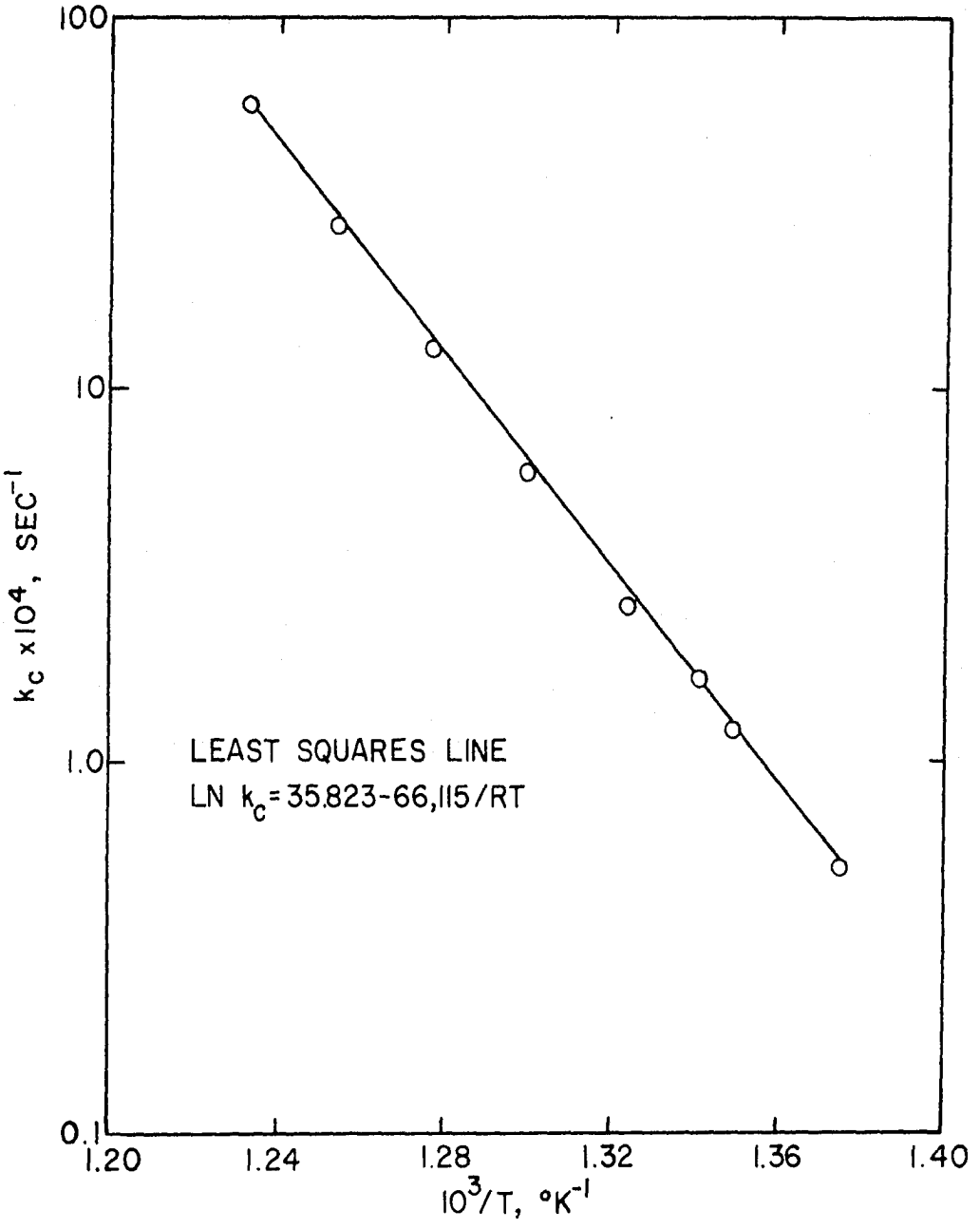


Figure 29. Arrhenius Correlation at 4.4 atms.

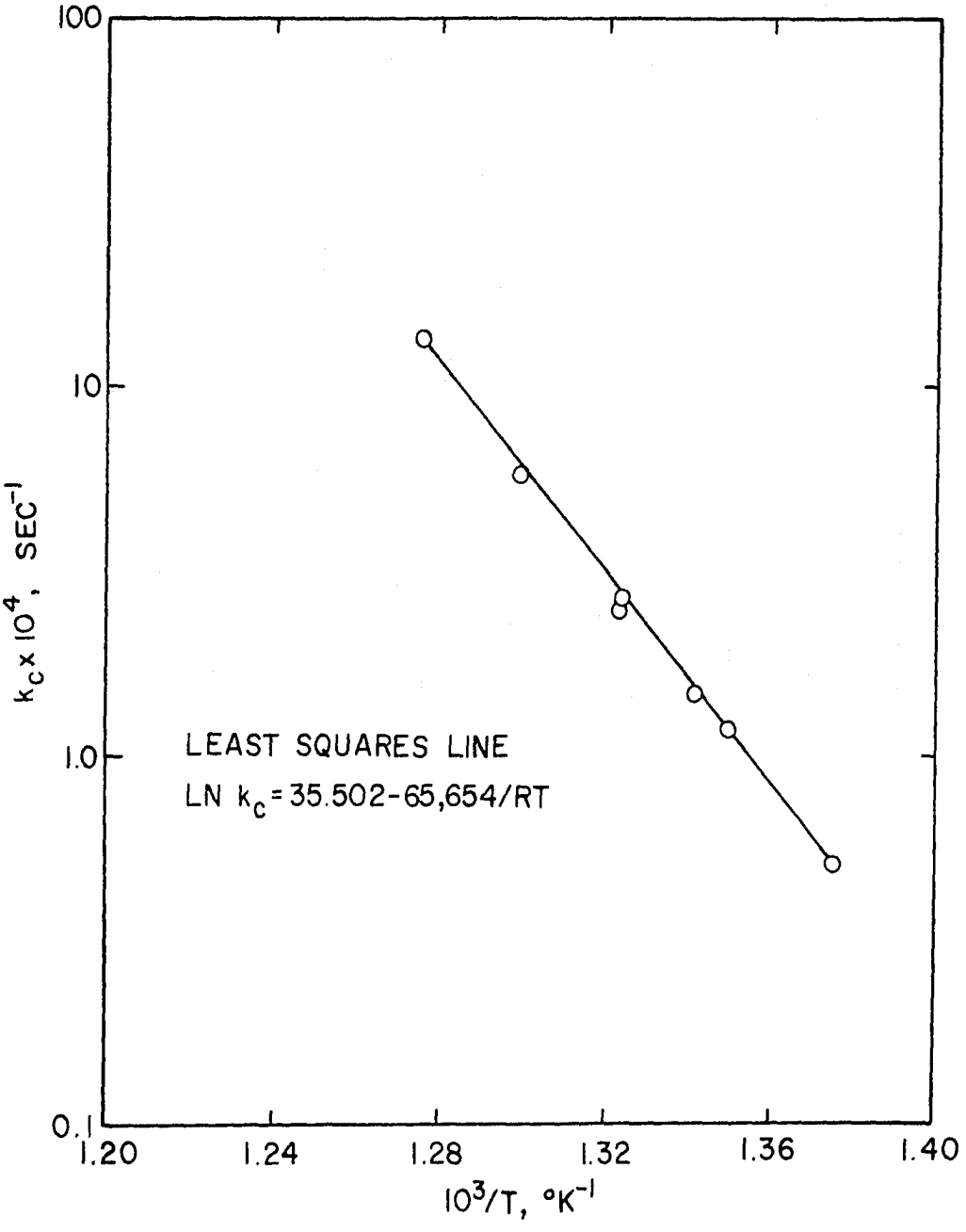


Figure 30. Arrhenius Correlation at 3.0 atms.

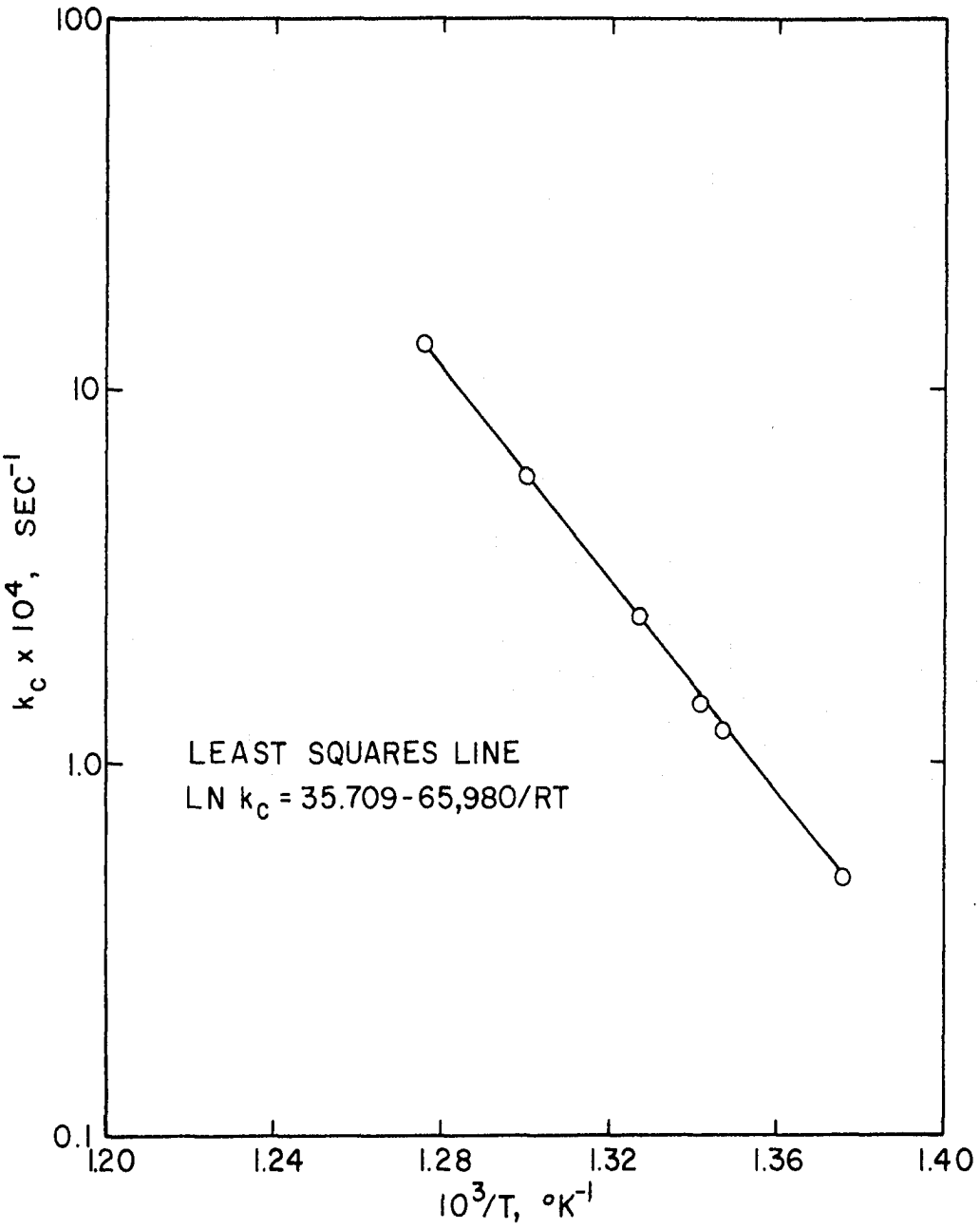


Figure 31. Arrhenius Correlation at 2.0 atms.

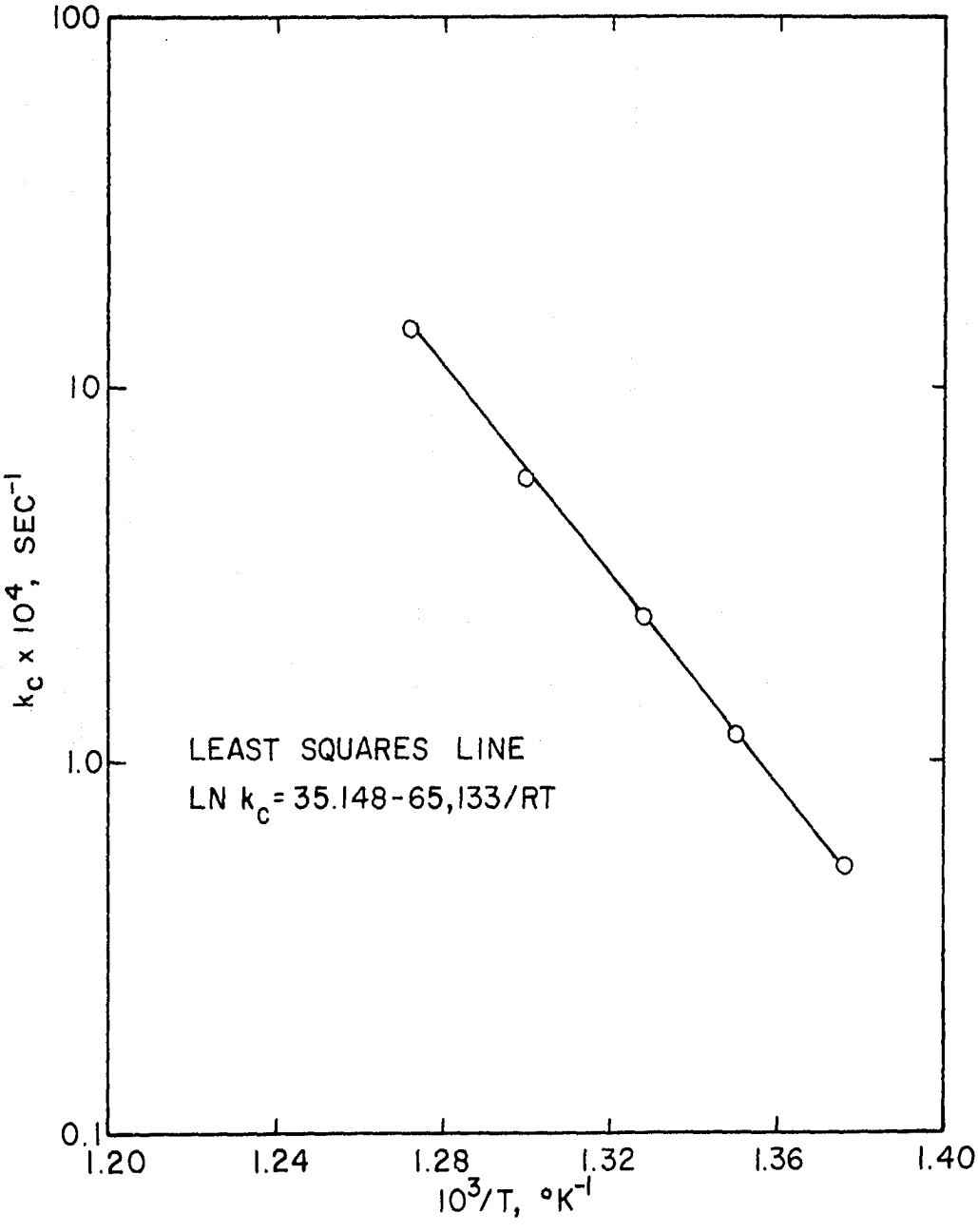


Figure 32. Arrheius Correlation at 1.3 atms.

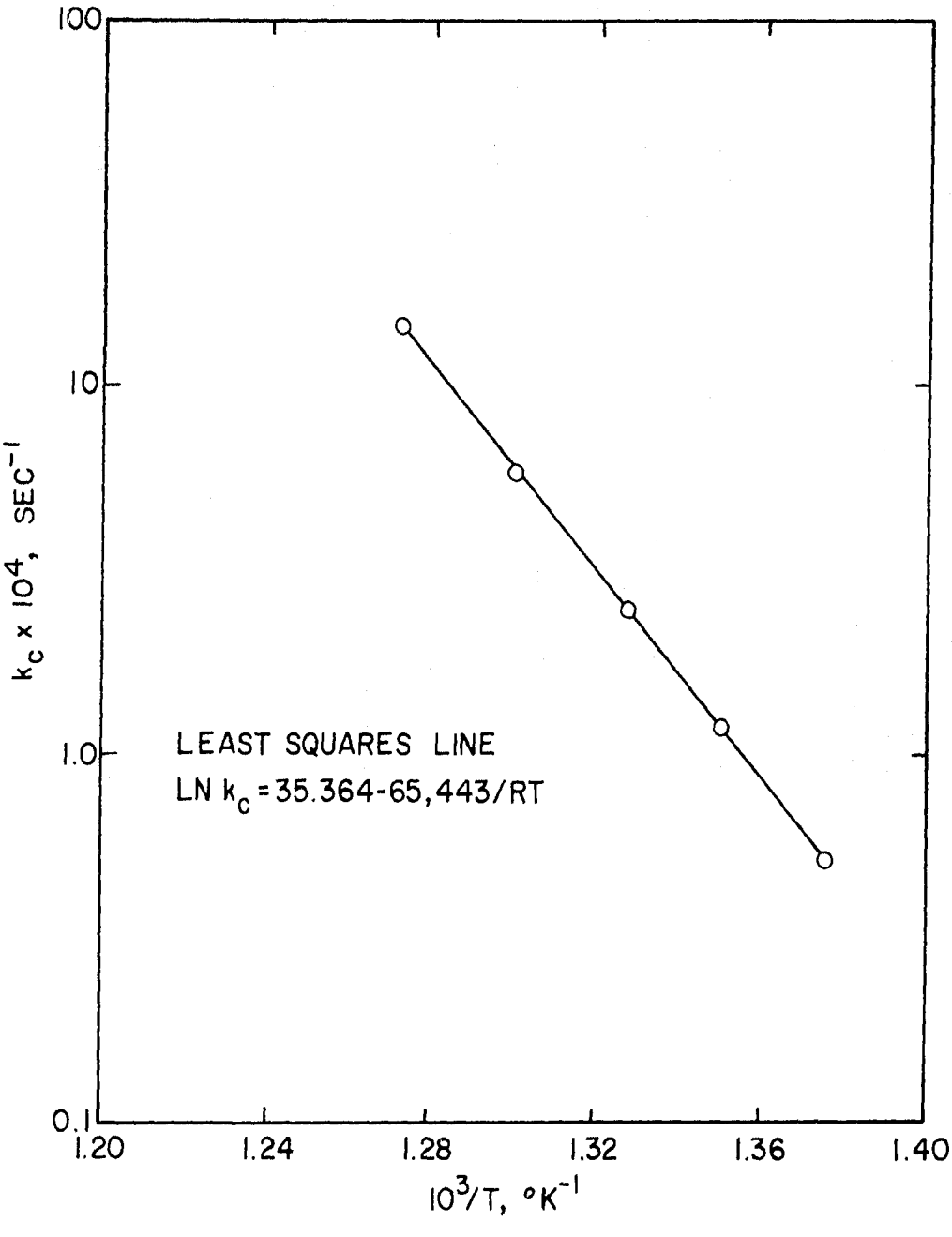


Figure 33. Arrhenius Correlation at 1.0 atms.

relationship. At each pressure level, the data were fitted to an equation of the form

$$\ell n\, k_c = \ell n(A) - E_o/RT$$

by the least squares technique. Results of these fittings are shown on each figure. Deviations between values of the rate constant computed from the least squares equation and experimental data points averaged about 2 percent; maximum deviations were less than 5 percent. These deviations were felt reasonable in light of the "expected" experimental error of ± 4 percent predicted in Chapter VII. Table 5 shows the pressure levels employed in this investigation along with the runs used in each Arrhenius plot.

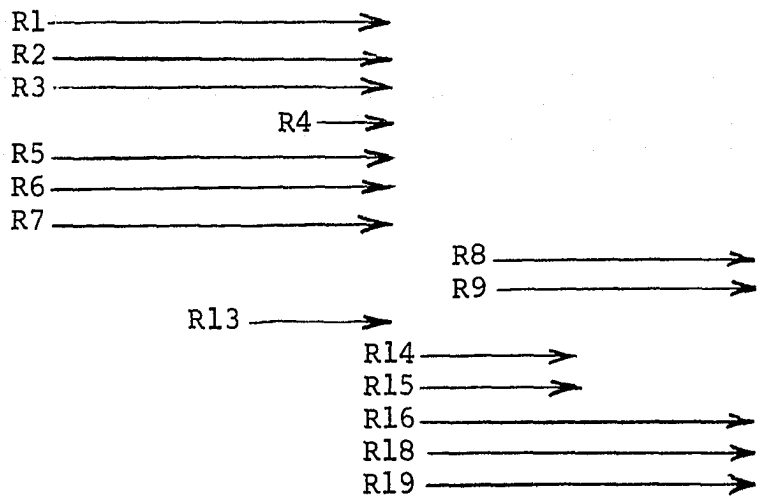
Values of Kassel's integral, Equation (II-24), were prepared at five temperature levels--454, 468, 482, 496, and 510°C. From these computations, the plot of I(T,P) versus ℓn(P), shown in Figure 34, was obtained. Values of I(T,P) thus obtained were used to compute hypothetical values of the rate constant at infinite pressure, k_∞. At each temperature level, the newly computed k_∞ values were averaged to obtain data relating k_∞ and temperature as shown in Table 6. An Arrhenius plot of this data, shown in Figure 35, gave the following correlation:

$$\ell n\, k_\infty = 35.984 - 66{,}316/RT \qquad \text{(VIII-1)}$$

TABLE 5

SUMMARY OF RUNS USED IN ARRHENIUS CORRELATION

Figure	25	26	27	28	29	30	31	32	33
Pressure									
(atms)	28	21	14.5	7.8	4.4	3.0	2.0	1.3	1.0
(psig)	400	300	200	100	50	30	15	5	1



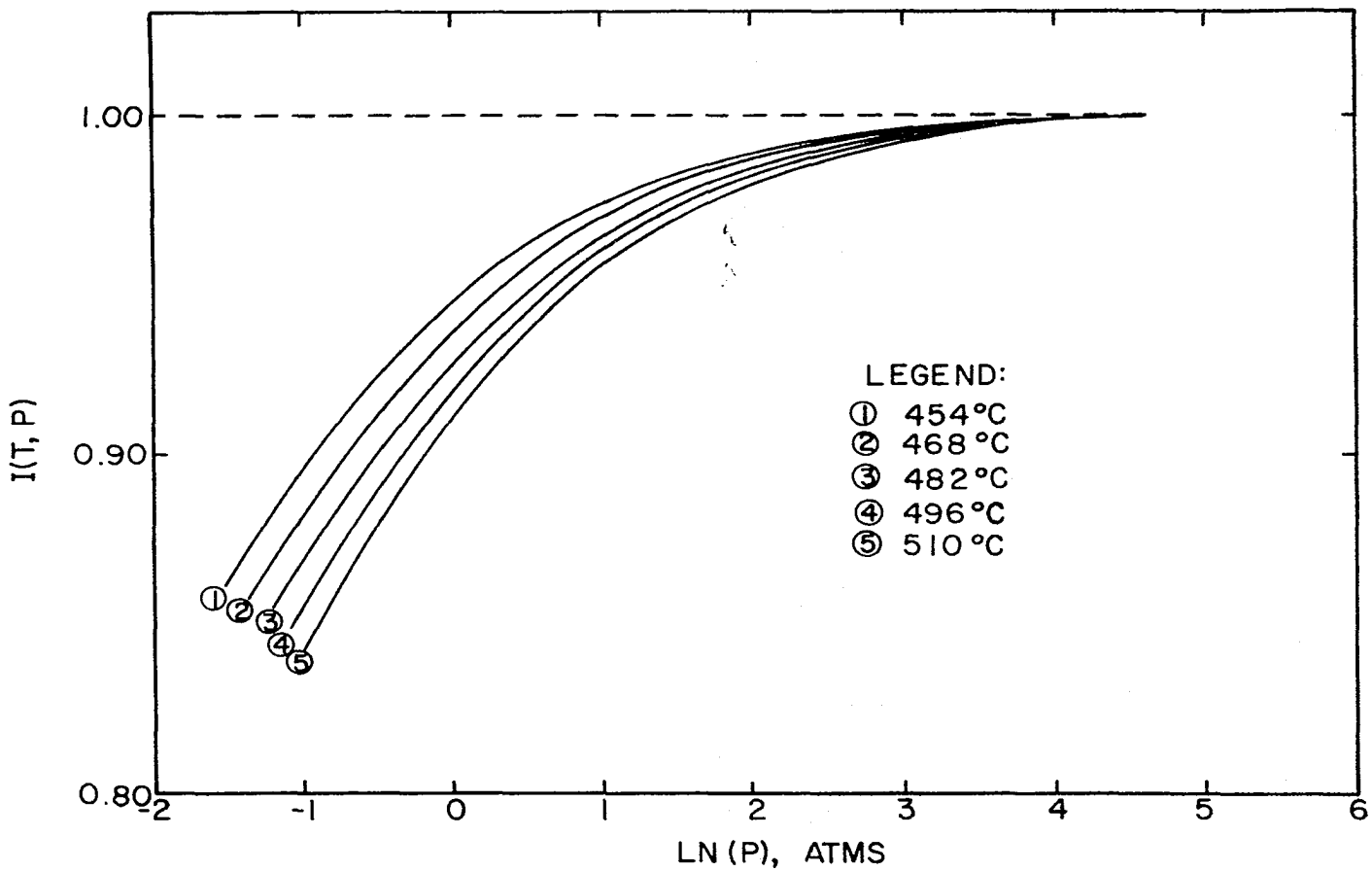


Figure 34. Plot of I(T,P) versus ℓn (P).

TABLE 6

RATE CONSTANT FOR INFINITE PRESSURE

T, °C	$k_c \times 10^4$, sec^{-1}
454.44	0.5115 ± 0.014
468.33	1.19 ± 0.03
482.22	2.77 ± 0.03
496.11	6.02 ± 0.08
510.00	13.28 ± 0.22

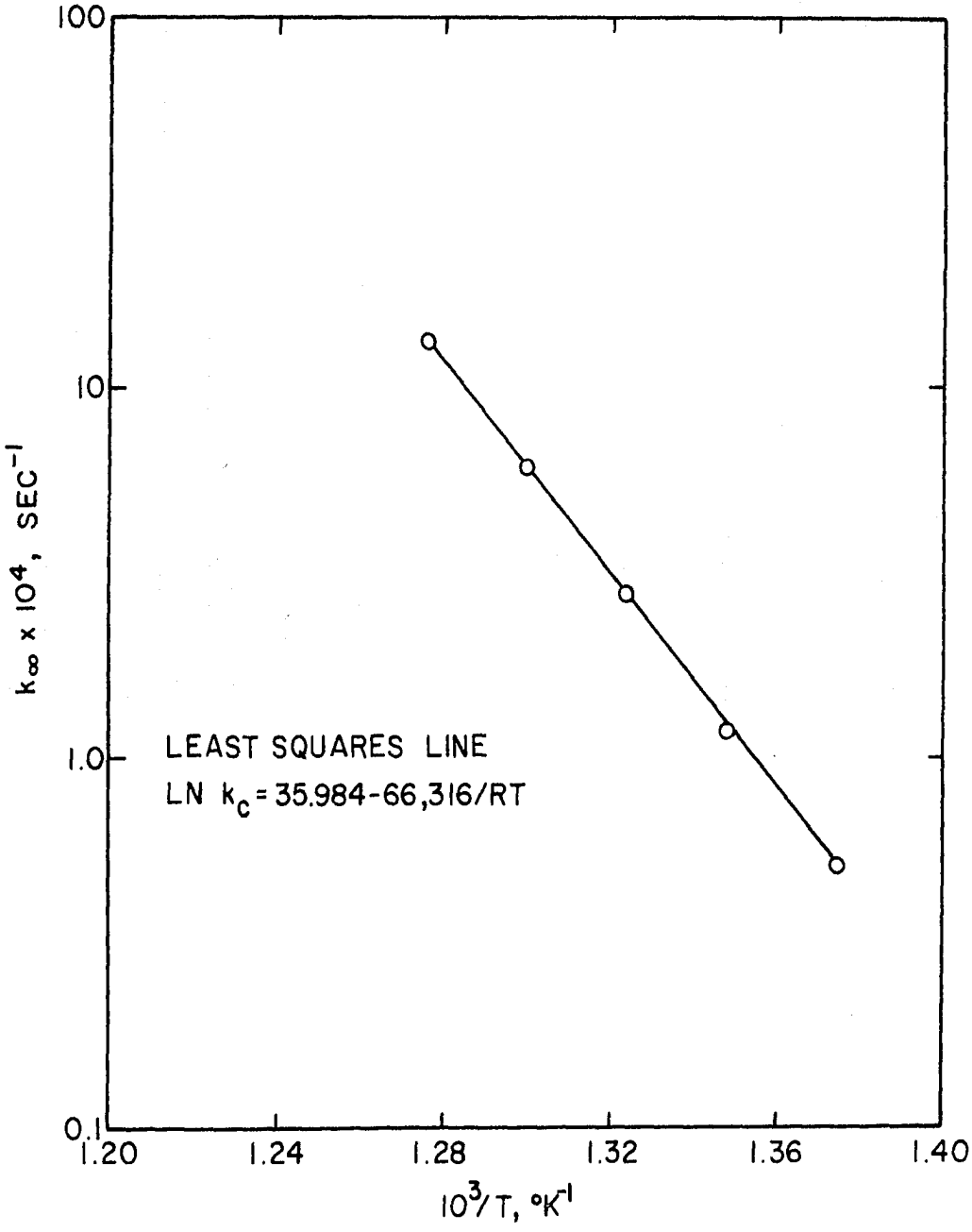


Figure 35. Arrhenius Correlation for Infinite Pressure.

Several investigators (C1), C3, (F1), (D2), of the cyclopropane isomerization reaction have computed Arrhenius parameters from their "infinite pressure" rate constant data. It is interesting to compare the results of extrapolations from pressures at or below one atmosphere to the results obtained from this investigation by extrapolation from higher pressures. Table 7 illustrates the range of Arrhenius parameters obtained and the maximum pressure used in each extrapolation. Although there is only a 5 percent spread in ℓn A and a 4 percent spread in the activation energy, sample values of k_∞ computed at 500°C show a 29 percent spread (5.9 to 8.1 x 10^{-4}). This deviation between investigators should be viewed in light of the $\pm$ 15 percent scatter of experimental data reported by some investigators (D2). The results of this study agree more closely with the more recent results of Falconer, Hunter and Trotman-Dickensen (F1) and Davis and Scott (D2) than with the earlier investigators.

The variation of the rate constant, k_c, with pressure has been discussed in Chapter II. The conclusions of that discussion were that the rate constant should increase with increasing pressure until some pressure, P_m, was reached. Beyond this pressure, the rate constant should decrease with increasing pressure. The variation of the rate constant with pressure was given by the integral of Equation (II-34):

TABLE 7

ARRHENIUS PARAMETERS FOR INFINITE PRESSURE RATE CONSTANTS

Reference Number	$\ell n(A)$	E_o, cal/g-mole	Max P atm
C1	34.89	65,000	1.
C3	36.502	67,500	--
F1	35.581	65,600	0.4
D2	35.431	65,570	1
This Study	35.984	66,316	28.1

$$\ln[k_c(P)] = \int_{P_1}^{P} \left[\frac{\partial \ln I(T,P)}{\partial P} - \frac{\bar{V}^* - \bar{V}_A}{RT} \right] dP + I_1 \qquad \text{(VIII-2)}$$

here I_1 is the logarithm of the rate constant at some pressure of reference P_1. As previously mentioned, values of $\bar{V}^*$, the specific volume of the activated complex, are not available. Therefore, the specific volume of propylene was chosen as a suitable approximation to $\bar{V}^*$. Experimental data of this investigation were available at the 482.2°C temperature level from 0.4 to 137 atmospheres to compare with the computed results of Equation (VIII-2). Figure 36 illustrates this comparison. A large majority of the experimental data falls within ± 1 percent of the predicted curve. The maximum value of the rate constant was computed to occur at 28 atmospheres, a reasonable value in light of the experimental data. Table 8 gives the specific volumes and other information needed to construct the curve in Figure 36.

Pipkin (P2), who conducted the first study of the thermal isomerization of cyclopropane at pressures substantially in excess of atmospheric, also observed a decrease in the rate constant with increasing pressure. Unfortunately, Pipkin was not able to show conclusively that his observed effect was due entirely to a change in reaction pressure. The main criticism of Pipkin's work was centered on the fact that he ran at a constant flow rate, therefore an increase in reactor

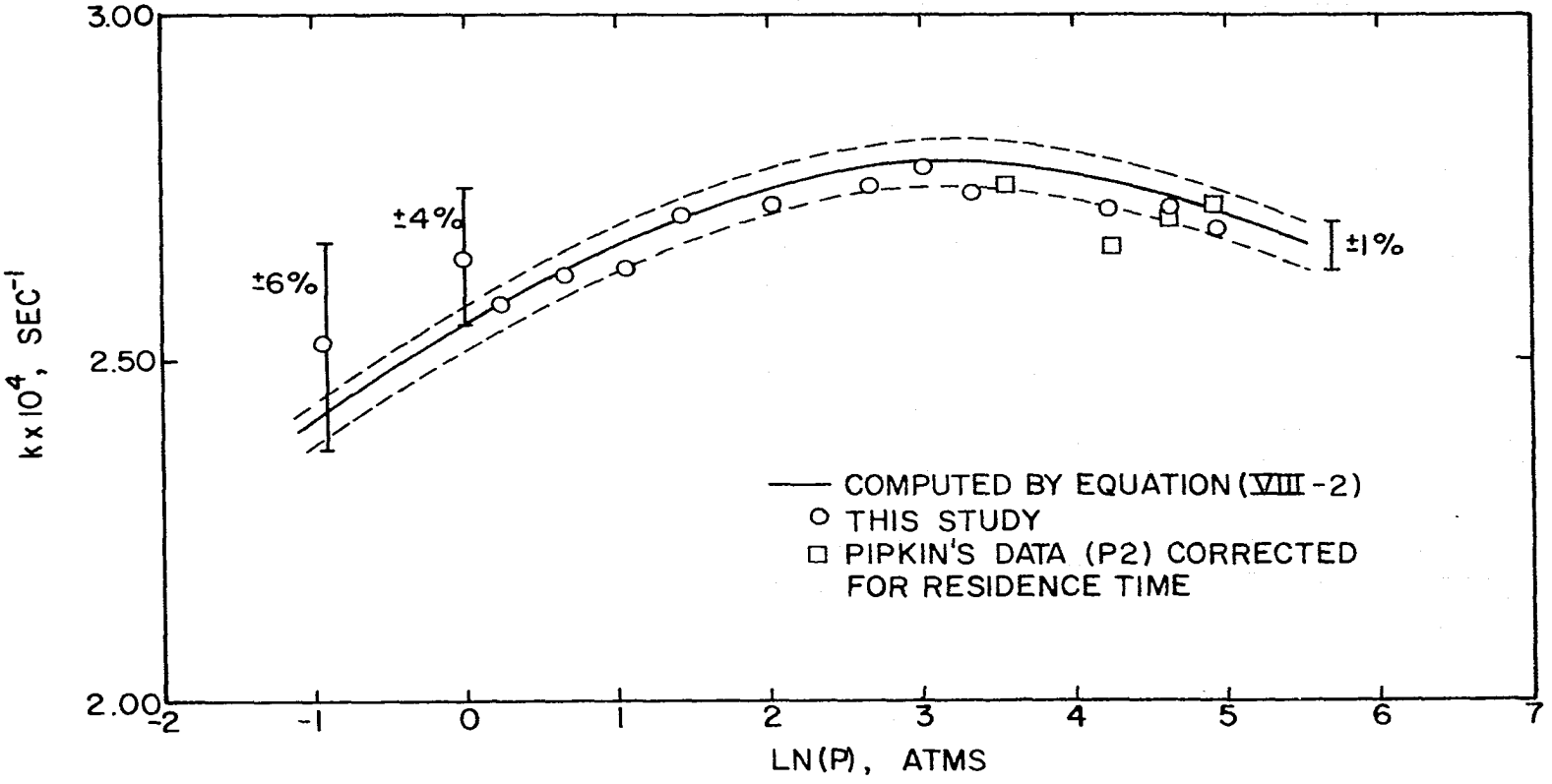


Figure 36. Variation of the Rate Constant with Pressure at 482.2°C.

TABLE 8

PARAMETERS USED IN EQUATION (VIII-2)
AT 482.2°C

Pressure (atms)	$\frac{\partial \ln I(T,P)}{\partial P} \times 10^3$	$\frac{\bar{V}^* - \bar{V}_A}{RT} \times 10^3$
1.5	29.3	0
2.5	16.1	0
5.0	3.7	0.158
8.0	1.67	0.159
13.0	0.883	0.162
15.0	0.566	0.163
20.0	0.388	0.166
25.0	0.210	0.169
30.0	0.156	0.172
45.0	0.068	0.180
50.0	0.042	0.183
60.0	0.025	0.188
80.0	0.020	0.199
90.0	0.018	0.205

$I_1 = \ln (2.77 \times 10^{-4})$ at 21 atmospheres

pressure increased his residence time. Since his longest residence times corresponded to his highest pressure, the possibility of undetected polymerization could not, at that time, be ruled out or accounted for. During the course of this study, an investigation into the effect of residence time on the rate constant was carried out. The results of this investigation are shown in Figure 37. The existence of a residence time effect is clearly shown and this effect is probably due to a polymerization and pyrolysis of the propylene product. Since this "residence time" effect had been strongly put forth as the explanation of Pipkin's observed decrease in rate constant with increasing pressure, an attempt was made to separate this effect from Pipkin's results. At each pressure level of Pipkin's investigation (35, 69, 103 and 137 atmospheres and 482.2°C), the rate constant and respective residence times for each pressure were averaged. The ratio k/k_o was obtained from Figure 37 and the relationship, $k_{cor} = k_\tau/[k/k_o]_\tau$, where k_{cor} is the corrected residence time, applied. The results of this correction are shown on Figure 36 and are labeled "Pipkin's Data (P2) corrected for residence time." In light of the ± 10 percent experimental error of Pipkin's data, his results agree well with the data of this study. It should be emphasized that the results of this investigation were obtained at residence times which were sufficiently low so that no residence

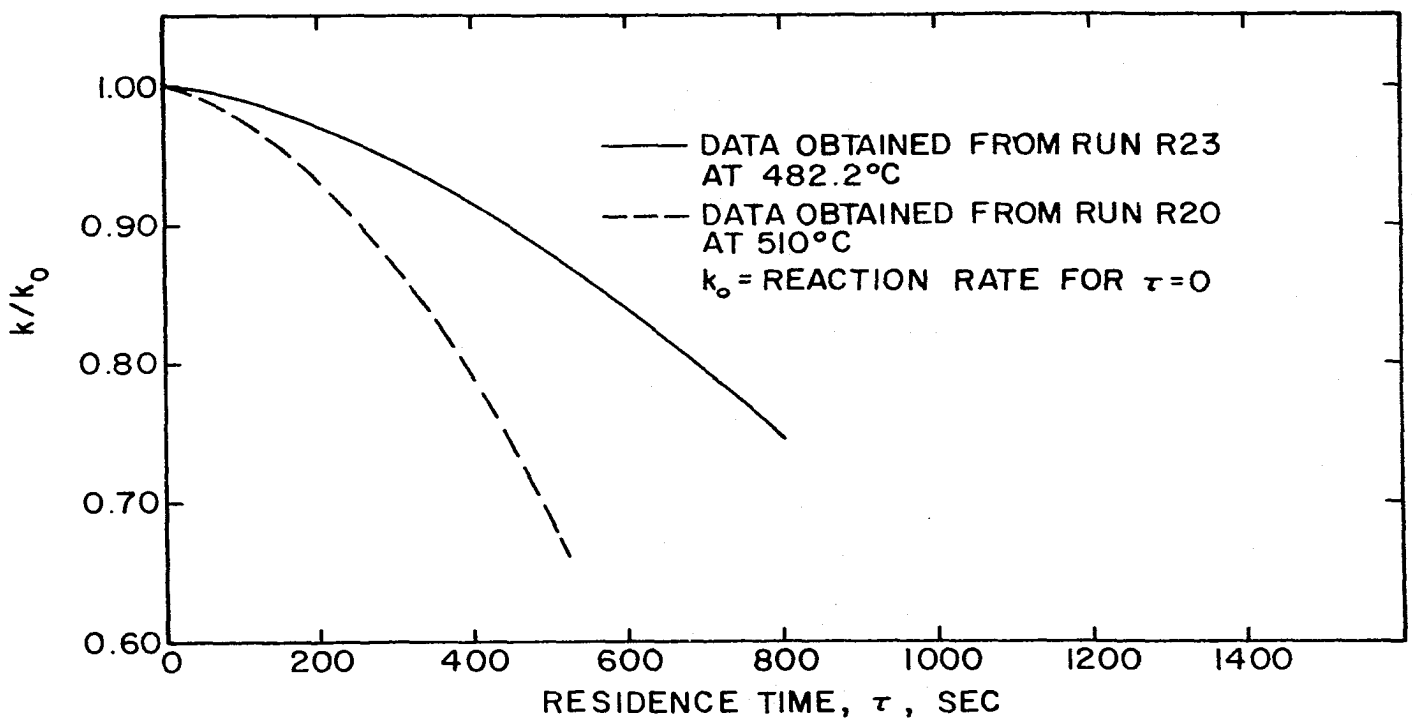


Figure 37. Effect of Residence Time on the Rate Constant at 482.2 and 510°C.

time corrections were required. In other words, it is doubtful that the decrease in rate constant shown in Figure 36 can be explained away by "undetected" polymerization arguments.

During the theoretical discussions of Chapter II, the term k_∞ was defined as a "supposedly" pressure independent rate constant referred to infinite pressure. The "correctness" of the interpretation of the term k_∞ is seriously questioned by the results of this investigation and the results of Pipkin (P2) as corrected for residence time. According to the theories of Kassel (K2), Rice and Ramsperger (R2) and Slater (S1), the unimolecular rate constant should be an ever increasing function of pressure, asympotically approaching the value of k_∞ (see Figure 34, here I(T,P) represents k/k_∞).

The results of this investigation show that the rate constant decreases with increasing pressure after some pressure P_m has been passed. Thus, the value of k_∞ computed from the curves of Kassel, etc. may be very different from the value of the rate constant at extremely high pressures. This difference is more clearly shown in Figure 38, where the inverse of the rate constant, $1/k_c$, is plotted with the inverse of pressure, 1/P. The development of Kassel and others predicts a positive slope for the curve $1/k_c$ versus 1/P. However, for very low values of 1/P (high pressures) the slope predicted from Equation (VIII-2)

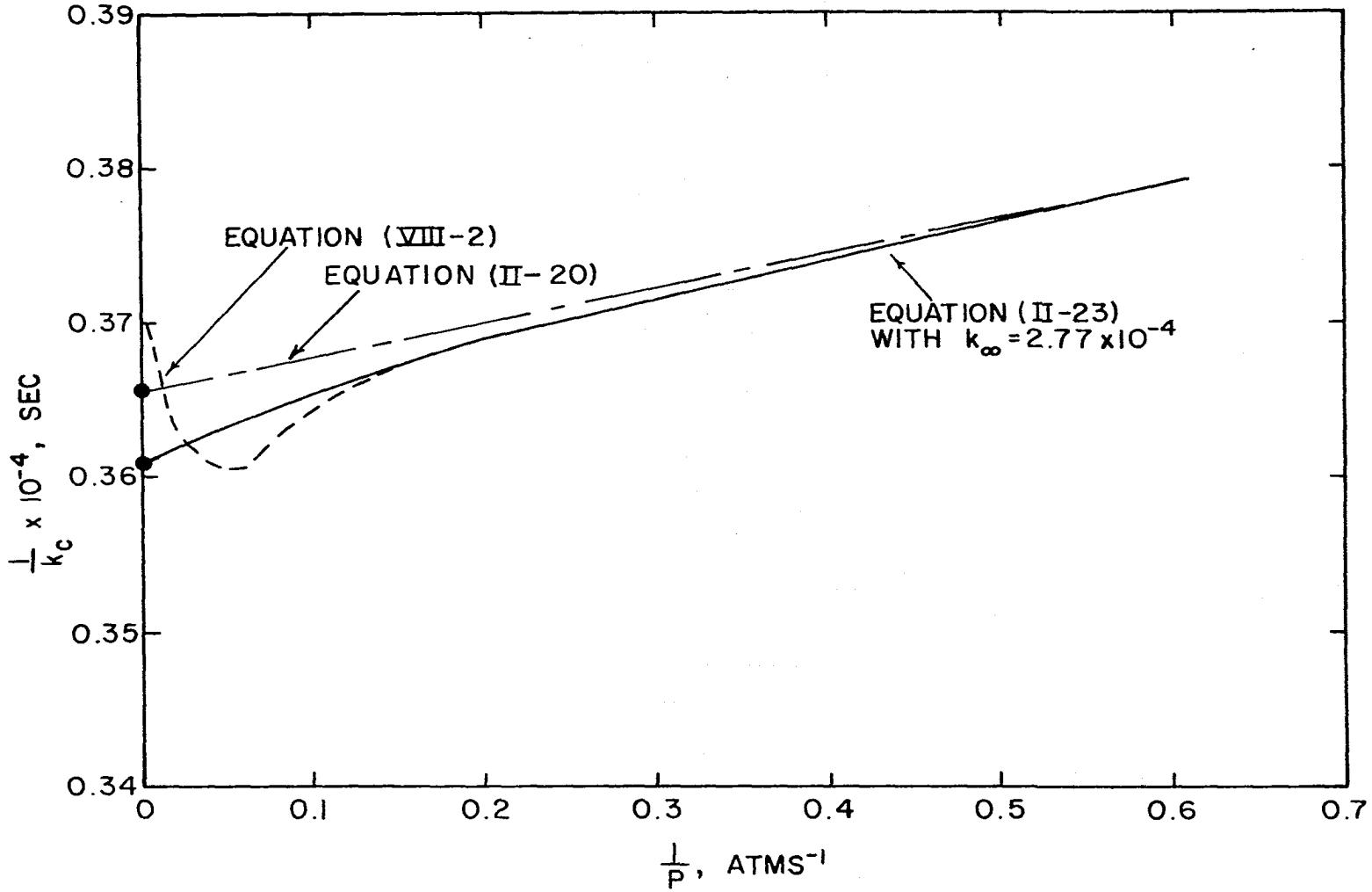


Figure 38. Plot of 1/k versus 1/P at 482.2°C.

is negative. The rate of change of $1/k_c$ with $1/P$ is very rapid in this region, further emphasizing the prediction that the value of k_∞ found by utilizing Equation (II-23), the intercept at $1/P=0$, may be very different from the experimental value of the rate constant found as $1/P \rightarrow 0$. The use of the term k_∞ as a rate constant referred to infinite pressure is incorrect, at least in numerical value.

Values of the rate constant computed from Equations (VIII-2), (II-37) and (II-38) are compared in Figure 39. As shown, the absolute reaction rate theory with a non-pressure dependent transmission coefficient [Equation (II-8)] predicts the variation in the rate constant with pressure at high pressures, but differs considerably at subatmospheric pressures. The theories of Kassel, Rice and Ramsperger, and Slater [Equation (II-23)] predict the rate constant variation up to 10 atms, but fail to show the decrease in rate constant with increasing pressure at high pressure. The theory developed in Chapter II [Equation (VIII-2)] describes the rate constant variation with pressure at both high and low pressures.

The rate constant based on thermodynamic activities, k_a, was computed utilizing the results of Pipkin's (P2) development:

$$k_a = \frac{k_c \rho_m}{f_i}$$

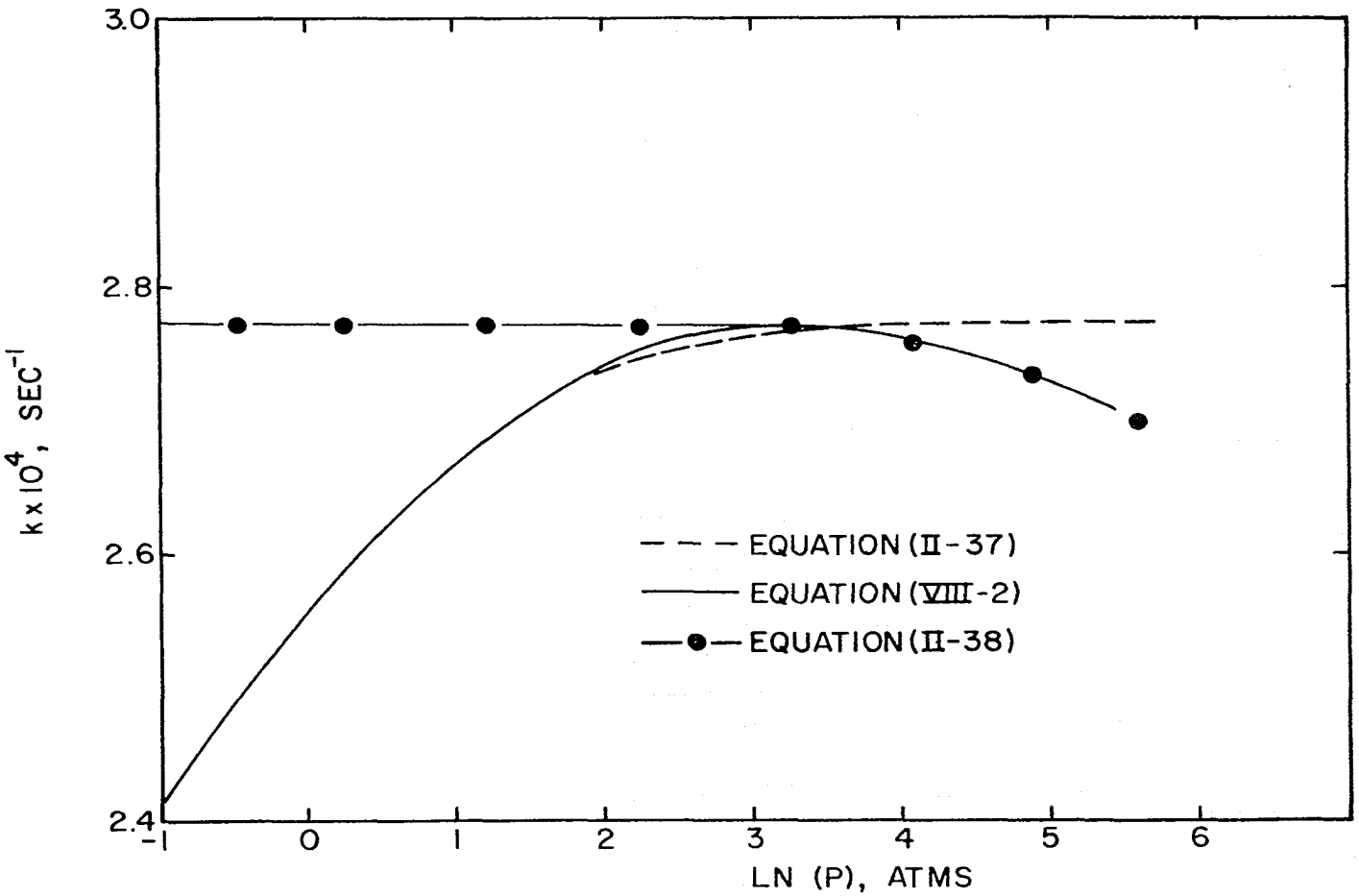


Figure 39. Comparison of Rate Constant Theories.

where ρ_m is the mixture molar density and f_i is the fugacity of pure cyclopropane. Values of the pure component fugacity were obtained by use of the BWR equation of state. As Figure 40 shows, both the concentration based rate constant and the activity based rate constant are functions of pressure. However, the activity based rate constant, k_a, appears "better behaved" with regard to pressure over the pressure range of this study.

As discussed in Chapter II, the activation energy, E_o, should also be a function of pressure. Using Equations (II-39) and (II-40), the activation energy from 10^{-5} to 150 atmospheres was computed. Figure 41 compares the results of this computation with the available experimental data. Table 9 lists the values of the activation energy used to construct the curve shown in Figure 41. As shown, the available data agree reasonably well with the computed curve.

The results of the 21 atms runs of this investigation can be compared to the results of Pipkin's study at 18 atms. Pipkin's 18 atms results should be free of the possibility of undetected polymerization previously discussed since the residence times for these runs were short. The results of this investigation can be expressed as:

$$\ell n\ (k_c) = 36.079 - 66{,}494/RT \qquad \text{(21 atms)}$$

Pipkin's results (P2) were:

$$\ell n\ (k_c) = 36.037 - 66{,}410/RT \qquad \text{(18 atms)}$$

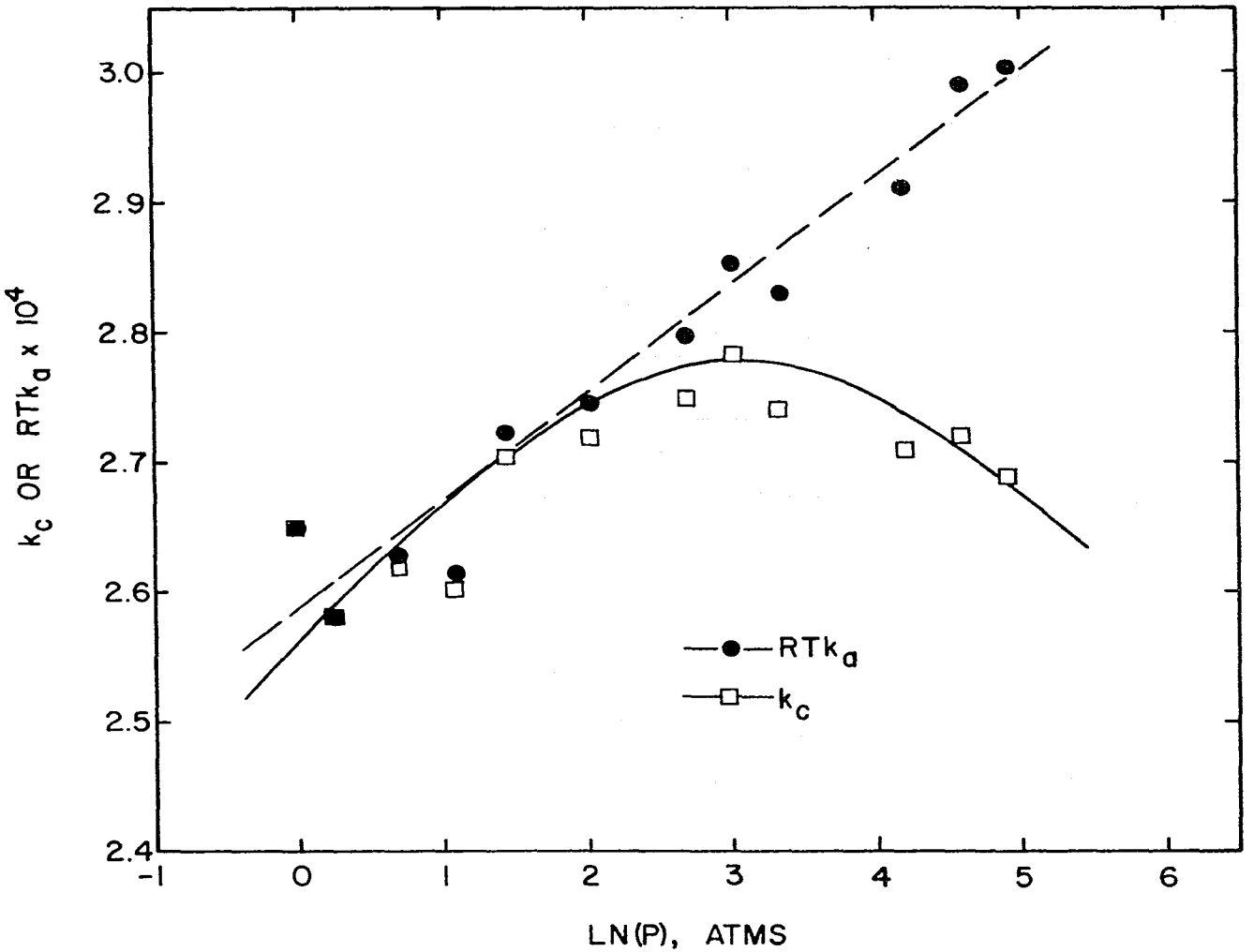


Figure 40. Comparison of k_c and RTk_a.

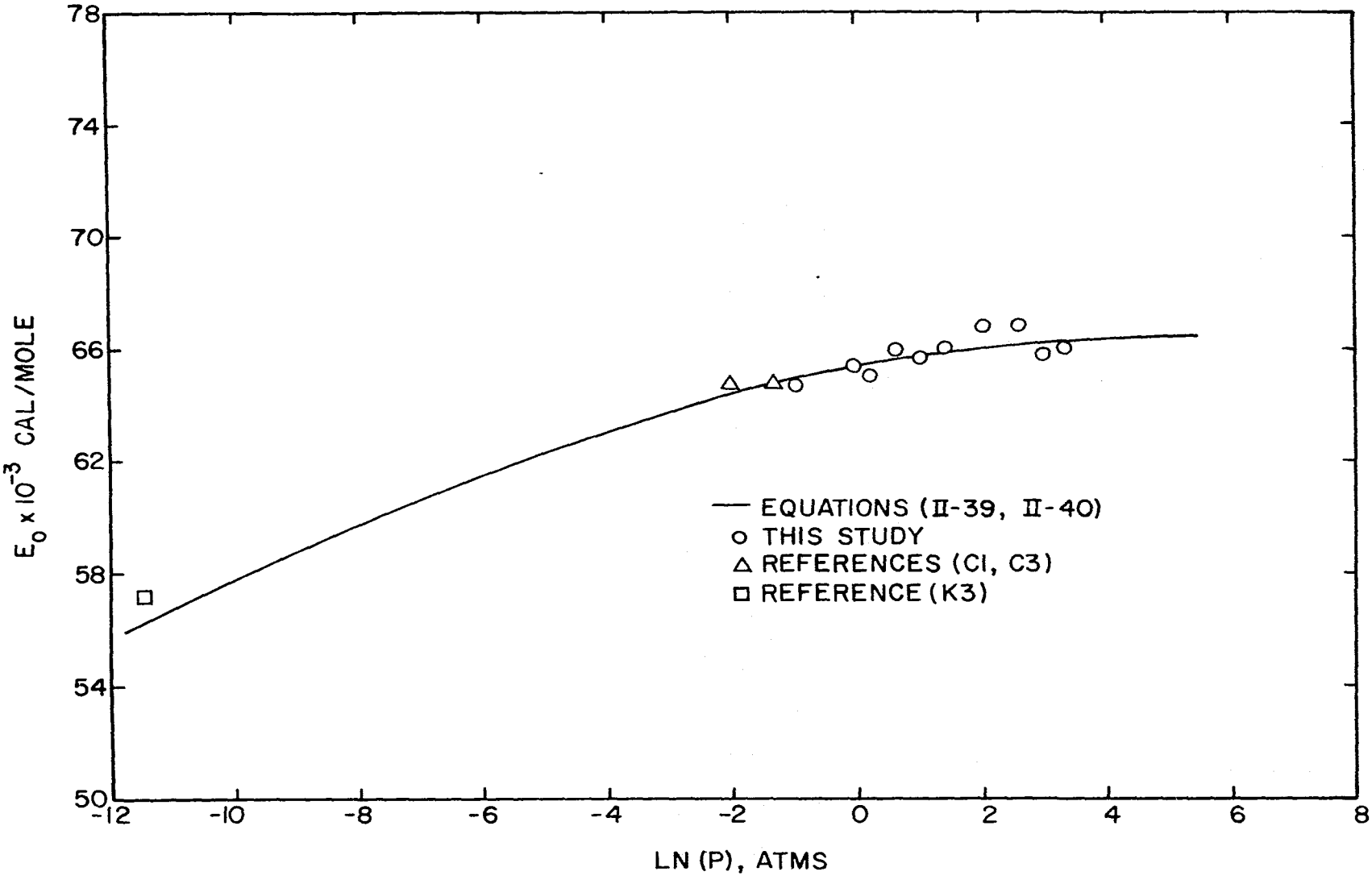


Figure 41. Variation of Activation Energy with Pressure.

TABLE 9

VARIATION OF ACTIVATION ENERGY WITH PRESSURE

P atms	E_o cal/mole
1×10^{-5}	56,450
0.01	62,220
0.02	62,850
0.05	63,650
0.20	64,720
0.37	65,100
1.00	65,550
20.0	66,000
150.0	66,500

The two correlations are in excellent agreement.

Another comparison between the results of this work and previous investigators is available at atmospheric pressure. Davis and Scott (D2) report the following Arrhenius parameters at atmospheric pressure:

$$\ell n\ (k_c) = 36.1923 - 66{,}950/RT \qquad (1\ atm)$$

The results of this work are:

$$\ell n\ (k_c) = 35.364 - 65{,}443/RT \qquad (1\ atm)$$

The two results are not in good agreement. It is interesting to note that the "infinite" pressure activation energy of 65,570 cal/mole computed by Davis and Scott is substantially less than their activation energy at atmospheric pressure. This result is in disagreement with the theoretical prediction for activation energy to increase with increasing pressure (see Figure 41). Further, Davis and Scott acknowledge deviations of 15 percent between their data and the derived Arrhenius correlation.

Rate constants were obtained at a pressure of 0.4 atms and for temperatures of 482.2 and 510°C. Due to difficulties in obtaining accurate flow measurement at subatmospheric pressure, the experimental error in these data is estimated to be ± 6 percent. The rate constant was found to be 11.76×10^{-4} at 510°C and 2.55×10^{-4} at 482.2°C. These results represent an average of all data at each

temperature level. Falconer, et al. (F1) report rate constants of 13.7×10^{-4} and 2.92×10^{-4} at 510 and 482.2°C. The results of Falconer, et al. appear high since their rate constants are greater than the highest rate constants (obtained in this study at about 30 atms) at each temperature level. Further, their values are higher than the computed "infinite" pressure rate constants determined from the data of this study.

Arrhenius parameters at 0.4 atms were found to be:

$$\ell n\ (k_c) = 34.831 - 64,701/RT$$

The activation energy of 64,701 cal/mole-°K at 0.4 atms is plotted in Figure 41 at $\ell n(P) = -0.93$. Considering that only two data points were available to compute E_o, the results agree favorably with the predicted curve.

CHAPTER IX

CONCLUSIONS

The conclusions derived from the results of this experimental investigation cover: the effect of temperature on the specific rate constant, the effect of pressure on the specific rate constant, the effect of pressure on the activation energy, the meaning of the rate constant at "infinite" pressure, and the usefulness of a flow apparatus for kinetic studies over wide ranges of pressure.

As expected, the temperature dependence for the rate data of this investigation was well represented by the Arrhenius relation: $\ln(k) = \ln(A) - E_o/RT$. Deviations between the Arrhenius relation and experimental data was generally well within the anticipated experimental error ($\pm$ 4%) of the investigation.

The analysis of Equation (II-36), indicating that the rate constant should increase with increasing pressure until some pressure P_m and then decrease with increasing pressure, was verified. The experimental results at 482.2°C agreed with the computed curve of rate constant versus pressure [Equations (II-36) or (VIII-2)] to within $\pm$ 1 percent, well within experimental error.

The effect of pressure on the activation energy was calculated using Equations (II-39) and (II-40). The available Arrhenius activation energies, E_o, agree within an average deviation of 0.6 percent of this calculation.

With reasonable certainty, the actual value of the rate constant at high pressures (over 100 atms) was shown to differ from the "infinite" pressure rate constant, k_∞, predicted from the theories of Kassel, etc. However, the rate constant at moderate pressures (5-40 atms) approached the numerical value of k_∞ very closely.

The use of a tubular, gold-lined, flow reactor was demonstrated to be useable from 0.4 to 137 atmospheres pressure in the study of the thermal isomerization of cyclopropane. Further, the use of a pressurized liquid flow system showed many advantages over a conventially pumped system, i.e.: large range of flow rates, ease of flow rate change and extreme consistency of flow rate.

NOMENCLATURE

a = thermodynamic activity

a' = constant in Equation A-2

A = component A in stoichiometric equation

A = frequency factor in Arrhenius equation

A^* = activated complex

A_o' = constant in Equation A-2

b' = constant in Equation A-2

B = component B in stoichoimetric equation

B_o' = constant in Equation A-2

c = dimensionless concentration, C/C_o

c' = constant in Equation A-2

C = concentration

C_o' = constant in Equation A-2

C_p = heat capacity at constant pressure

d = reactor diameter

D = diffusion coefficient

D = term in Equation II-23, $1.0/[\Gamma(s)(RT)^s]$

E_o = energy of activation

E_∞ = energy of activation referred to infinite pressure

F = partition function

F_o = volumetric flow rate at STP

G = Gibbs free energy

$\Delta G°$ = standard state free energy change associated with reaction

h = Planck's constant

H = enthalpy

H = heat transfer coefficient

H_{rxn} = heat of reaction

ΔH_{rxn} = rate of heat generation by reaction

I = integral defined by Equation II-23

k = specific reaction rate, sec^{-1}

K = thermal conductivity

K = equilibrium constant

K_B = Boltzman constant

L = axial length of reactor

M = molecular weight

n = number of moles

N = collision term, Equation II-4

P = pressure

r = rate of reaction

r = radius variable

R = reactor radius

R = resistance

R = gas law constant, 1.987 cal/mole-°K

R_1 = gas law constant, 8.314×10^7 gm cm^2/sec^2-mole-°K

R_2 = gas law constant, 0.08205 liter-atm/mole-°K

R_e = Reynolds number, $d\langle v\rangle\rho/\mu$

s = number of oscillators in Equation II-23

S^{o} = standard state entropy

t = time

T = temperature

U = dimensionless radius, r/R

V = local velocity of flow

V^{*} = molar average velocity

$\langle v \rangle$ = bulk velocity

V = reactor volume

x = mole fraction

Z = axial distance

Greek

α = dimensionless parameter, $D/k_c R^2$

Δ = symbol for difference

∂ = partial derivative

ϑ = dimensionless temperature, T/T_w

λ = contact time parameter, $k_c Z/2\langle v \rangle$

μ = viscosity

ν = dimensionless radial distance, r/R

ρ = density

ρ_o = density at STP

τ = residence time

σ = molecular radius

π = reduced pressure, P/P_c

Ω = collision integral

Subscripts

a = definition in terms of activity

A = component A (usually cyclopropane)

b = backward

B = component B (usually propylene)

c = definition in terms of concentration

f = forward

i = variable i or inlet condition

m = mixture property

o = outlet condition

r = radial

w = wall

Z = axial

∞ = refers to infinite pressure

Superscripts

* = activated complex

$\bar{}$ = molar units

REFERENCES

B1. Benedict, M., George B. Webb and L. C. Rubin, "An Empirical Equation for Thermodynamic Properties of Liqht Hydrocarbons and their Mixtures," J. Chem. Phys. 10, 747-58 (1942).

B2. Bird, R. B., W. E. Stewart, and E. N. Lightfoot, "Transport Phenomena," p. 557, John Wiley and Sons, Inc., New York (1962).

B3. Blades, A. T., "The Hydrogen Isotope Effect in the Pyrolysis of Cyclopropane," Can. J. Chem. 39, 1401 (1961).

B4. Bosworth, R. C. L., "Distribution of Reaction Times for Laminar Flow in Cylindrical Reactors," Phil. Maq. (London) (No. 7), 39, 847 (1948).

C1. Chambers, T. S. and G. B. Kistiakowsky, "Kinetics of the Thermal Isomerization of Cyclopropane," J. Am. Chem. Soc. 56, 399-405 (1934).

C2. Cleland, F. A. and R. H. Wilhelm, "Diffusion and Reaction in Viscous-flow Tubular Reactor," A.I.Ch.E. J. 2, 489 (1956).

C3. Corner, E. S. and R. N. Pease, "Kinetics and Mechanism of the Isomerization of Cyclopropane," J. Am. Chem. Soc. 67, 2067-2071 (1945).

D1. Danckwerts, P. V., "Continuous Flow Systems," Chem. Eng. Sci. 2, 1-13 (1953).

D2. Davis, B. R. and D. S. Scott, "Rate of Isomerization of Cyclopropane in a Flow Reactor," Ind. Eng. Chem. 3, (1964).

E1. Edmister, W. C., J. Vairogs and A. J. Klekers, "A Generalized B-W-R Equation of State," A.I.Ch.E. J. 14 (3), 479-82 (1968).

F1. Falconer, W. E., T. F. Hunter and A. F. Trotman-Dickenson, "The Thermal Isomerization of Cyclopropane," J. Chem. Soc. 164, 609 (1961).

G1. Gonikberg, M.G., "Chemical Equilibria and Reaction Rates at High Pressures," Translated by the Israel Program for Scientific Translations (1963).

H1. Hinshelwood, C. N., "On the Theory of Unimolecular Reactions," Proc. Roy. Soc., 113A, 230 (1926).

H2. Hirschfelder, J. O., R. B. Bird and E. L. Spotz, J. Chem. Physics 16, 968 (1948).

K1. Kassel, L. S., "Kinetics of Homogeneous Gas Reactions," The Chemical Catalog Co., Inc., New York (1932).

K2. Kassel, L. S., "Studies in Homogeneous Gas Reactions," J. Phys. Chem., 32, 235 (1928).

K3. Kennedy, A. D. and H. O. Pritchard, "The Thermal Isomerization of Cyclopropane at Low Pressures," J. Phys. Chem. 67, 161 (1963).

L0. Laidler, K. J., "Chemical Kinetics," 49-198, McGraw-Hill Book Company, New York (1965).

L1. Langrish, J. and H. O. Pritchard, "Secondary Effects in the Thermal Decomposition of Cyclopropane and Cyclobutane," J. Phys. Chem. 62, 761 (1958).

L2. Lapidus, L., Digital Computation for Chemical Engineers, 178, McGraw-Hill Book Company, Inc., New York (1962).

L3. Lee, A. L., K. E. Starling, J. P. Dolan and R. T. Ellington, "Viscosity Correlation for Light Hydrocarbon Systems," A.I.Ch.E. J. 10 (5), 694-97 (1964).

L4. Lindemann, F. A., "The Radiation Theory of Chemical Action," Trans. Faraday Soc. 17, 598 (1922).

L5. Lindquist, R. H. and G. K. Rollefson, "Relative Rates of Isomerization of Cyclopropane and Cyclopropane-t_1," J. Chem. Phys. 24, 725 (1956).

L6. Lyderson, A. L., R. A. Greenkorn and O. A. Hougen, Univ. Wisc. Exptl. Stat. Rept. 4, (1955).

N1. Nelson, L. C. and E. F. Obert, "Generalized Compressibility Charts," Chem. Eng., July (1954).

P1. Perrin, J., Ann. Phys. 11 (9), 1 (1919).

P2. Pipkin, O. A., "Thermal Isomerization of Cyclopropane at Elevated Pressures," Ph.D. Thesis, University of Oklahoma, Norman, Oklahoma (1964).

P3. Pritchard, H. O., R. G. Sowden and A. F. Trotman-Dickenson, "The Isomerization of Cyclopropane--A Quasi-Unimolecular Reaction," J. Am. Chem. Soc. 74, 4472 (1952).

P4. Pritchard, H. O., R. G. Sowden and A. F. Trotman-Dickenson, The Isomerization of Cyclopropane--A Quasi-Unimolecular Reaction," Proc. Royal Soc. A217, 563 (1953).

R1. Rabinovich, B. S., E. W. Schlag and K. B. Wiberg, "Geometrical and Structural Unimolecular Isomerization of Symcyclopropane-d_2," J. Chem. Phys. 28, 504 (1958).

R2. Rice, O. K. and H. C. Ramsperger, "Theories of Unimolecular Gas Reactions at Low Pressure," J. Am. Chem. Soc. 49, 1617 (1927).

R3. Roberts, R. M., "Catalytic Isomerization of Cyclopropane," J. Phys. Chem. 63, 1400 (1959).

S1. Slater, N. B., "Theory of Unimolecular Reactions," Cornell University Press, Ithaca, N. Y. (1959).

S2. Slater, N. B., "The Theoretical Rate of Isomerization of Cyclopropane," Proc. Royal Soc. (London) A218, 224 (1953).

S3. Slater, N. B., Theoretical Temperature Dependence of the Rate of Isomerization of Cyclopropane," J. Chem. Soc. 164, 606 (1961).

T1. Trautz, M. and K. Winkler, J. Prakt. Chem. 104 (2) 53 (1922).

W1. Weston, Jr., R. E., "Effect of Pressure on the Isotope Effect in a Unimolecular Gaseous Reaction: Tritium and Carbon-13 Effects in the Isomerization of Cyclopropane," J. Chem. Physics 26, 975 (1957).

W2. Weston, Jr., R. E., "Tritium Isotope Effect in the Isomerization of Cyclopropane," J. Chem. Phys. 23, 988 (1955).

APPENDIX A

CALCULATION OF PHYSICAL PROPERTIES

In any kinetic study conducted in a gaseous flow system, accurate values of certain physical properties are required. The most important property is the density of the reacting gases, for the residence time is directly related to the density:

$$\tau = V\rho_{RC}F_o/\rho_o \qquad \text{(A-1)}$$

where: τ = residence time

V = reactor volume

ρ_{RC} = density at reactor conditions

ρ_o = density at standard conditions

F_o = flow rate at standard conditions

Equation (A-1), of course, implies the assumption of plug flow which will be examined in Appendix B. In analyzing the results of this investigation, a reduced form of the Benedict-Webb-Rubin equation of state (B1) developed by Edmister, Vairogs and Klerkers (E1) was used. Briefly, Edmister's generalization of the BWR equation involved placing the original equation, in which pressure was a function of density, temperature and eight constants

specific for each pure substance, into an equation in which the reduced pressure is a function of the reduced temperature, reduced density and eight constants, each of which was a simple function of the acentric factor. Their equations are:

$$\pi = \theta\rho_r + (B_o'\theta - A_o' - C_o'/\theta^2)\rho_r^2 + (b'\theta - a)\rho_r^3 + (a'\alpha)\rho_r^6 + \frac{C'\rho_r^3}{\theta^2}(1 + \gamma'\rho_r^2)\exp(-\gamma\rho_r^2) \qquad \text{(A-2)}$$

where: $\pi = P/P_c$

$\theta = T/T_c$

$\rho_r = \rho RT_c/P_c$

A'_o, B'_o etc $= \Phi(\omega)$

In testing Equation (A-2), Edmister found it to be comparable to the original BWR equation in accuracy. Figure 42 shows the compressibility of pure cyclopropane computed from Equation (A-2) compared with the generalized prediction methods of Nelson and Obert (N1) and Lyderson, Greenkorn and Hougen (L6).

Due to the good agreement between Equation (A-2) and the generalized methods, Equation (A-2) was used to compute cyclopropane densities for all runs in this study. Since the density of cyclopropane and propylene differ by less than 1% over the temperature and pressure ranges

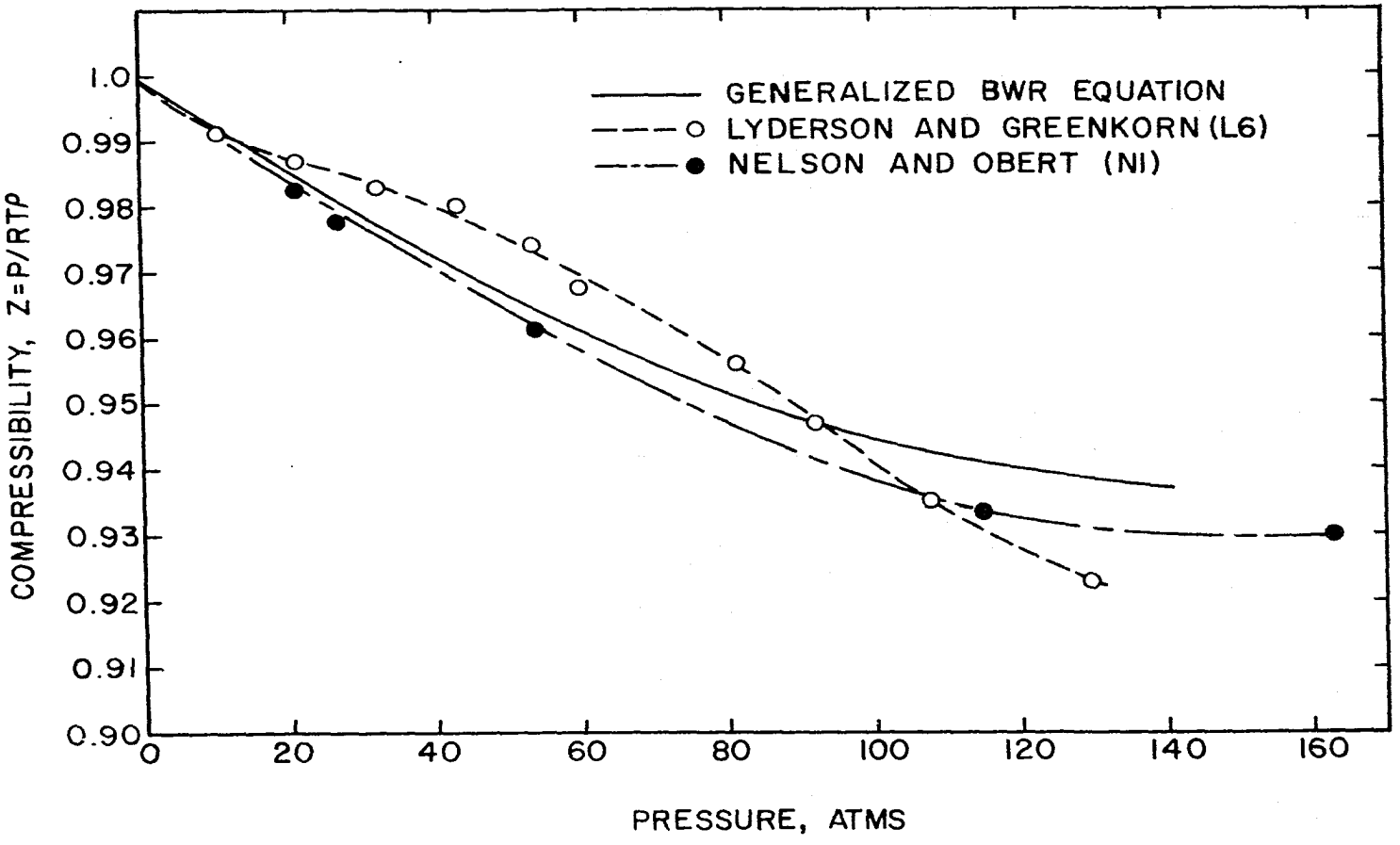


Figure 42. Compressibility of Cyclopropane at 482.2°C.

covered in this investigation, the density of pure cyclopropane was taken as the density of the reactant gases.

Viscosity and diffusion coefficient are important parameters in determining whether or not the assumption of plug flow is valid for a tubular reactor. Viscosity values are necessary in determining the Reynolds number:

$$R_e = d\langle V\rangle\rho/\mu \qquad \text{(A-3)}$$

where: d = tube diameter

$\langle V\rangle$ = bulk velocity

ρ = density

μ = viscosity

It is generally accepted that for Reynolds numbers below 2100, and in the absence of diffusion effects, laminar flow is prevalent. The viscosity correlation of Lee, Starling, Dolan and Ellington (L3) was chosen as the most appropriate method of computing gas phase viscosity at the conditions employed in this study. Their correlation is semiempirical, relating viscosity to temperature, molecular weight and density in the following equations:

$$\mu = K \exp(X\rho^Y) \qquad \text{(A-4)}$$

$$K = (7.77 + .0063M)T^{1.5}/(122.4 + 12.9M + T) \qquad \text{(A-5)}$$

$$X = 2.57 + 1914.5/T + .0095M \qquad \text{(A-6)}$$

$$Y = 1.11 + .04\,X \qquad \text{(A-7)}$$

where: μ = viscosity in micropoise

ρ = density in g/cm^3

M = molecular weight

T = temperature in °R

Equation (A-4) represented the viscosity of propane to within 1 percent over a wide range of temperatures and pressures. It should be similarly accurate for computing cyclopropane or propylene viscosity.

All runs in this investigation were conducted at Reynolds numbers below 2100. However, the assumption of plug flow was made in analyzing the kinetic data. It is the purpose of Appendix B to justify this assumption, therefore only the method of computing the diffusion coefficient will be discussed in this section. The correlation frequently attributed to Hirschfelder, Bird, and Spotz (H2) was used to determine diffusion coefficients in this study. Other correlations are available but they do not offer substantial increases in accuracy to warrant their use. The HBS equation is:

$$D_{12} = \frac{0.001858T^{3/2}\,[(M_1+M_2)/M_1M_2]^{1/2}}{P\,\sigma_{12}{}^2\Omega_D} \qquad \text{(A-8)}$$

where T = temperature in °K

M = molecular weight

P = pressure in atmospheres

$\sigma_{12} = (\sigma_1+\sigma_2)/2$ = collision diameter in angstroms

Ω_D = collision integral for diffusion

It is not possible to predict the accuracy of Equation (A-8) as experimental data for the cyclopropane-propylene system are not available. Table 10 of Appendix B lists the values of ρ, μ, and D used to examine the effects of diffusion in a tubular reactor.

APPENDIX B

EVALUATION OF THE EFFECTS OF LONGITUDINAL AND AXIAL DIFFUSION IN A TUBULAR REACTOR

One of the most frequent simplifying assumptions made in the analysis of kinetic data from tubular reactors is that of plug flow. When well developed turbulent flow exists, this assumption is usually satisfactory. In the laminar flow region, plug flow can be correctly assumed only under certain conditions. It is the purpose of this section to develop criteria for determining when the plug flow assumption is valid and to establish the effects of longitudinal diffusion on the expected conversion.

In the absence of diffusion, natural convection and thermal effects, the radial velocity distribution is given by the well known Poiseuille equation:

$$V(r) = 2\langle v \rangle \ (1-r^2/R^2) \qquad \text{(B-1)}$$

It is evident that the center streamline (r = 0) will have a smaller residence (reaction) time than any element at a greater radius. This condition gives rise to a distribution

of residence times which has been discussed by Bosworth (B4). If radial diffusion is present, the picture becomes more complicated. Cleland and Wilhelm (C2), using numerical integration, solved the basic partial differential equation describing the concentration field in a circular tube where a fluid in laminar flow is undergoing a first order reaction. In dimensionless form, the equation which they solved was:

$$-(1-\nu^2)\frac{\partial c}{\partial \lambda} + \alpha \frac{\partial^2 c}{\partial \nu^2} + \frac{1}{\nu}\frac{\partial c}{\partial \nu} - c = 0 \qquad \text{(B-2)}$$

with boundary conditions:

(1) $c = 1$ at $\lambda = 0$

(2) $\partial c/d\nu = 0$ at $\nu = 1$ and at $\nu = 0$

where: $\lambda = k_c Z/2\langle v \rangle$

$c = c/c_o$

$\alpha = D/k_c R^2$

$\nu = r/R$

Equation (B-2) involves the following assumptions:

(1) isothermal conditions,

(2) laminar flow fully developed,

(3) axial diffusion small in comparison to radial diffusion,

(4) constant diffusivity.

Cleland and Wilhelm solved Equation (B-2) for values of α and λ for which $\alpha\lambda = 1$.

Generally, the values of α encountered in this investigation were much larger than those covered by Cleland and Wilhelm and the values of λ much smaller. Therefore Equation (B-2) and associated boundary conditions were solved by a method similar to that used by Lapidus (L2) for a new range of parameters.

The results of the numerical solution indicated that the ratio α/λ could be used as the criteria for determining validity of the plug flow assumption. Figure 43 shows the relationship between α/λ and the maximum percent error involved in assuming plug flow. The percent error was determined as follows:

$$\text{Percent error} = 100\left|(C_{PF} - C_{NI})/C_{NI}\right| \quad \text{(B-3)}$$

where: C_{PF} = plug flow concentration

C_{NI} = numerical integration concentration

For values of α/λ greater than 9, the error in assuming plug flow will be less than 0.5 percent. In general, values of α/λ for this investigation were larger than 100, so the assumption of plug flow in analyzing the results appears valid.

Danckwerts (D1) has analyzed the effect of longitudinal diffusion on tubular reactor conversion in the absence of velocity gradients. He found that while longitudinal diffusion tends to lower the conversion below that expected for plug flow, the effect is negligible provided $k_c^2 DL/\langle v\rangle^3 \ll 1$ holds. All runs in this study fulfilled

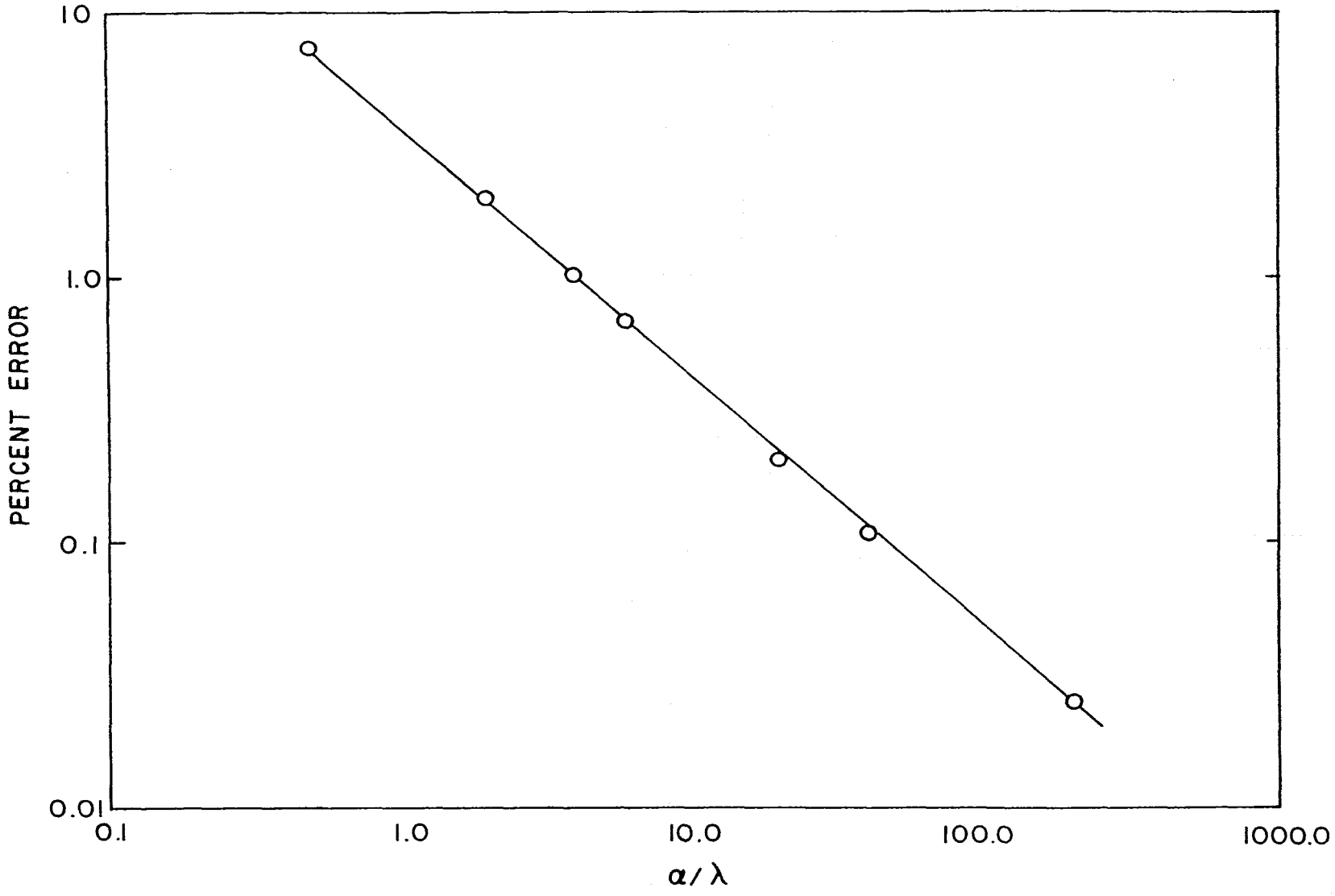


Figure 43. Error in Assuming Plug Flow.

this criterion.

In summary, it can be said that: (1) all runs in this study existed in the laminar flow region, (2) the plug flow assumption was valid in the kinetic data analysis and (3) longitudinal diffusion had a negligible effect on conversion levels. Values of the parameters α, λ and $k_c^2 DL/\langle v \rangle^3$ were computed for each run using the physical property estimation techniques discussed in Appendix A. The results are tabulated in Table 10.

TABLE 10

RESULTS OF PARAMETER CALCULATIONS

Run Number	Density (mole/liter)	Viscosity (micropoise)	Diffusion (cm^2/sec)	V_s (cm/sec)	α/λ	$K_c^2 DL/\nu_s^3$ ($\times 10^8$)	Reynolds Number
R1-50	0.0706	199.4	0.0874	6.79	210,000	.982	81
R1-100	0.1254	200.0	0.0493	5.00	86,000	1.41	106
R1-200	0.2371	201.3	0.0262	5.16	46,200	.691	205
R1-300	0.3486	202.8	0.0179	5.22	30,700	.473	302
R1-400	0.4609	204.5	0.0136	5.35	24,600	.321	407
R2-50	0.0681	205.5	0.0930	14.89	22,600	2.15	167
R2-100	0.1215	206.0	0.0522	11.43	8,400	3.08	227
R2-200	0.2281	207.3	0.0279	10.32	4,440	2.08	383
R2-300	0.3353	208.8	0.0191	10.29	2,860	1.48	557
R2-400	0.4434	210.4	0.0145	10.51	2,190	1.06	747
R3-50	0.0654	211.4	0.0994	68.29	5,230	.504	713
R3-100	0.1170	212.0	0.0557	38.11	1,590	1.67	709
R3-200	0.2196	213.2	0.0297	20.10	453	6.00	698
R3-300	0.3230	214.7	0.0203	13.49	210	13.30	684
R3-400	0.4273	216.2	0.0154	10.12	120	24.03	674
R4-50	0.0732	193.3	0.0820	6.88	5,550,000	.032	88
R4-100	0.1301	193.8	0.0462	4.52	2,440,000	.053	102
R4-200	0.2464	195.1	0.0245	2.30	682,000	.207	98
R4-300	0.3627	196.7	0.0167	2.52	488,000	.111	157
R4-400	0.4803	198.5	0.0127	2.62	335,000	.086	214
R5-50	0.0665	208.5	0.0965	46.35	15,400	.351	499
R5-100	0.1187	209.0	0.0542	26.07	5,100	1.06	499
R5-200	0.2233	210.4	0.0289	13.74	1,300	4.22	492
R5-300	0.3285	211.8	0.0197	10.03	670	7.14	524
R5-400	0.4347	213.4	0.0149	8.34	420	9.32	573
R6-50	0.0689	202.5	0.0908	8.60	57,000	2.44	99
R6-100	0.1236	203.1	0.0507	6.36	22,700	3.49	131
R6-200	0.2317	204.3	0.0271	3.83	7,600	8.21	146
R6-300	0.3411	205.8	0.0185	3.58	4,650	7.08	200
R6-400	0.4523	207.5	0.0140	3.56	3,550	5.37	262
R7-50	0.0655	211.4	0.0993	53.79	4,100	1.03	562
R7-100	0.1171	212.0	0.0556	36.95	1,650	1.71	688
R7-200	0.2196	213.2	0.0297	20.66	500	5.07	718
R7-300	0.3237	214.6	0.0202	15.31	250	8.67	778
R7-400	0.4278	216.2	0.0153	11.60	140	15.36	773
R8-30	0.0471	205.6	0.135	13.90	26,500	4.39	107
R8-15	0.0309	205.4	0.205	17.74	52,300	3.19	90
R8-5	0.0206	205.7	0.309	14.25	54,300	10.76	48
R8-atms	0.161	205.7	0.395	18.44	87,900	6.49	49

TABLE 10 (Continued)

Run Number	Density (mole/liter)	Viscosity (micropoise)	Diffusion (cm^2/sec)	$\bar{v}$ (cm/sec)	η/λ	$K_c^2 DL/\bar{v}$ ($\times 10^8$)	Reynolds Number
R9-30	0.0492	199.0	0.125	2.85	154,500	15.57	24
R9-30A	0.0487	199.0	0.126	3.73	199,000	7.19	31
R9-15	0.0323	198.9	0.191	4.41	355,000	6.54	24
R9-5	0.0210	198.8	0.293	6.60	849,000	2.90	24
R9-atms	0.0168	198.8	0.366	7.61	1,150,000	2.49	22
R10-30	0.0483	199.1	0.1276	2.49	105,800	30.99	20
R10-30A	0.0486	199.1	0.1268	6.77	302,000	14.43	56
R10-15	0.0321	198.9	0.1920	4.07	257,000	10.77	22
R10-5	0.0209	198.9	0.2944	5.69	506,000	6.59	20
R10-atms	0.0167	198.9	0.3683	7.49	871,000	3.45	21
R11-30	0.0451	211.2	0.1442	22.80	1,360	36.7	164
R11-15	0.0298	211.1	0.2180	34.24	1,500	33.8	163
R13-200	0.2364	201.4	0.0263	3.65	35,500	1.81	144
R13-100	0.1257	200.1	0.0492	7.14	134,500	0.439	151
R13-50	0.0708	199.5	0.0872	10.21	341,000	0.266	122
R14-50	0.0690	202.6	0.0907	4.98	31,900	12.90	57
R14-30	0.0478	202.4	0.1311	7.02	70,700	6.11	56
R14-15	0.0315	202.3	0.1991	10.76	163,500	2.60	56
R15-50	0.0709	197.4	0.0860	2.71	278,000	4.49	33
R15-30	0.0492	197.2	0.1240	4.24	616,000	1.73	36
R15-15	0.0327	197.1	0.1866	6.40	1,441,000	0.733	36
R16-50	0.0730	193.4	0.0822	2.50	1,950,000	0.690	32
R16-30	0.0505	193.2	0.1189	3.58	4,280,000	0.320	32
R16-15	0.0333	193.1	0.1800	5.30	9,860,000	0.145	31
R16-5	0.0220	193.0	0.2723	8.35	21,300,000	0.062	32
R16-atms	0.0173	193.0	0.3458	7.57	25,000,000	0.104	23
R18-50	0.0689	202.5	0.0908	5.33	34,300	10.54	61
R18-30	0.0477	202.3	0.1310	7.26	69,600	5.81	58
R18-15	0.0313	202.2	0.1997	11.13	164,300	2.43	58
R18-5	0.0206	202.1	0.3032	16.77	395,000	1.03	58
R18-atms	0.0164	202.1	0.3808	21.09	611,000	0.663	58
R19-50	0.0720	196.5	0.0846	2.69	399,000	3.09	33
R19-30	0.0496	196.3	0.1226	3.82	861,000	1.48	33
R19-15	0.0327	196.2	0.1860	5.57	1,800,000	0.769	31
R19-5	0.0215	196.1	0.2830	8.74	4,500,000	0.287	32
R19-atms	0.0169	196.1	0.3598	11.08	7,180,000	0.183	32

TABLE 10 (continued)

Run Number	Density (mole/liter)	Viscosity (micropoise)	Diffusion (cm^2/sec)	V_∞ (cm/sec)	r/λ	$K_c^2 DL/V_\infty^3$ ($\times 10^8$)	Reynolds Number
R20-400-1	0.4444	210.4	0.0144	6.03	1473.	4.82	428
R20-400-2	0.4442	210.4	0.0144	3.76	928.	19.66	267
R20-400-3	0.4448	210.3	0.0144	10.95	2597.	0.828	777
R20-400-4	0.4441	210.4	0.0144	2.09	561.	105.10	149
R20-400-5	0.4443	210.4	0.0144	1.07	458.	488.10	76
R21-0.4-1	0.0061	205.0	1.034	18.93	348,300.	10.64	19
R21-0.4-2	0.0062	205.0	1.024	13.21	248,438.	30.09	13
R21-0.4-3	0.0062	205.0	1.027	9.78	198,202.	69.13	10
R22-0.4-1	0.0064	199.0	0.968	8.51	3,333,333.	4.83	9
R22-0.4-2	0.0063	199.0	0.973	7.37	2,793,388.	7.75	8
R23-1	1.1497	217.2	0.0055	3.22	6306.	0.583	566
R23-2	1.1503	217.2	0.0055	6.07	11320.	0.091	1069
R23-3	1.1504	217.2	0.0055	1.50	3180.	5.30	264
R23-4	1.1549	217.3	0.0055	0.61	1986.	51.78	107
R24-1000	1.1515	217.2	0.0055	7.14	14311.	0.052	1258
R24-1500	1.7352	230.3	0.0037	6.14	8050.	0.056	1523
R24-2000	2.3221	245.5	0.0028	5.83	5977.	0.047	1796

APPENDIX C

COMPUTER PROGRAM FOR ANALYSIS OF EXPERIMENTAL DATA

R1-50	Run Number
28.70	Barometric Pressure, In. Hg
25.0	Room Temp, °C
922.0 7.0	Control Setting, Crse-Fine
8.0	Air Flow Indicator Rdg
9.2	Propane Rotameter Rdg
55.321	Bridge Reading, Ohms
0.0076	Bridge Correction, Ohms
26.5	Bridge Temp, °C
50.0	Reactor Pressure, PSIG
27.4	Flow Meter Temp, °C
1.54	Flow Meter ΔP, In. Hg.
78.6	Flow Time, Sec
461.97	Flow Range
1	Flow Meter Code, 1 = SBM 2 = WTM
3.75	Flow Rotameter Rdg
1 6	Sample #, Reactor-Preh
0.9972	Inlet Conc
0.9771	Outlet Conc
1	Temperature Code

Remarks: very smooth run

Figure 44. Sample Input Data.

```
//ISO  JOB RS-02349,JOHNSON,MSGLEVEL=1
C    PROGRAM TO ANALYZE DATA FOR STUDY OF THE THERMAL ISOMERIZATION OF  CYCLO-
C         PROPANE
C
C    NOMENCLATURE
C    ************
C
C         PBAR  = BAROMETRIC PRESSURE, INCHES HG
C         TRM   = ROOM TEMPERATURE, DEG C
C         CRSE  = COARSE CONTROL SETTING
C         CFNE  = FINE CONTROL SETTING
C         FLA   = AIR FLOW INDICATOR
C         FPR   = PROPANE ROTAMETER
C         RMB   = MUELLER BRIDGE READING, OHMS
C         TMB   = MUELLER BRIDGE TEMPERATURE, DEG C
C         BC    = MUELLER BRIDGE CORRECTION, OHMS
C         NCODE = FLOW METER CODE, 1=SBM  2=WTM
C         TFM   = FLOW METER TEMPERATURE, DEG C
C         DELP  = FLOW METER DELTA P, INCHES HG
C         TMF   = FLOW TIME, SEC
C         RNGE  = FLOW METER RANGE
C         RFR   = FLOW ROTAMETER READING
C         MVTS  = BATH THERMOCOUPLE, MV
C         NSAMP = SAMPLE NUMBER
C         CONCI = INLET CONCENTRATION, MOLE FRACTION
C         CONCO = OUTLET CONCENTRATION, MOLE FRACTION
C         TF    = REACTOR TEMPERATURE, DEG F
C         TC    =                    , DEG C
C         RT    = CORRECTED MUELLER BRIDGE RESISTANCE, OHMS
C
C         PR    = REACTOR PRESSURE, PSIG
     5 FORMAT(6A4)
    10 FORMAT(F10.3,F10.3)
    15 FORMAT(F10.4)
    20 FORMAT(2I5)
    25 FORMAT(F10.5)
```

```
 35 FORMAT(1H+,T40,6A4)
100 FORMAT(1H ,15X,'DATA ANALYSIS FOR RUN')
105 FORMAT(1H0)
110 FORMAT(1H ,'SUMMARY OF RUN VARIABLES')
115 FORMAT(1H ,'******* ** *** *********')
120 FORMAT(1H ,5X,'BAROMETRIC PRESSURE      = ',F6.2,' INCHES HG')
125 FORMAT(1H ,5X,'ROOM TEMPERATURE         = ',F6.2,' DEG C')
130 FORMAT(1H ,5X,'BAILEY CONTROL SETTINGS  = ',F7.1,' COURSE',3X,F5.1
   1,' FINE')
135 FORMAT(1H ,5X,'AIR FLOW INDICATOR       = ',F5.2)
140 FORMAT(1H ,5X,'PROPANE ROTAMETER        = ',F6.2)
145 FORMAT(1H ,5X,'FLOW METER CODE          = ',I2)
150 FORMAT(1H ,5X,'FLOW METER TEMPERATURE   = ',F5.1,' DEG C')
155 FORMAT(1H ,5X,'FLOW METER DELTA P       = ',F6.3,' INCHES HG')
160 FORMAT(1H ,5X,'SAMPLE NUMBER FOR REACTOR= ',I2,3X,'FOR PREHEATOR =
   1 ',I2)
165 FORMAT(1H ,'UNCORRECTED REACTOR CONDITIONS')
170 FORMAT(1H ,'********** ******* **********')
175 FORMAT(1H ,5X,'REACTOR PRESSURE         = ',F6.1,' PSIG')
180 FORMAT(1H ,5X,'BRIDGE RESISTANCE        = ',F7.3,' OHMS')
185 FORMAT(1H ,5X,'BRIDGE TEMPERATURE       = ',F5.1,' DEG C')
190 FORMAT(1H ,5X,'INLET CONCENTRATION      = ',F7.4)
195 FORMAT(1H ,5X,'OUTLET CONCENTRATION     = ',F7.4)
200 FORMAT(1H ,'CORRECTED REACTOR CONDITIONS')
205 FORMAT(1H ,'********** ******* **********')
210 FORMAT(1H ,5X,'BRIDGE RESISTANCE        = ',F7.3,' OHMS')
215 FORMAT(1H ,5X,'REACTOR TEMPERATURE      = ',F8.2,' DEG F',3X,F8.2,
   1' DEG C')
220 FORMAT(1H ,5X,'REACTOR PRESSURE         = ',F6.1,'7PSIG',3X,F7.1,'
   1 PSIA')
225 FORMAT(1H ,5X,'INLET CONCENTRATION      = ',F7.4)
230 FORMAT(1H ,5X,'OUTLET CONCENTRATION     = ',F7.4)
235 FORMAT(1H ,'SUMMARY OF RATE VARIABLES')
240 FORMAT(1H ,'******* ** **** *********')
245 FORMAT(1H ,5X,'TEMPERATURE          = ',F8.2,' DEG F',3X,F8.2,' DEG
   1 C')
```

```
  250 FORMAT(1H ,5X,'PRESSURE                = ',F7.1,' PSIA')
  255 FORMAT(1H ,5X,'RESIDENCE TIME          = ',F7.2,' SEC')
  260 FORMAT(1H ,5X,'DENSITY AT RC           = ',F7.4,' MOLES/LITER')
  265 FORMAT(1H ,5X,'DENSITY AT STP          = ',F7.4,' MOLES/LITER')
  270 FORMAT(1H ,5X,'FLOW RATE AT STP        = ',F9.2,' ML/SEC')
  275 FORMAT(1H ,5X,'ROTAMETER RATE          = ',F9.2,' ML/SEC')
  280 FORMAT(1H ,5X,'RATE CONSTANT           = ',E11.4,' PER SEC')
  285 FORMAT(1H ,'**********  END OF RUN ANALYSIS')
 9191 FORMAT(1H1)
C   READ INPUT DATA
C
      COMMON RT,TF,TC,TR,TK,CI,CO,TAU,FLOW,RHO,RHOS,FLOW1,RKC
      READ(1,20) NSETS
      DO 500 JKL=1, NSETS
      READ(1,5) Q1,Q2,Q3,Q4,Q5,Q6
      READ(1,10) PBAR
      READ(1,10) TRM
      READ(1,10) CRSE, CFNE
      READ(1,10) FLA
      READ(1,10) FPR
      READ(1,10) RMB
      READ(1,15) BC
      READ(1,10) TMB
      READ(1,10) PR
      READ(1,10) TFM
      READ(1,10) DELP
      READ(1,10) TMF
      READ(1,10) RNGE
      READ(1,20) NCODE
      READ(1,10) RFR
      READ(1,20) NSAMP, NSAMP1
      READ(1,25) CONCI
      READ(1,25) CONCO
      READ(1,20) NTEMP
C
C    BEGIN CALCULATIONS
```

```
C
      CALL BRIDGE(RMB,TMB,BC,NTEMP)
      CALL CONC(CONCI,CONCO)
      CALL PVT(   PR,PBAR)
      CALL FLCOR(NCODE,TFM,DELP,TMF,RNGE,RFR,PBAR)
      CALL RATE(PR)
C
C     PRINT OUT RESULTS
C
      WRITE(3,9191)
      WRITE(3,100)
      WRITE(3,35) Q1,Q2,Q3,Q4,Q5,Q6
      WRITE(3,105)
      WRITE(3,110)
      WRITE(3,115)
      WRITE(3,105)
      WRITE(3,120) PBAR
      WRITE(3,125) TRM
      WRITE(3,130) CRSE, CFNE
      WRITE(3,135) FLA
      WRITE(3,140) FPR
      WRITE(3,145) NCODE
      WRITE(3,150) TFM
      WRITE(3,155) DELP
      WRITE(3,160) NSAMP, NSAMP1
      WRITE(3,105)
      WRITE(3,165)
      WRITE(3,170)
      WRITE(3,105)
      WRITE(3,175) PR
      WRITE(3,180) RMB
      WRITE(3,185) TMB
      WRITE(3,190) CONCI
      WRITE(3,195) CONCO
      WRITE(3,105)
      WRITE(3,200)
```

```
      WRITE(3,205)
      WRITE(3,105)
      WRITE(3,210) RT
      WRITE(3,215) TF, TC
      PR1=PR+ (PBAR/29.92)*14.7
      WRITE(3,220) PR, PR1
      WRITE(3,225) CI
      WRITE(3,230) CO
      WRITE(3,105)
      WRITE(3,235)
      WRITE(3,240)
      WRITE(3,105)
      WRITE(3,245) TF, TC
      WRITE(3,250) PR1
      WRITE(3,255) TAU
      WRITE(3,260) RHO
      WRITE(3,265) RHOS
      WRITE(3,270) FLOW
      WRITE(3,275) FLOW1
      WRITE(3,280) RKC
      WRITE(3,105)
      WRITE(3,285)
  500 CONTINUE
      STOP
      END
C    SUBROUTINE TO COMPUTE CORRECTED MUELLER BRIDGE RESISTANCE AND REACTOR TEMP
C
      SUBROUTINE BRIDGE(RMB,TMB,BC,NTEMP)
      COMMON RT, TF, TC, TR, TK
      RMB1=RMB- 40.00
      RMB1=RMB1+ BC
      CF1= 0.99933+ 0.000036074*TMB- 0.00000042969*TMB*TMB
      R1=RMB1*CF1
      R2= 40.00+ 0.0421+ 0.0001834*TMB
      GO TO(50,100,150), NTEMP
   50 CONTINUE
```

```
      RT=R1+ R2
      TF=-424.36+ 22.3826*RT+ 0.007611*RT*RT+ 0.000362*RT*RT*RT
      GO TO 200
  100 CONTINUE
      RT=R1+ R2
      TF=-425.82+ 22.3867*RT+ 0.004196*RT*RT+0.0004027039*RT*RT*RT
      GO TO 200
  150 CONTINUE
      RT=RMB+ BC
      TF= 63.40+ 41.898*RT
  200 CONTINUE
      TC=(TF-32.0)/1.8
      TR=TF+459.6
      TK=TC+273.16
      RETURN
      END
C    SUBROUTINE TO COMPUTE DENSITY
C
      SUBROUTINE PVT(PR,PBAR)
      COMMON RT,TF,TC,TR,TK,CI,CO,TAU,FLOW,RHO,RHOS
      R=0.08205
      OMEG1=0.135
      GAM=0.052058- 0.09064*OMEG1+ 0.10506*OMEG1**2
      C=0.035694+ 0.185297*OMEG1- 0.230125*OMEG1**2
      A=0.0235866+ 0.290284*OMEG1- 0.295413*OMEG1**2
      B=0.0275404+ 0.131009*OMEG1- 0.134924*OMEG1**2
      C1=0.098224+ 0.401236*OMEG1- 0.0397267*OMEG1**2
      A0=0.343258- 0.127521*OMEG1- 0.509131*OMEG1**2
      B0=0.113747+ 0.127349*OMEG1- 0.243280*OMEG1**2
      ALPH=0.0000875/A
      T1=TK/397.6
      PRED=(PR/14.696+ PBAR/29.92)/54.2
      D=0.0
      COR=0.1
      DIFFE=10.0
      ZZ=0.00001
```

```
  101 IF(DIFFE-ZZ) 112,112,102
  102 DO 106 J=1, 200
      D=D+ COR
      PI=T1*D+(BO*T1-AO-C1/(T1*T1))*D*D+(B*T1-A)*D**3+(A*ALPH)*D**6+
     1(C*D**3/(T1*T1))*(1.0+GAM*D*D)*EXP(-GAM*D*D)
      DIFE=PRED-PI
      DIFFE=ABS(DIFE)
  103 IF(DIFE) 107,107,106
  106 CONTINUE
  107 IF(COR-0.00001) 112,112,109
  109 D=D-COR
      COR=0.1*COR
      GO TO 101
  112 CONTINUE
      RHO=D*54.2/(R*397.6)
      RHOS=0.04296
      RETURN
      END
C   SUBROUTINE TO COMPUTE FLOW RATES AT STP(60 F, 1 ATMS) AND RESIDENCE TIME
C        IN REACTOR
C
      SUBROUTINE FLCOR(NCODE,TFM,DELP,TMF,RNGE,RFR,PBAR)
      COMMON RT,TF,TC,TR,TK,CI,CO,TAU,FLOW,RHO,RHOS,FLOW1
      VP= 0.47296+ 0.037868*TFM+ 0.00043951*TFM*TFM+ 0.00004361*TFM*TFM*
     1TFM
      VP=VP/2.54
      PFM=PBAR+ DELP- VP
      FACT1=PFM/29.92
      FACT2=(520.0)/((TFM+273.2)*1.8)
      GO TO (10,15,10),NCODE
   10 FLOW=(RNGE*FACT1*FACT2)/TMF
      TAU=(239.9/FLOW)*(RHO/RHOS)
      GO TO 20
   15 FLOW=(RNGE*FACT1*FACT2)/TMF
      FLOW=FLOW/0.0000353
      TAU=(239.9/FLOW)*(RHO/RHOS)
```

```
   20 CONTINUE
      FLOW1=-1.5595+ 0.69845*RFR+ 0.0059885*RFR*RFR
      FLOW1=FLOW1/(.00353*60.0)
      RETURN
      END
C    SUBROUTINE TO COMPUTE CORRECTED CONCENTRATIONS
C
      SUBROUTINE CONC(CONCI,CONCO)
      COMMON RT,TF,TC,TR,TK,CI,CO
      IF(CONCO-0.8000)10,15,15
   10 CO=0.0256+ 0.97987*CONCO
      GO TO 20
   15 CO=0.0511+ 0.94874*CONCO
   20 CONTINUE
      CI=0.0511+ 0.94874*CONCI
      RETURN
      END
C    SUBROUTINE TO COMPUTE RATE CONSTANT
C
      SUBROUTINE RATE(PR)
      COMMON RT,TF,TC,TR,TK,CI,CO,TAU,FLOW,RHO,RHOS,FLOW1,RKC
      RKC=ALOG(CI/CO)/TAU
      RETURN
      END
```

```
                    DATA ANALYSIS FOR RUN   R1-50

 SUMMARY OF RUN VARIABLES
 ******* ** *** *********

      BAROMETRIC PRESSURE      =  28.70 INCHES HG
      ROOM TEMPERATURE         =  25.00 DEG C
      BAILEY CONTROL SETTINGS  =   922.0 COURSE     7.0 FINE
      AIR FLOW INDICATOR       =  8.00
      PROPANE ROTAMETER        =   9.20
      FLOW METER CODE          =  1
      FLOW METER TEMPERATURE   =  27.4 DEG C
      FLOW METER DELTA P       =  1.540 INCHES HG
      SAMPLE NUMBER FOR REACTOR=  1    FOR PREHEATOR =  0

 UNCORRECTED REACTOR CONDITIONS
 ********** ******* **********

      REACTOR PRESSURE         =   50.0 PSIG
      BRIDGE RESISTANCE        =  55.321 OHMS
      BRIDGE TEMPERATURE       =  26.5 DEG C
      INLET CONCENTRATION      =  0.9972
      OUTLET CONCENTRATION     =  0.9771

 CORRECTED REACTOR CONDITIONS
 ********* ******* **********

      BRIDGE RESISTANCE        =  55.375 OHMS
      REACTOR TEMPERATURE      =   899.89 DEG F     482.16 DEG C
      REACTOR PRESSURE         =   50.07PSIG       64.1 PSIA
      INLET CONCENTRATION      =  0.9972
      OUTLET CONCENTRATION     =  0.9781

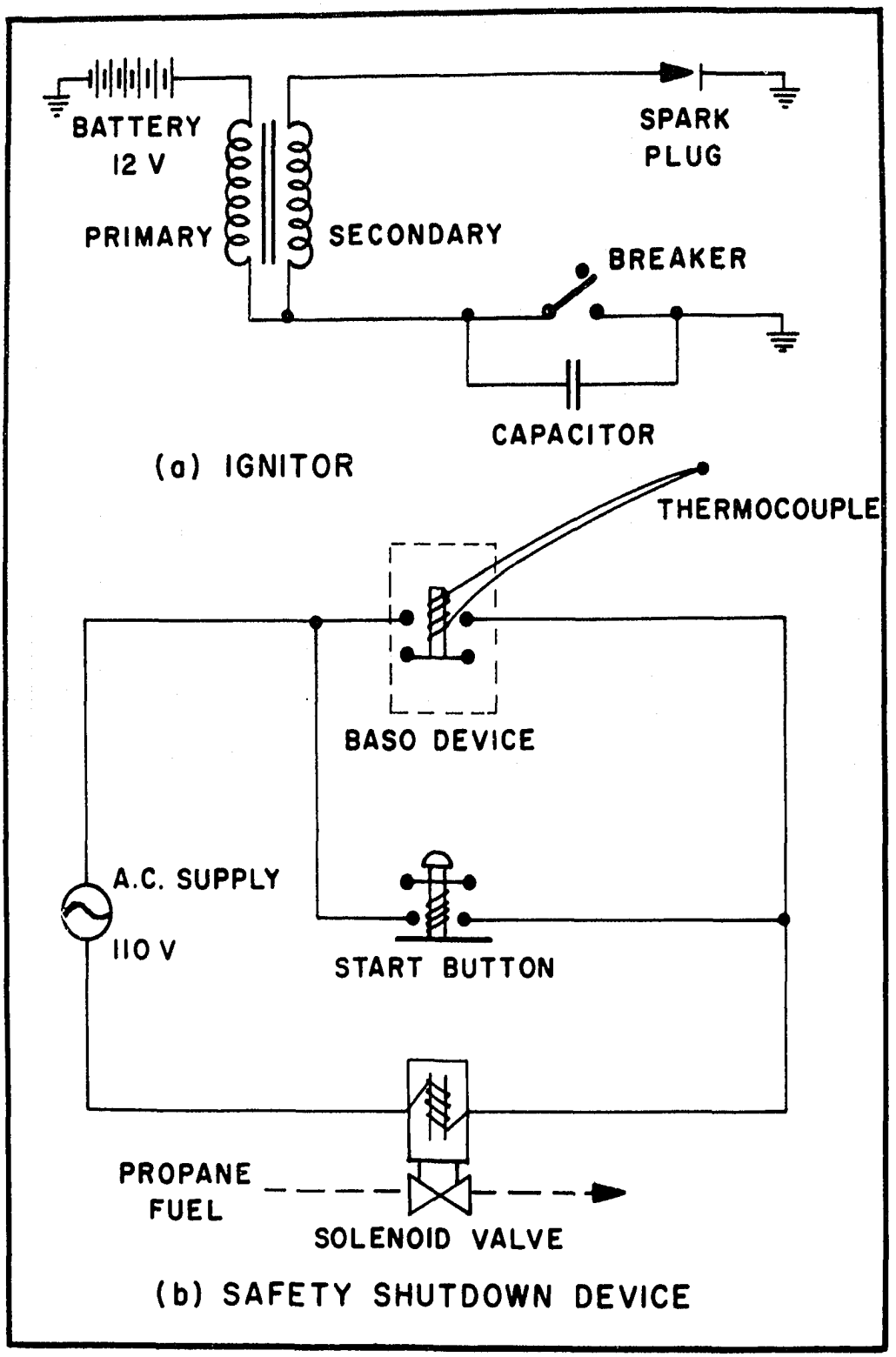
 SUMMARY OF RATE VARIABLES
 ******* ** **** *********

      TEMPERATURE              =   899.89 DEG F     482.16 DEG C
      PRESSURE                 =    64.1 PSIA
      RESIDENCE TIME           =   71.59 SEC
      DENSITY AT RC            =  0.0706 MOLES/LITER
12    DENSITY AT STP           =  0.0430 MOLES/LITER
11    FLOW RATE AT STP         =       5.51 ML/SEC
10    ROTAMETER RATE           =       5.40 ML/SEC
 9    RATE CONSTANT            =  0.2697E-03 PER SEC
 8
 7
 6  **********  END OF RUN ANALYSIS
```

Figure 45. Sample Computer Results.

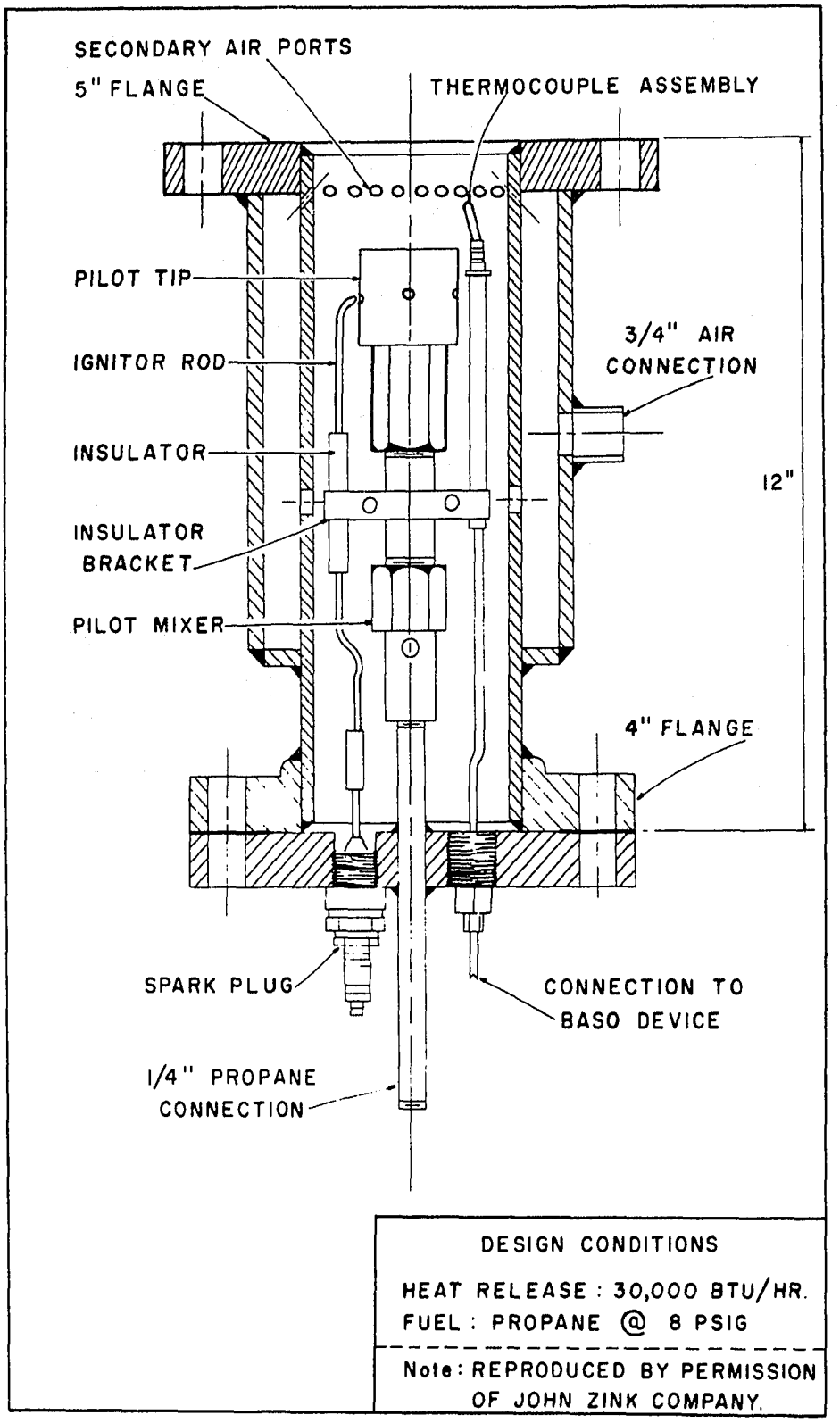
APPENDIX D

SAND BATH DIAGRAMS



BURNER IGNITION SYSTEM
ELECTRICAL CIRCUIT DIAGRAMS

Figure 46. Burner Ignition System Electrical Circuit Diagrams.



SECTIONAL ELEVATION OF BURNER FOR SAND BATH HEATER

Figure 47. Sectional Elevation of Burner for Sand Bath Heater.

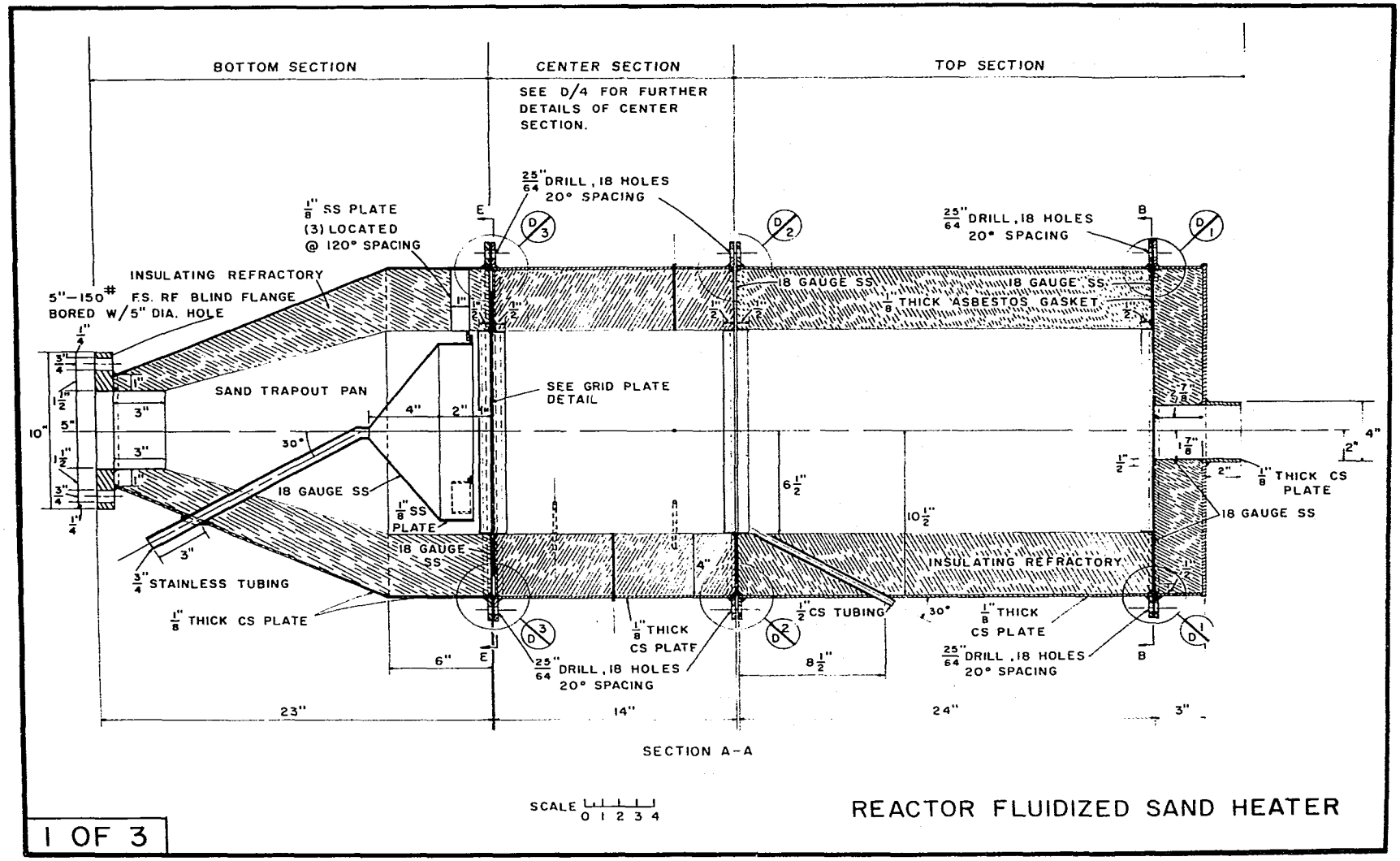


Figure 48. Reactor Fluidized Sand Heater.

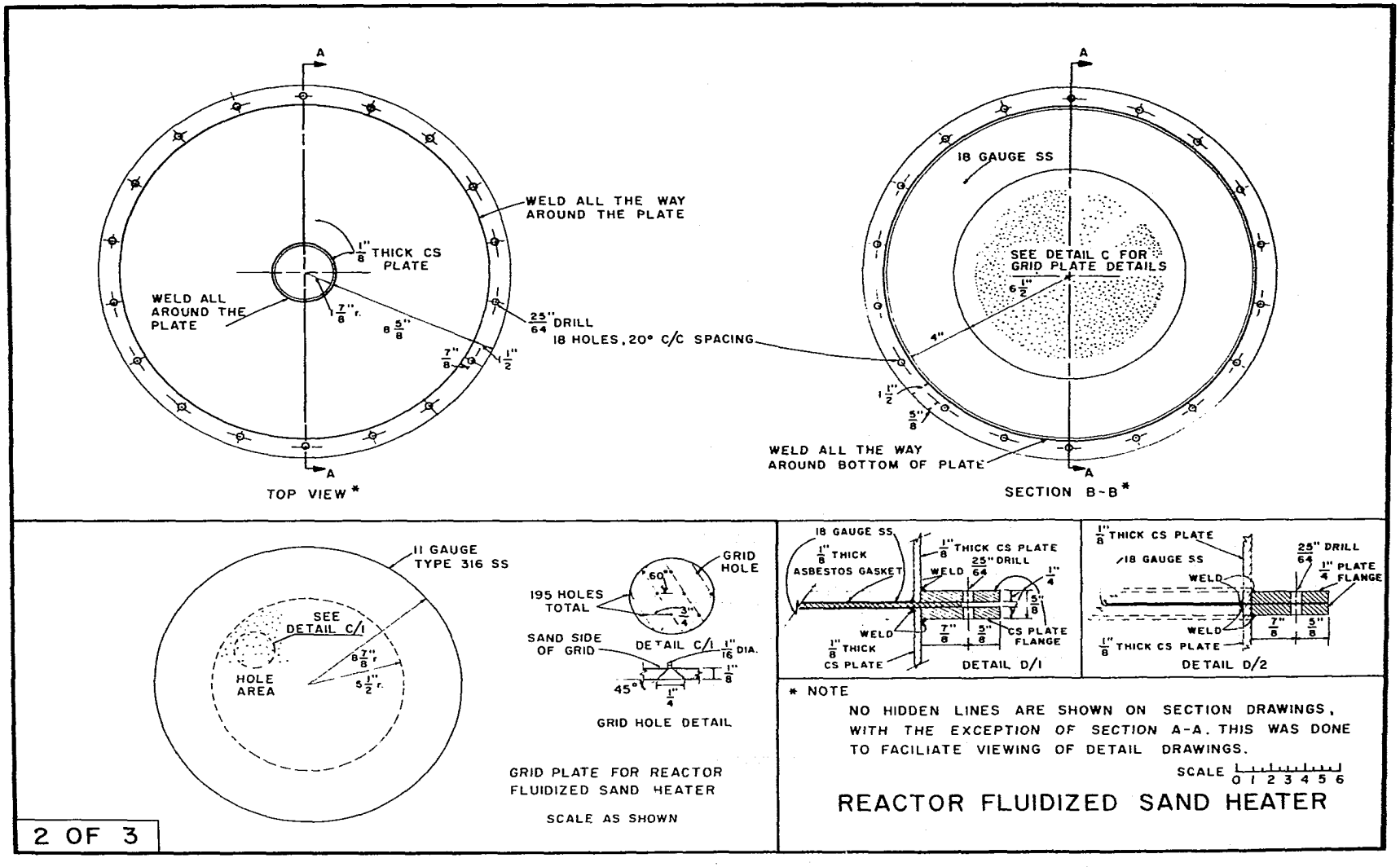


Figure 49. Reactor Fluidized Sand Heater--Sectional.

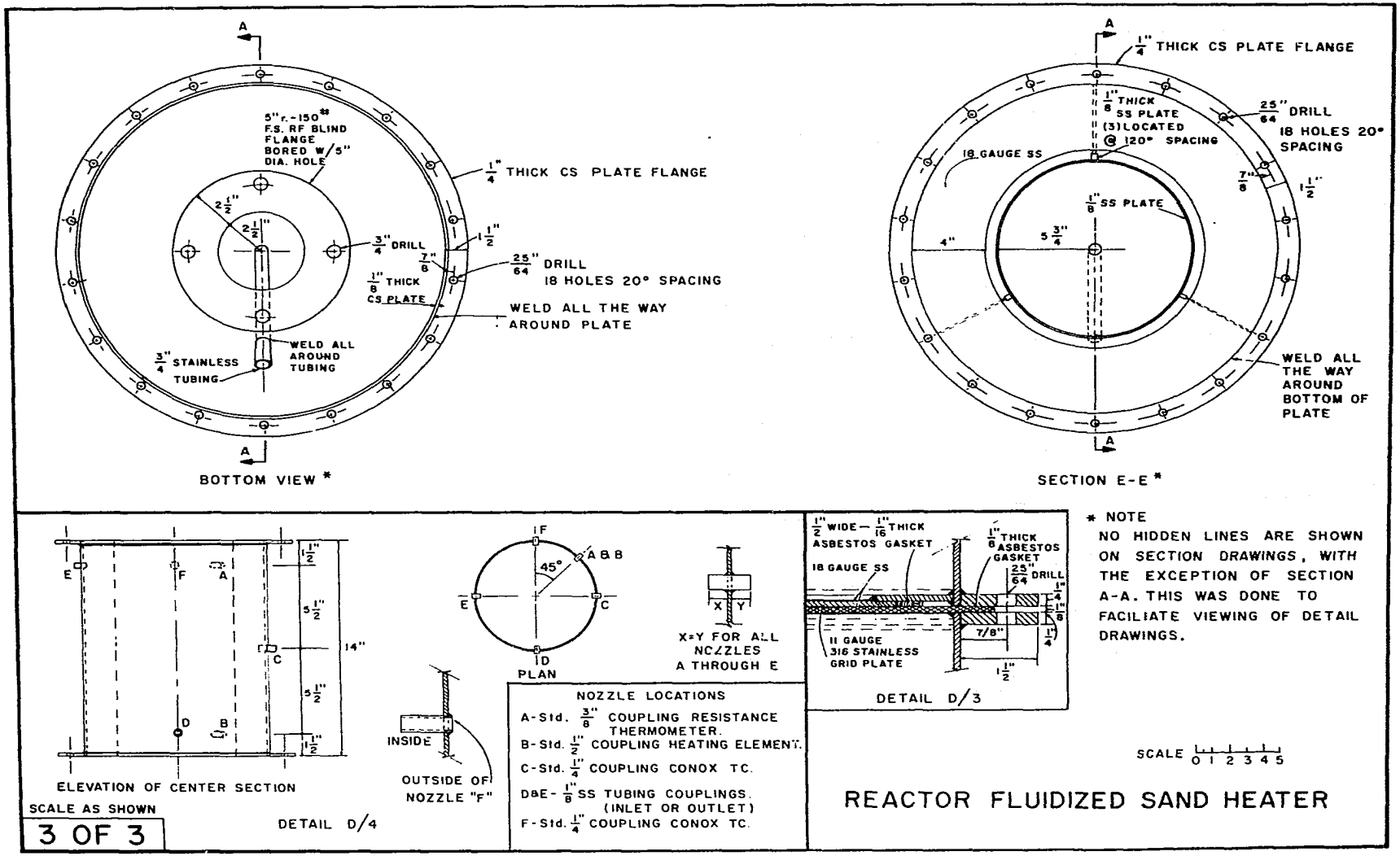


Figure 50. Reactor Fluidized Sand Heater--Grid Plate.

APPENDIX E

SUMMARY OF EXPERIMENTAL DATA

TABLE 11

SUMMARY OF EXPERIMENTAL RUNS

Run Number	Temperature °C	Temperature °F	Pressure atms.	Flow ml./sec. (STP)	Density moles/l.	τ sec	Cyclopropane Concentration inlet	Cyclopropane Concentration outlet	Conversion %	k x 10^4 sec^{-1}	Material Balance (out/in)x100	Comments
RI-50	482.16	899.89	4.36	5.51	0.0706	71.57	0.9972	0.9781	1.92	2.698		
RI-100	482.17	899.91	7.74	7.19	0.1254	97.34	0.9974	0.9714	2.61	2.713		
RI-200	482.16	899.89	14.57	14.05	0.2371	94.24	0.9974	0.9719	2.56	2.740		
RI-300	482.26	900.07	21.34	20.88	0.3486	93.23	0.9975	0.9719	2.57	2.791		
RI-400	482.25	900.04	28.11	28.33	0.4609	90.83	0.9976	0.9730	2.47	2.746		
R2-50	510.08	950.14	4.37	11.65	0.0681	32.65	0.9970	0.9570	4.01	12.55		
R2-100	510.22	950.40	7.78	15.94	0.1215	42.56	0.9965	0.9409	5.58	13.49	101.9	
R2-100A	510.22	950.40	7.78	16.20	0.1215	41.89	0.9965	0.9409	5.58	13.70		
R2-200	510.14	950.25	14.55	27.03	0.2281	47.13	0.9966	0.9373	5.95	13.01	102.1	
R2-300	510.21	950.38	21.33	39.62	0.3353	47.26	0.9968	0.9363	7.07	13.26	101.5	
R2-400	510.20	950.36	28.13	53.54	0.4434	46.25	0.9967	0.9371	5.98	13.33	101.8	
R3-50	538.20	1000.76	4.35	51.33	0.0654	7.12	0.9970	0.9568	4.03	57.86	103.9	a
R3-100	538.22	1000.79	7.76	51.18	0.1170	12.76	0.9963	0.9246	7.19	58.53	102.0	a
R3-200	538.30	1000.93	14.53	50.70	0.2196	24.19	0.9951	0.8571	13.87	58.28	103.9	a
R3-300	538.29	1000.92	21.32	50.03	0.3230	36.05	0.9939	0.8069	18.81	57.79	100.6	a
R3-400	538.19	1000.75	28.14	49.66	0.4273	48.05	0.9927	0.7511	24.34	58.05		a
R4-50	454.09	849.36	4.35	5.78	0.0732	70.72	0.9980	0.9944	0.36	0.5116		
R4-100	454.02	849.24	7.72	6.75	0.1301	107.56	0.9980	0.9930	0.50	0.4695		
R4-200	453.95	849.11	14.55	6.51	0.2464	211.48	0.9980	0.9884	0.96	0.4607		
R4-300	453.97	849.15	21.32	10.51	0.3627	192.68	0.9978	0.9888	0.90	0.4709		
R4-400	454.25	849.66	28.12	14.46	0.4803	185.44	0.9980	0.9887	0.93	0.5047		
R5-50	524.41	975.94	4.34	35.41	0.0665	10.49	0.9973	0.9691	2.83	27.33	99.70	
R5-100	524.41	975.94	7.74	35.54	0.1187	18.65	0.9966	0.9481	4.87	26.75	101.3	
R5-200	524.67	976.40	14.52	35.24	0.2233	35.38	0.9958	0.9017	9.45	28.03	99.80	
R5-300	524.64	976.36	21.30	37.82	0.3285	48.50	0.9952	0.8708	12.50	27.53	99.80	
R5-400	524.53	976.15	28.11	41.63	0.4347	58.31	0.9943	0.8474	14.77	27.43	101.3	
R6-50	496.50	925.70	4.34	6.80	0.0689	56.54	0.9969	0.9640	3.30	5.940		
R6-100	496.45	925.62	7.78	9.03	0.1236	76.48	0.9972	0.9521	4.52	6.046		
R6-200	496.31	925.37	14.52	10.19	0.2317	127.05	0.9964	0.9241	7.26	5.929		
R6-300	496.41	925.53	21.30	14.03	0.3411	135.75	0.9963	0.9179	7.87	6.042		
R6-400	496.36	925.45	28.15	18.51	0.4523	136.42	0.9962	0.9179	7.86	6.006		
R7-50	538.19	1000.74	4.35	40.44	0.0655	9.04	0.9968	0.9460	5.10	57.78		b
R7-100	538.14	1000.66	7.77	49.68	0.1171	13.16	0.9964	0.9249	7.17	56.62	99.44	b
R7-200	538.00	1000.41	14.53	52.13	0.2196	23.53	0.9953	0.8727	12.32	55.86	100.71	b
R7-300	538.03	1000.45	21.36	56.90	0.3236	31.76	0.9943	0.8311	16.41	56.47	101.80	b
R7-400	538.14	1000.66	28.18	56.97	0.4278	41.93	0.9929	0.7822	21.22	56.94	99.92	b
R8-30	511.37	952.47	3.03	7.52	0.0471	34.97	0.9969	0.9511	4.59	13.45		
R8-15	511.12	952.01	1.98	6.29	0.0309	27.41	0.9972	0.9593	3.80	13.40		
R8-5	512.73	954.90	1.33	3.36	0.0206	34.13	0.9967	0.9488	4.80	14.43		
R8-atms	512.86	955.16	1.03	3.41	0.0161	26.37	0.9972	0.9595	3.78	14.60		
R9-30	481.23	898.22	3.04	1.61	0.0492	170.85	0.9967	0.9561	4.07	2.434		
R9-30A	481.12	898.02	3.01	2.09	0.0487	130.42	0.9971	0.9655	3.17	2.469		

TABLE 11 (continued)

Run Number	Temperature °C	Temperature °F	Pressure atms.	Flow ml/sec. (STP)	Density moles/l.	τ sec	Cyclopropane Concentration inlet	Cyclopropane Concentration outlet	Conversion %	k x 10^4 sec^{-1}	Material Balance (out/in)x100	Comments
R9-15	481.17	898.11	1.99	1.64	0.0323	110.21	0.9971	0.9703	2.69	2.468		
R9-5	481.12	898.01	1.30	1.59	0.0210	73.71	0.9974	0.9797	1.77	2.422		
R9-atms	481.16	898.09	1.04	1.47	0.0168	63.87	0.9974	0.9816	1.58	2.492		
R10-30	481.37	898.47	2.98	1.38	0.0483	195.37	0.9955	0.9428	5.29	2.782		
R10-30A	481.48	898.66	3.00	3.78	0.0486	71.84	0.9970	0.9778	1.93	2.702		
R10-15	481.34	898.42	1.98	1.50	0.0321	119.44	0.9964	0.9637	3.28	2.796		
R10-5	481.49	898.69	1.29	1.37	0.0209	85.46	0.9968	0.9722	2.47	2.921		
R10-atms	481.45	898.61	1.03	1.44	0.0167	64.88	0.9971	0.9788	1.84	2.857		
R11-30	538.11	1000.59	2.99	11.80	0.0451	21.33	0.9943	0.8404	15.48	78.93		c
R11-15	538.02	1000.43	1.98	11.72	0.0298	14.20	0.9945	0.8467	14.86	113.3		c
R12	--	--	--	--	--	--	--	--	--	--		d
R13-200	482.64	900.75	14.53	9.92	0.2364	133.05	0.9971	0.9609	3.63	2.634		
R13-100	482.55	900.59	7.76	10.30	0.1257	68.13	0.9977	0.9802	1.75	2.591		
R13-50	482.58	900.64	4.37	8.30	0.0708	47.64	0.9978	0.9856	1.22	2.590		
R14-50	496.74	926.14	4.35	3.95	0.0690	97.64	0.9957	0.9387	5.72	6.029		
R14-30	496.58	925.84	3.01	3.85	0.0478	69.30	0.9966	0.9575	3.92	5.774		
R14-15	496.62	925.92	1.98	3.89	0.0315	45.19	0.9971	0.9713	2.59	5.803		
R15-50	472.78	883.01	4.34	2.21	0.0709	179.31	0.9969	0.9710	2.60	1.468		
R15-30	472.69	882.84	3.01	2.40	0.0492	114.75	0.9972	0.9804	1.68	1.480		
R15-15	472.91	883.24	2.00	2.40	0.0327	76.01	0.9976	0.9866	1.10	1.459		
R16-50	454.67	850.40	4.35	2.10	0.0730	194.50	0.9979	0.9879	1.00	0.5207		
R16-30	454.75	850.56	3.01	2.08	0.0505	135.81	0.9978	0.9910	0.68	0.5058		
R16-15	454.78	850.61	1.99	2.03	0.0333	91.71	0.9979	0.9934	0.45	0.4986		
R16-5	454.83	850.69	1.31	2.11	0.0220	58.24	0.9979	0.9949	0.30	0.5230		
R16-atms	454.84	850.72	1.03	1.51	0.0173	64.23	0.9978	0.9945	0.33	0.5190		
R17	--	--	--	--	--	--	--	--	--	--		e
R18-50	496.47	925.65	4.34	4.22	0.0689	91.25	0.9961	0.9428	5.35	6.028		
R18-30	496.27	925.29	3.01	3.98	0.0477	66.96	0.9968	0.9580	3.89	5.930		
R18-15	496.39	925.51	1.97	4.01	0.0313	43.67	0.9973	0.9719	2.55	5.892		
R18-5	496.42	925.56	1.30	3.97	0.0206	29.00	0.9978	0.9804	1.74	5.754		
R18-atms	496.21	925.18	1.03	3.97	0.0164	23.06	0.9978	0.9845	1.33	5.811		
R19-50	468.70	875.66	4.37	2.22	0.0720	180.67	0.9975	0.9758	2.18	1.213		
R19-30	468.64	875.56	3.01	2.18	0.0496	127.17	0.9975	0.9826	1.49	1.183		
R19-15	468.80	875.85	1.99	2.09	0.0327	87.22	0.9978	0.9872	1.06	1.217		
R19-5	468.82	875.87	1.31	2.15	0.0215	55.63	0.9978	0.9912	0.66	1.183		
R19-atms	468.88	875.98	1.03	2.15	0.0169	43.88	0.9978	0.9926	0.52	1.195		
R20-400-1	510.07	950.12	28.18	30.76	0.4444	80.68	0.9927	0.8989	9.45	12.31		f
R20-400-2	509.98	949.96	28.17	19.19	0.4442	129.29	0.9929	0.8475	14.65	12.25		f
R20-400-3	509.74	949.53	28.20	55.92	0.4448	44.42	0.9965	0.9427	5.40	12.49		f
R20-400-4	510.07	950.12	28.16	10.68	0.4441	232.14	0.9879	0.7518	23.90	11.77		f
R20-400-5	510.08	950.15	28.18	5.48	0.4443	452.51	0.9807	0.6432	34.41	9.321		f
R21-0.4-1	510.11	950.20	0.393	1.323	0.0061	25.68	0.9964	0.9654	3.12	12.22		
R21-0.4-2	510.17	950.30	0.397	0.935	0.0062	36.82	0.9956	0.9532	4.25	11.83		
R21-0.4-3	510.10	950.18	0.395	0.690	0.0062	49.73	0.9952	0.9403	5.50	11.41		
R22-0.4-1	482.24	900.03	0.394	0.620	0.0064	57.17	0.9970	0.9827	1.44	2.52		
R22-0.4-2	482.22	900.00	0.392	0.535	0.0063	65.94	0.9969	0.9801	1.69	2.57		

TABLE 11 (continued)

Run Number	Temperature °C	Temperature °F	Pressure atms.	Flow ml./sec. (STP)	Density moles/l.	τ sec	Cyclopropane Concentration inlet	Cyclopropane Concentration outlet	Conversion %	k x 10^4 sec^{-1}	Material Balance (out/in)x100	Comments
R23-1	900.07	482.26	68.89	42.49	1.1497	151.09	0.9963	0.9566	3.98	2.695		g
R23-2	900.03	482.24	68.93	80.20	1.1503	80.10	0.9976	0.9757	2.20	2.761		g
R23-3	900.03	482.24	68.93	19.84	1.1504	323.80	0.9952	0.9151	8.05	2.591		g
R23-4	900.11	482.28	69.20	8.04	1.1549	802.52	0.9908	0.8386	15.36	2.079		g
R24-1000	900.04	482.24	69.01	94.37	1.1515	68.14	0.9979	0.9800	1.79	2.661		
R24-1500	899.69	482.05	102.96	122.37	1.7352	79.18	0.9978	0.9768	2.10	2.694		
R24-2000	899.47	481.93	137.19	155.35	2.3221	83.47	0.9978	0.9760	2.18	2.638		

Footnote Comments on Experimental Runs

a - first occurrence of preheater plugging. Gold lining found constricted at preheater inlet

b - second occurrence of preheater plugging. Same problem as in comment (a).

c - third occurrence of preheater plugging. Gold lined preheater removed and replaced with unlined preheater.

d - air purged through reactor while at run temperature to remove any carbon deposits which had accumulated on reactor lining.

e - same as (d).

f - first run made at high residence times to evaluate the effect of residence time on the rate constant.

g - second run at high residence times to evaluate the effect of residence time on the rate constant.